A SCIENTIFIC APPROACH TO THE DESIGN OF COMPUTER CONTROLLED MANIPULATORS

J. L. Nevins, et al

Charles Stark Draper Laboratory, Incorporated

Prepared for:

Defense Advanced Research Projects Agency

August 1974

R-837

A Scientific Approach to the Design of Computer Controlled Manipulators

by

J. L. Nevins, D. E. Whitney, A. E. Woodin
S. Drake, M. Lynch, D. Seltzer, R. Sturges, P. Watson

Contract DAH-C-15-73-C-0278 with the Defense Advanced Research Projects Agency, ARPA Order No. 2455, Project Code 3D30

August 1974

The Charles Stark Draper Laboratory, Inc.
Cambridge, Massachusetts

Approved: N. E. Sears by ear Date: 22 Oct. 74
N. Sears

ACKNOWLEDGEMENT

This report was prepared by The Charles Stark Draper Laboratory, Inc., under contract DAH-C-15-73-C-0278 with the Defense Advanced Research Projects Agency, ARPA Order No. 2455, Project Code 3D30.

TABLE OF CONTENTS

TABLE OF CONTENTS (cont)

TABLE OF CONTENTS (cont)

TABLE OF CONTENTS (cont)

SECURITY CLASSIFICATION OF THIS PAGE (When Data Entered)

REPORT DOCUMENTATION PAGE	READ INSTRUCTIONS BEFORE COMPLETING FORM
1. REPORT NUMBER	2. GOVT ACCESSION NO.	3. RECIPIENT'S CATALOG NUMBER: AD-A007 582
4. TITLE (and Subtitle): A SCIENTIFIC APPROACH TO THE DESIGN OF COMPUTER CONTROLLED MANIPULATORS	5. TYPE OF REPORT & PERIOD COVERED
	6. PERFORMING ORG. REPORT NUMBER: R-837
7. AUTHOR(s): J.L. Nevins D.E. Whitney A.E. Woodin S. Drake M. Lynch, D. Seltzer R. Sturges P. Watson	8. CONTRACT OR GRANT NUMBER(s): DAH-C-15-73-C-0278
9. PERFORMING ORGANIZATION NAME AND ADDRESS: Charles Stark Draper Laboratory, Inc. 68 Albany Street Cambridge, Mass. 02139	10. PROGRAM ELEMENT, PROJECT, TASK AREA & WORK UNIT NUMBERS: ARPA Order No. 2455 Proj. Code 3D30
11. CONTROLLING OFFICE NAME AND ADDRESS: Advanced Research Projects Agency 1400 Wilson Boulevard Arlington, Virginia 22209	12. REPORT DATE: August 1974
	13. NUMBER OF PAGES: 185
14. MONITORING AGENCY NAME & ADDRESS(if different from Controlling Office)	15. SECURITY CLASS. (of this report): unclassified
	15a. DECLASSIFICATION/DOWNGRADING SCHEDULE

16. DISTRIBUTION STATEMENT (of this Report)

Approved for public release; distribution unlimited.

17. DISTRIBUTION STATEMENT (of the abstract entered in Block 20, if different from Report)

18. SUPPLEMENTARY NOTES

19. KEY WORDS (Continue on reverse side if necessary and identify by block number)

20. ABSTRACT (Continue on reverse side if necessary and identify by block number)

I. INTRODUCTION

A. Research Objectives

The purpose of this study was to develop a science for the design of computer controlled manipulator systems which could be scaled for small manipulators. At the outset of the study the lack of specific tasks or the specific scale of a design environment forced consideration of a working volume consistent with people in order to determine the relationships between tasks, task scale and performance requirements for actuators, sensors (both force and position), etc.

The work therefore had four principal activities, namely:

a. establish a scientific base for determining manipulator requirements as a function of task and task scale

b. identification and development of general design tools needed

c. implementation of a design for a laboratory system to determine the validity of the approach

d. evaluation of design concepts via simulations and small laboratory experiments

In addition, a survey was made of existing manipulator systems and a novel, patentable, hydraulic actuator was conceived and documented.

1. Arm Design Considerations

Arm design is really a misnomer. One cannot consider an arm out of context of the tasks expected to be performed or the environment that the tasks will be performed in. For example, Figure I-1 diagrams the interlationships that must be considered between technology, environment, parts design, and task descriptors if the focus is

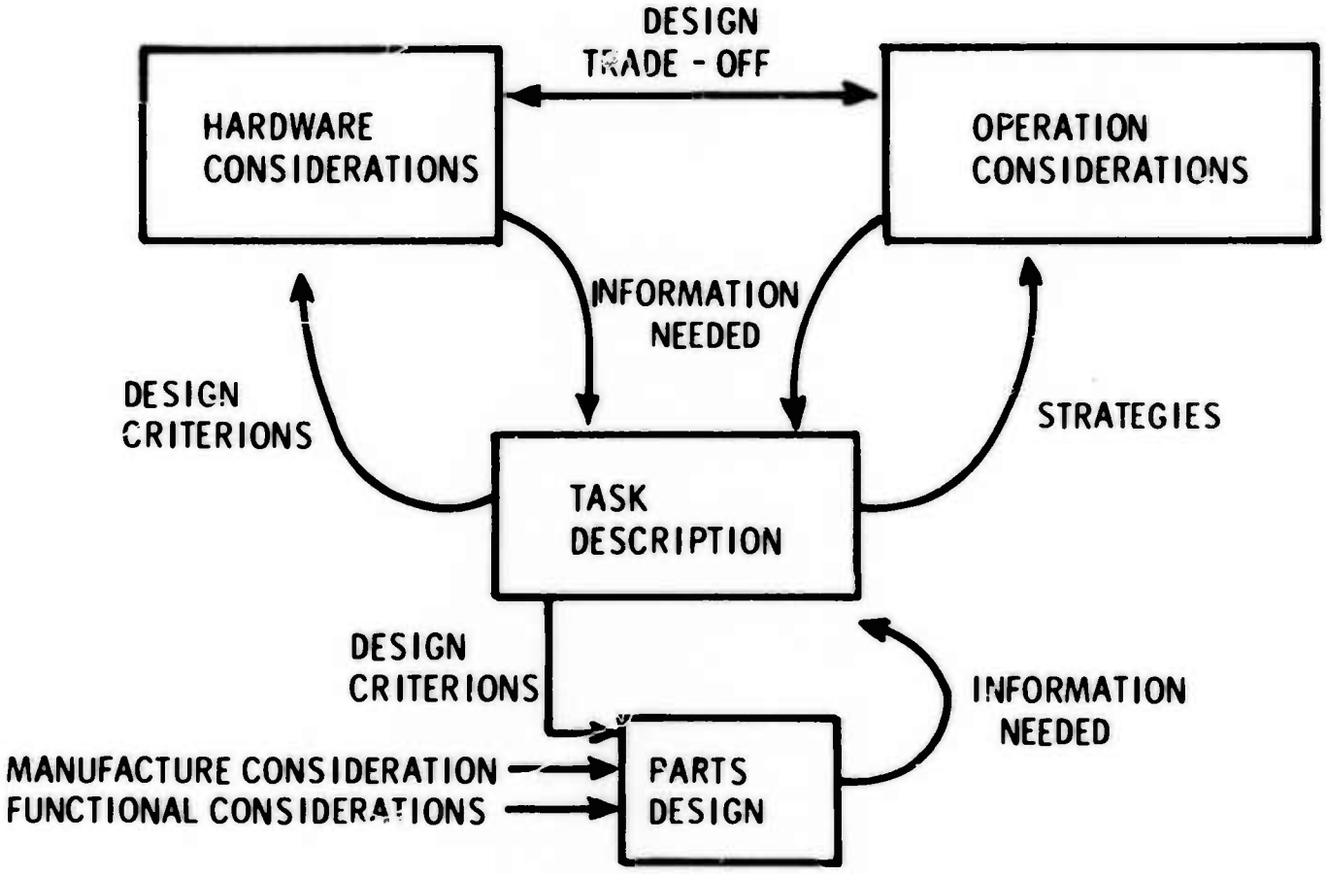

Figure I-1 Interaction of Elements in Assembly System Design

manipulator systems for assembly in a manufacturing environment.

Besides these issues, other studies[1, 2] have shown that the definition of industrial assembly requires consideration of a whole spectrum of issues besides motion systems as illustrated by Table 1. In general, motion or manipulator systems must be concerned with fetching parts, holding parts, and assembling parts. These alone imply many degrees-of-freedom not normally considered in the simple arm requirement that the end point of the manipulator be able to achieve all possible state points in some arbitrary working volume.

Further, these studies[1] showed that the three tasks (fetching parts, holding parts, and the assembly process) can be categorized into gross and fine motions. Gross motions are the large, rapid, less accurate motions necessary to move objects from one location to another. These motions can usually be done in an open-loop control manner with minimum information required from the environment. Fine motions are the small precise motions needed when two objects interact. It is this latter motion which is most dependent on the information acquired from the environment.

An interface region has also been defined between gross motion and fine motion to identify the boundary of uncertainty in knowledge of the location of parts, their size variation or the imprecise technology (sensor arrays, mechanical systems, control strategies, etc.) available for accomplishing the desired motion.

For other tasks, other considerations as well as the above must be taken into account. Two thumbnail design scenarios might serve to illustrate these points. Suppose one wishes to use a small arm (50 cm reach) to remove or insert common integrated circuits. It is known that each pin on such a circuit module requires a force of about 200g to insert it. Thus, a common 8 pin module will require 1.6 kilogram of force at the hand or 0.8 kilogram-meter of stall torque at the shoulder of the arm which does the inserting or removing. This stipulates a minimum static strength for this actuator. Other actuators with axes parallel to this one, at the elbow or wrist, will have to be capable of correspondingly

TABLE 1 ASSEMBLY SYSTEM ELEMENTS

(1) PARTS MANAGEMENT, GROSS AND FINE

Gross (scheduling): inventory orders, conveyors, dispatchers, etc.

Fine (parts feeding): shakers, conveyors, etc. (note the trend to make parts on site).

(2) INSPECTION, EXPLICIT AND IMPLICIT

Explicit (are all the holes present?)

Implicit (do the parts go together as expected?)

(3) MOTION, TO BRING THE FED, INSPECTED PARTS TOGETHER POSSIBLY USING JIGS AND FIXTURES

(4) FASTENING, USING SCREWS, RIVETS, GLUE, ETC.

(If not glue, then fastening involves additional assembly tasks).

(5) NON-DESTRUCTIVE TESTING (e.g., TEST FOR FREE MOTION).

(6) DIAGNOSTICS

(If some assemblies fail, find out why and correct parts manufacture or assembly)

(7) MONITORING

(To determine if the assembly system is operating properly)

calculated stall torques. A separate calculation is required for the torques required to accelerate and decelerate the arm. See below. Here it sufficies to say that the specified payloads are a tiny fraction of the arm's total weight, which therefore governs the dynamic and gravity torque problem independent of payload. If speed is not a factor, then insertion forces will determine the actuator characteristics.

As a second example, consider the arm studied in detail in this report (Fig. I-2). Here, payloads will be a substantial fraction of the arm's weight, perhaps 20% to 30%. This percentage is beyond the capabilities of current industrial robots. Their efficiency of design might yield only 10 to 15%. That is, their arms are quite heavy in comparison to the objects they are designed to move about. High speeds and payload requirements dominate the torque sizing problem for the arm designed here, far exceeding gravity or insertion forces. It is possible to solve this problem badly and end up with unbalanced capabilities among the actuators. Weak wrists are common among commercial industrial arms. Procedures for avoiding such difficulties are given in this report, along with the necessary technology of actuators, actuator location and transmission methods, and computer techniques for performing the balance.

Similar calculations, based on arm size and task characteristics, are required to determine the accuracy, and therefore the technology required for joint position sensors. Technology limitations in sensors and structure may lead to the conclusion that a single arm cannot be built which simultaneously has the required reach (a gross motion characteristic) and the required accuracy and ability to make very small motions (fine motion characteristics). A properly designed system capable of dealing meaningfully with such a task would therfore consist of two or more mobility systems.

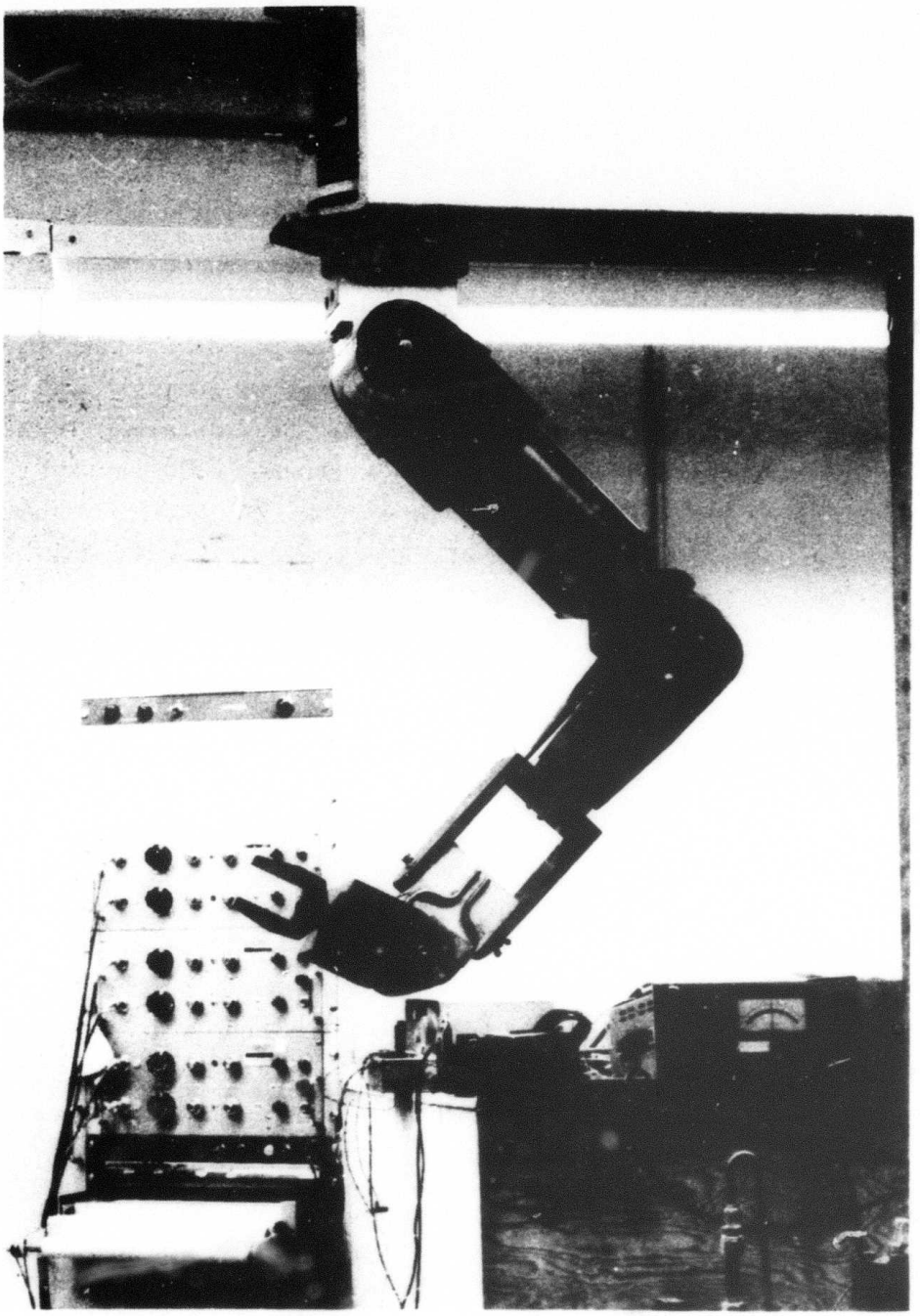

Figure I-2 Mockup of POPEYE, the Arm Studied in this Report

2. Design Method

To deal with this problem in a systematic way, therefore, required detail consideration of manipulator tasks and an environment. With contractor agency support it was decided to use the detailed task and environment analysis being done under an NSF sponsored research grant* into "Exploratory Research in Industrial Modular Assembly."[1, 2]

This work was concerned with a system organized about force and torque sensor arrays for performing industrial mechanical assembly within a working volume of 0.3 meter cubed (1 foot cubed). This approach for assembly is similar to the way a blind person might assemble things — by touch and feel. In order that this kind of system be efficient its world must be highly structured. That is, the location of parts, jigs, tools, etc. must be known a priori to some tolerance. Otherwise, a great deal of time would be required to grope around and find things. Groping around, or a less structured world, was left to later considerations of higher level systems that include visual or non-visual imaging sensors.

The decision to use the NSF sponsored work had the following advantages:

a. It was concerned with a work volume in which tasks can easily be identified and studied.

b. It gave access to detailed task analysis being performed on a variety of mechanical assemblies.

c. Since assembly is a composite of many kinds of tasks the lack of task specificity would not be a problem.

d. The dynamic coupling of manipulator requirements and task and task scale could be analyzed to determine the design tools needed.

* NSF Grant No. GI-39432X and GI-43787

B. Design Goals for a Research Arm

The principal activity of this work was to implement a research tool (arm) for determining the validity of the approach taken. The design goals were as follows:

a. examine the dynamic geometry requirements for motion/manipulator systems for a variety of tasks and task scale

b. determine both the static and dynamic relationship between the requirements for actuators, sensors, kinematics, structures and task and task scale

c. explore various task execution strategies and the associated environment-task related information needed and assess the impact which strategy/information have on arm performance requirements.

What was found was that the design effort for this research tool became the prime focus for all the other work. That is, arm design clearly identified the performance that could be obtained and this in turn sharpened the categorization of the gross and fine motion regions and caused an interface region to be defined that encompassed the combined uncertainties of the technology and the pieces to be assembled.

The following conclusions could therefore be drawn from this activity:

a. arm design requires a use context

b. context provides scale, speed, loads, accuracies - also strategies, information, (system organization?), and servo sensor loop closure

c. both design and use are not well understood disciplines

d. parallel development of each discipline stimulates both and identifies the real world constraints

e. developments at this level provide the lower order systems necessary for interacting with an environment and coupling it with eventual high order artificial intelligence planning systems

f. it would appear that the existence of technologically real lower order systems would aid and stimulate the development of effective and realistic higher order planning systems just as consideration of task contexts stimulates the development of lower order systems.

C. Report Organization

In six major sections this report discusses a survey of existing arms (Section II), basic trade offs and considerations in arm design (Section III), the technical aspects of design and design tools for a scientific approach to arm design (Section IV), discussion of the Draper Lab. Arm Design which has been nick named POPEYE (Section V), details of POPEYE's specification (Section VI), and SectionVII POPEYE's subsystems.

A wooden mockup of POPEYE shown in its actual mounting is illustrated by Figure I-2.

II. SURVEY OF EXISTING ARMS

A. Purpose of Survey

The ultimate goal of this research was to gain knowledge applicable to the design and use of very small robot arms for miniature assembly tasks. It was decided that a larger size would be more appropriate as a start to bring out the generic problems, since very small arms pose some special design difficulties as well as general ones.

A survey of existing robot arms was undertaken to see what could be learned. We were interested in how such general problems as servo control, kinematic configuration, actuator type, transmissions and angle readouts were attacked. We also needed to know if any existing robot could be utilized to test assembly strategies. This would be useful for parallel work going on* as well as showing how the problems of implementing such strategies influenced arm design. The survey therefore concentrated on accuracy, payload and speed characteristics suitable for man-sized tasks. (No commercial industrial mini-robots were available at the time the survey was conducted.)

B. Criteria for an Arm

The criteria used for the design of an arm are given elsewhere in this report (e.g., see Sections III & VI). It suffices to say here that the static characteristics (size, reach, stiffness, load capacity, etc.) of an arm are determined by the nature of the assembly task (size, weight, etc.) and the dynamic characteristics are determined by how fast the assembly is to be accomplished. Also, it was assumed at the outset that the six degrees of freedom needed for assembly could not be divided up between an arm and

* NSF Grant GI 39432X and GI 43787

a pallet orienter. The requirement that the arm retain all six degrees of freedom would make it simpler to couple into an existing assembly line. Extra degrees of freedom in a pallet orienter are not ruled out, of course.

C. Sources of Information

The information for this survey came from three sources:

1. "Industrial Robots - A Survey", published by International Fluidics Services Ltd., 1972
2. "The Robots Are Here", Assembly Engineering, Vol. 15/No.4, April 1972
3. Information direct from the robot manufacturer in the form of brochures, drawings, and specificiations.

Source number 1 was originally a Swedish report but was updated and enlarged by Dr. Brian Rook of the University of Birmingham. This survey is especially useful for information concerning the many robots being built in Japan. Sources 2 and 3 were used to gather information on the robots built in this country.

D. Survey Results

Some of the data sheets for the robots that looked interesting are included in Appendix 1 of this report. An interesting robot is one that satisfies any one or more of the requirements of load capacity ($\geq$ 10 kgm), accuracy ($<$ 1 mm), or number of degrees of freedom ($\geq$ 6). The list shown in the appendix is not intended to be exhaustive. On the contrary, there are many more robots, especially from Japan, with similar characteristics. To get a more exhaustive survey the references cited above should be consulted.

From an examination of the available data on industrial robots one can make the following observations.

1. Arm and Wrist Motions

With few exceptions industrial robots accomplish the three translational degrees of freedom necessary for arm motion using either cylindrical (r, θ, z) or spherical (r, ω, θ) coordinates. Typical examples of these are shown in Figure II-1. Also shown in these figures is the general outline of the work volumes. These motion geometries optimize the quantity of work volume for a given base size. Furthermore, these work volumes are optimized for the work volumes normally used by humans while working at machines currently found in industry. For example, the sequential task — (a) pick up piece from incoming conveyor line, (b) place piece in machine, (c) place piece on outgoing conveyor line — is a typical task well suited to the work volume geometries of these robots.

The wrist motions are limited to one and two degrees of freedom making the total number of degrees of freedom four or five. The exceptions to this are the UNIMATE MK. II, both series 2000 and 4000, and a few of the Japanese designs.

2. Control

Control for these industrial robots runs the range from energy absorbing mechanical stops coupled with simple relay sequential

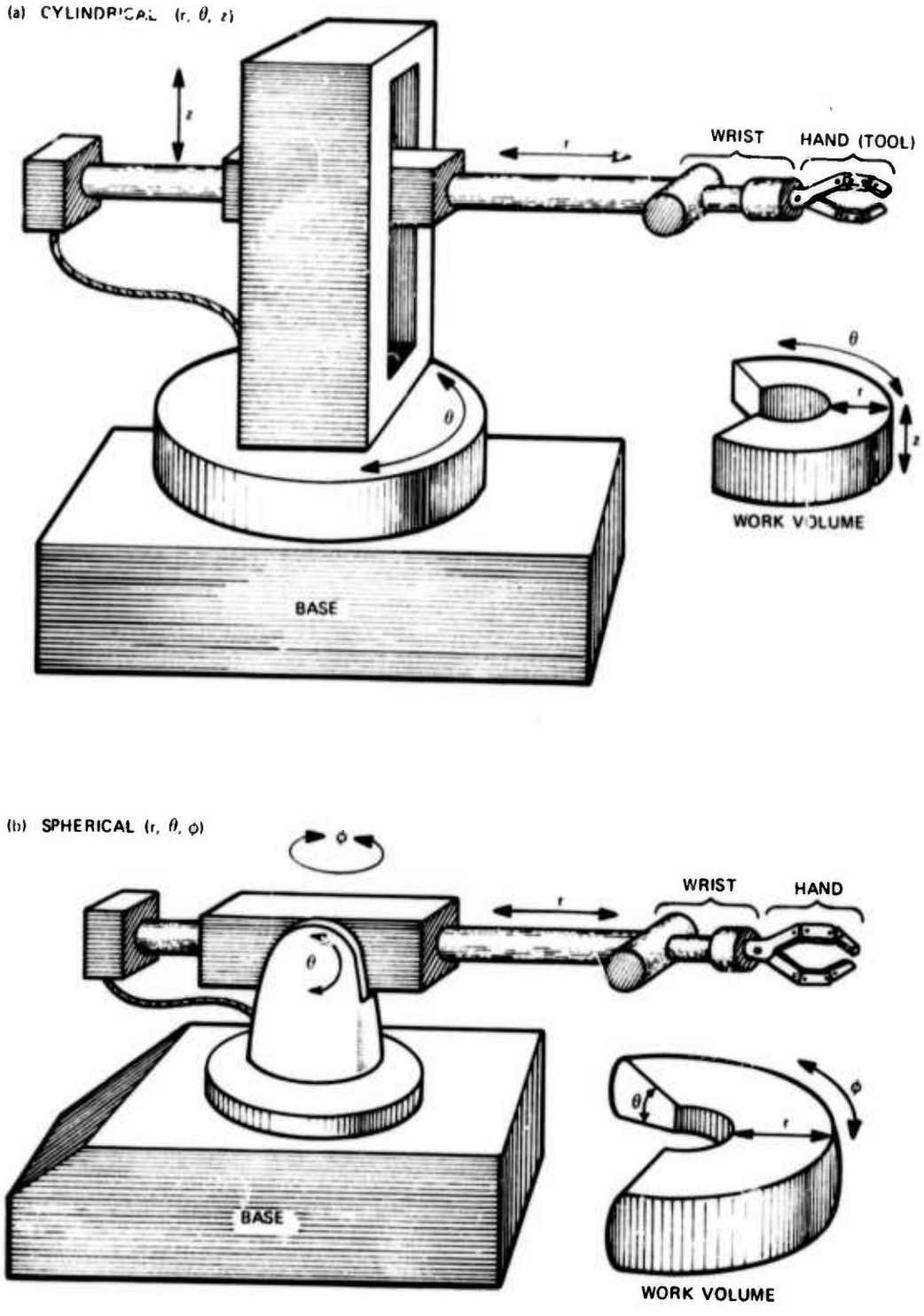

Figure II-1. Illustrating Robot Motion Geometries and Work Volume.

logic, to continuous path control employing position feedback, electronic memory (e.g., magnetic drum, tape, or wire) and logic circuits. Most controllers are the so-called point-to-point variety, where each degree of freedom is commanded to move in sequence. The effect of this is that the robot hand moves in a sequential series of straight lines or circles. The advantage of this type of control is that it is conservative of memory locations, potentiometers, etc.

In one of the more sophisticated control systems the robot is "taught" by leading it through the desired task pattern while recording the desired positions in memory. Three classes of position entries can be recorded; low accuracy, intermediate accuracy, and high accuracy. The first two are used at intermediate points in the task pattern so that the servos do not have to slow or stop when passing through these points. The high accuracy entry of course brings the arm to a stop and positions it to its rated accuracy. A schematic of this system is shown in Figure II-2. The hand held teach controller allows the task programmer to get close to the task stations so that he can make more accurate entries.

3. Power Actuators

Most available industrial robots employ either hydraulic or pneumatic actuators. Most of these are in the form of pistons which are directly connected or coupled through rack and pinion gears and/or sprocket chains. A few, such as the Sundstrand and the experimental "Scheinman Arm" use electric motors and gearing.

4. Hands (End Effectors, Grippers)

A study of the hands used with the various robots is also a study of the various tasks that these robots have been put to. Each robot comes with one or two "standard" hands usually in the form of two finger, parallel grippers. However, many of the tasks have special attributes about them (Geometry, fragileness, surface texture, etc.) that require special tooling at the hand. Because of this, most arms come with mechanical interfaces at the wrist that allow for quick removal and replacement of hands. Source 1 above has an excellent review of some

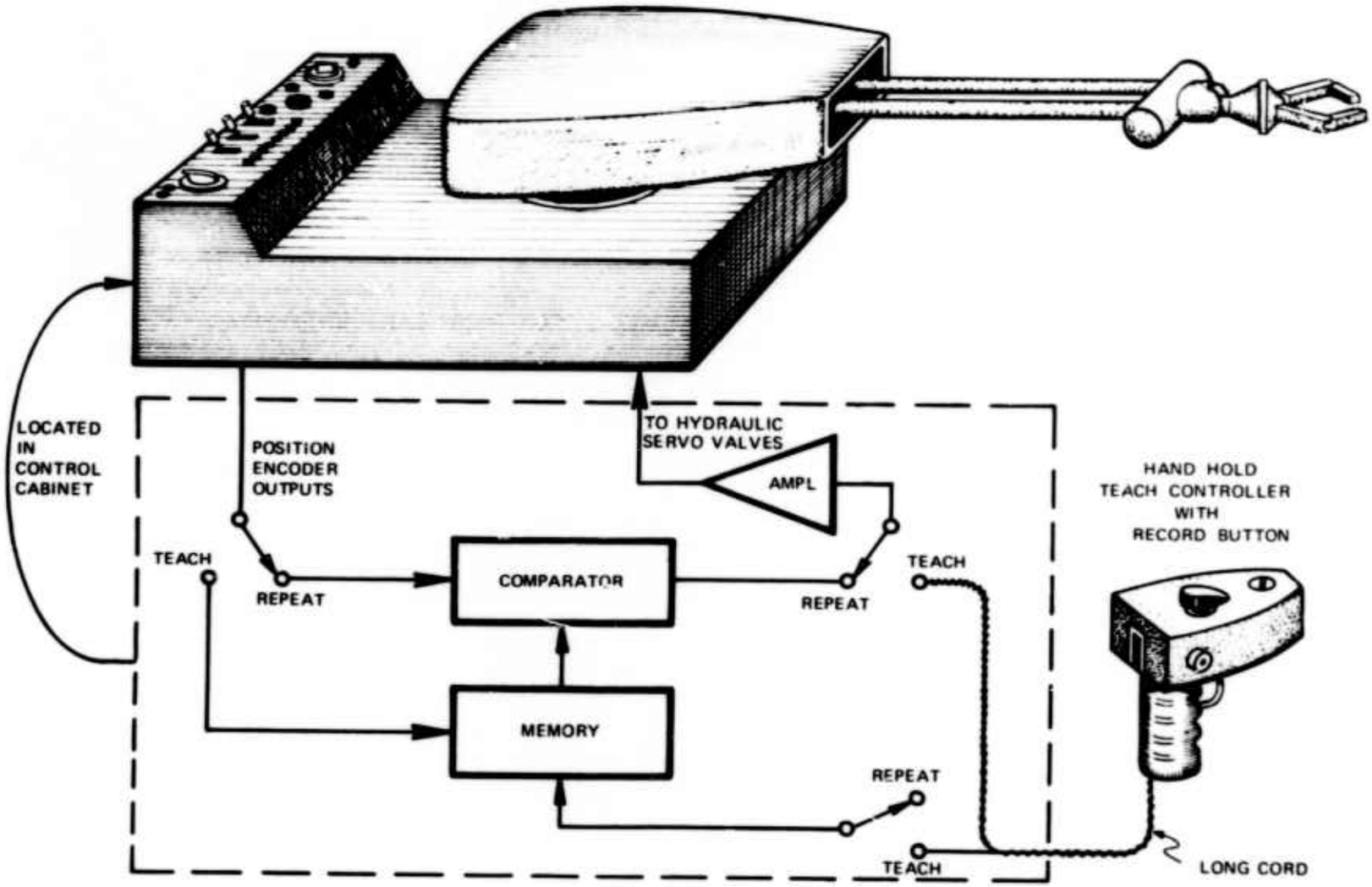

Figure II-2. Unimate Industrial Robot

of the hand designs that have been employed (see pages 8-10 of Source 1).

5. Areas of Application

Since the passage of the Occupational Safety and Health Act of 1970 (OSHA) many tasks previously done by humans are now being automated. As OSHA standards extend to cover other tasks more opportunities will offer themselves for automatic equipment. Many of these tasks fall within the domain of capability of the industrial robot. This is especially true for tasks that are monotonous or involve dangerous environments. Examples are: conveyor line feeding, unloading die casting machines; servicing machines such as machine tools, presses, stakers, punches, riveters. These tasks are easily handled by point-to-point or continuous-path controlled robots. Tasks such as spray painting and spot welding require robots with continuous-path controls.

E. Robot Assemblers

Very little has been accomplished in the area of assembly using presently available industrial robots. Exceptions to this observation are notable in the following areas.

1. Using a specialized tool in the place of the robot hand, two parts are fastened together. Examples are: screw machines, nut runners, pop riveters, and spot welders.

2. Using fixtures and gravitational force, two or three parts are stacked, then loaded or held in a fastening machine such as a staking or riveting machine.

3. A combination of 1 and 2.

These assembly techniques will get greater use as more subassemblies are deliberately designed or redesigned so as to take advantage of the assembly capabilities of present arms. Likewise as arm designers produce faster, stronger (greater pay load) and more

precise (greater positional accuracy) arms the range and variety of assembly tasks amenable to solution by the use of industrial robots will become very much greater.

Even greater numbers of applications will present themselves when the industrial robot is designed to take into consideration the special needs of the assembly process as well as the large scale mobility needs common to many pick and place applications. Reaching out, grabbing a part, and moving it to a new location often represent only the initial phases of an assembly task. For example, the control of small motions the direction of which is being determined by the interactive force between the two pieces being assembled (active accommodation)* might be the next phase required for successful assembly. The next phase may be to switch control modes such that the two pieces being assembled are allowed to guide themselves together along their mutually interacting surfaces (passive accommodation). It may be recognized that this example describes the task of putting a peg in a hole, one or both having chamfered ends.

The point being made in the previous paragraph is that the next generation industrial robot that is designed for the express purpose of assembly will have to have the attributes of an assembler as well as a pick and place robot. Greater accuracy, pay load range, dexterity, and speed will be required. The incorporation of accurate position and sensitive force feedback will also be needed. The Sections which follow discuss the major system and component design problems involved in creating high performance assembly robots. Only the general aspects suitable for all sizes of arms are discussed. No attention is given to the special problems which very small size presents.

* See Section III-D.

III. BASIC TRADEOFFS AND CONSIDERATIONS IN ARM DESIGN

A. Introduction

This section of the report discusses the issues which influence arm design, and describes (but does not solve) various technical problems and tradeoffs which must be considered. Section IV presents technical solutions in the form of tools applicable to the design of arms in a wide range of sizes. These matters are discussed in reference [1] as to their effect on assembler system architecture and for the insight they yield into the assembly problem in general. Here they are discussed to show how they impact the design of an arm and give rise to specific design approaches and design tools for specifying and evaluating assembler arms.

B. The Assembly Problem and Its Impact on Arm Design

Figure III-1 is an attempt to organize the processes and methods of assembly*. The process is described in two stages, parts presentation and assembly, the two separated by the point at which the part is interfaced firmly to that portion of the assembly device which carries the part to its final destination in the assembly and assembles it. According to this definition, everything else is parts presentation. The boundary between parts presentation and assembly occurs for manual assembly approximately at the point where the person grasps the part from the bin, conveyor or whatever, except in some cases where the person reorients the part in his hand or places the part in an assembly tool or fixture. For fixed automation, it would appear that the entire process is really part presentation. This is especially evident in bowl feeding of small parts, where the feeder removes uncertainty of the order of a meter and replaces it with uncertainty on the order of half a millimeter.

The entire assembly process appears, in fact, as a staged process of removal of uncertainty until positions and orientations are known with enough certainty so that assembly can occur. This does not necessarily mean that uncertainty is removed merely by navigation. This is clearly

* Many items on this figure are estimates.

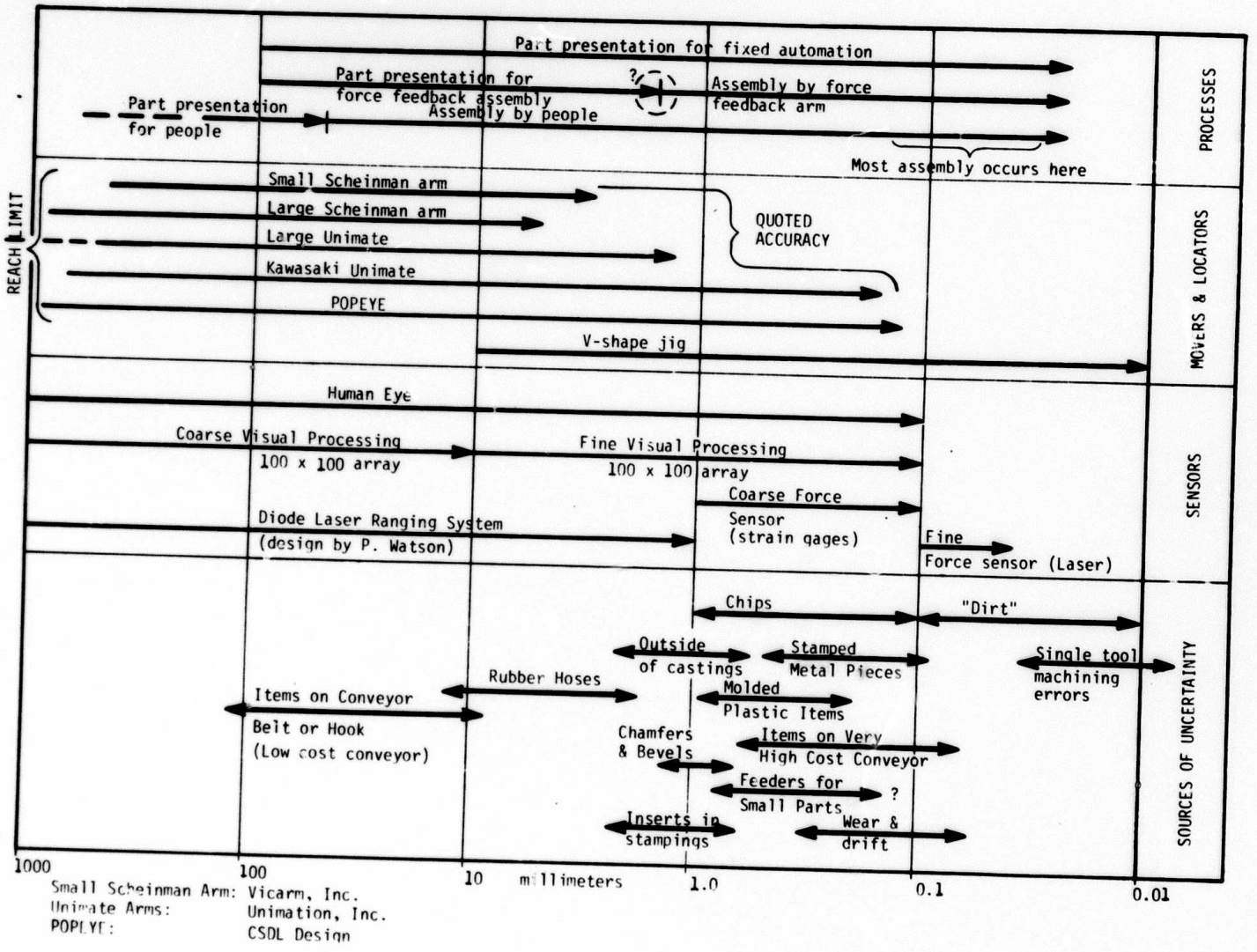

Small Scheinman Arm: Vicarm, Inc.
Unimate Arms: Unimation, Inc.
POPEYE: CSDL Design

Figure III-1

not true for manual assembly, because people cannot navigate objects open loop with sufficient accuracy. The ability of force feedback to reduce uncertainty by testing, taking data during attempts at assembly, is one of our research topics, and a major question is where the boundary between part presentation and assembly can be placed for the purposes of force feedback assembly. The farther to the left on Figure III-1 it can be put, the better, because this reduces constraints on part feeding mechanisms, although it puts added burdens on the strategy-making process of evaluating the force feedback data. It also removes much of the physical hardware used for uncertainty removal by fixed automation, freeing the assembler to be reprogrammed to do other tasks.

It would appear from our studies of a washing machine gearbox that its internal uncertainties are so small that once the parts are brought to final positions to within that uncertainty then assembly will occur. This is clearly the strategy inherent in fixed automation, and seems to be successful on carefully machined items like the gearbox, small engines, and so on. This method will not work on parts whose uncertainty is relatively large compared to the clearances through which the parts must be pushed or moved, because merely knowing where the parts are at some convenient reference points will not guarantee that the crucial mating sections will be in the correct relative positions.

Although this argument divides items assemblable by fixed automation from those which are not, it does not mean that gearbox-like items must be assembled by fixed automation. But if one can bring the parts of the gearbox to within 1 mm of certainty, then it may be relatively easy to bring them to within 0.1 mm and use a spring-loaded jig to remove the rest of the uncertainty. (0.02 mm is really necessary) Most fixed automation machines attempt the entire uncertainty reduction to the 0.02 mm level by rigid structures. Anything less rigid and precise may not stand up in industrial environments. Somewhat less precision might reduce design and setup costs of such machines, as well as maintenance and adjustments during operation.

Research sponsored by NSF is pursuing the above issues as they pertain to assembly system architecture. For our purposes here, these issues strongly influence arm design because they illustrate different scenarios by which assembly could be accomplished. Some combination of arms, feeders, sensors and control algorithms must be used to reduce uncertainty to the level where assembly can occur. In particular, the "uncertainty gap" between 1.0 mm and 0.1 mm contains most of the significant uncertainties in parts, feeders and arm.

Part uncertainties are determined mostly by their function: items like engines, shafts, gearboxes and so on, which transmit large amounts of mechanical power, are carefully machined to small clearances, small tolerances, good surface finish and small uncertainties in key internal dimensions within each part. Plastic parts usually have good surface finishes but may bulge or shrink after being molded. Stamped metal pieces may become bent in handling. These latter two types of part will function well in their bent or bulged condition if the deformation is not too large. But assembly will be hampered.

Feeder uncertainties are mostly a function of the degree of feeding accuracy needed by the assembly system. The cost of part feeding rises rapidly as part size increases and as more uncertainty removal is demanded of the feeder.

Arm uncertainties are governed by technological limitations on structure, sensors, control algorithms, design techniques, physical size of the arm, and the amount of money available. There is a tradeoff between arm size and feeder size, both governed by part size. Minimal investment in feeders will require large arms merely to reach for the parts. A strong arm capable of rapidly moving heavy parts (10 Kg) will be large simply to support itself and its actuators. Large investment in feeders will increase the degree of fixed automation associated with what is supposed to be flexible automation. Furthermore, automatic assembly of large numbers of small parts of low uncertainty is common practice. Thus, a major research problem is how to design an arm to transport

large items of medium uncertainty from medium uncertainty feeders to receiving parts of similar uncertainty and successfully assemble them. It is clear that multiple sensor systems integrated into the servo and strategy control systems of the arm will be needed to bridge the uncertainty gaps. This in turn requires the following kinds of tools for a scientific approach to arm design:

- kinematic synthesis to generate candidate arm configurations
- methods of obtaining geometric and dynamic equations of motion for use in speed, mass and actuator studies
- servo control techniques for obtaining fast, smooth motion and utilization of sensor data in a tight closed loop
- structural analysis methods for studying low weight high speed designs and their vibration modes
- error analysis techniques for predicting arm uncertainties from component inaccuracies

C. Major Design - Control Issues

Four main questions thus dominate design of a mechanical arm:

What is the arm going to do?

How shall it be built?

How shall it be controlled?

How shall it utilize sensory data?

The first concerns task specifications like reach, speed, and payload. The second concerns structure and actuators. The third involves both simple stabilization, vibration supression, and general strategy of operation for high efficiency and accuracy with low over-shoot and power consumption. The fourth concerns feedback sensors in the hand, joints and elsewhere.

A comparison of current industrial robots and the people they augment or replace yields some insights. A typical step in the manual assembly of a washing machine gearcase reads "Obtain pinion and assemble to gearcase." That is, fetch some object and do something with it. More concretely, a gross motion (much larger than the pinion itself) followed by some fine motions (usually much smaller than the pinion or whatever). Most industrial robots are incapable of fine motions because they were designed for gross motions and because fine motions require sensory feedback from the task of a kind which no current industrial robots have access to.

An important measure for both human and robot arms is the ratio of gross motion time to fine motion time. A high ratio may indicate wasted time in mere parts feeding activities which crowds the time needed for the careful work of assembly. But, for people, the gross motion time is fairly consistently lower-bounded for a given task. Overall task time is usually shortened by strategies which group many gross motions, such as carrying several little parts simultaneously, and take advantage of the human hand's dexterity. One can hope to build a robot arm strong enough to exceed a human's gross motion speed. Some of the problems of doing so are discussed below.

Exceeding a human's fine motion speed, which includes measurement and strategy - invocation time along with mere speed of motion, is much more difficult. The human equipment actually consists of two devices, an arm of 5 degrees of freedom which positions the hand and wrist, plus the hand, a fine motion device with several dozen degrees of freedom and many sensors. One can gain some design freedom in a robot fine motion

device by separating it from the gross motion device but this still leaves the robot at a disadvantage. Current technology and understanding of the problem indicate that

1. robot gross motion must be very fast to gain time for fine motion to occur, or else strategies like multipart handling must be adopted
2. robot fine motion must be specialized and carefully designed with limited degrees of freedom and other simplifications
3. contradictions could arise in attempting to build an arm which simultaneously is intended to perform both gross and fine motions economically, especially if the arm is physically large

A relation between structure and servo occurs in design of industrial arms where unwanted interactions between servo and structural natural frequencies could occur or an attempt to avoid these interactions could result in a structurally overdesigned arm. Some examples below discuss these points.

Questions Related to Gross Motion Patterns

1. how large is the arm to be and what kinematic articulations should it have
2. how fast should it be able to make a gross motion of some meaningful size
3. what range of inertial and gravitational loads must it be able to carry at the above speeds.

Remarks: It is generally true that the more specialized or dedicated an arm is, the fewer degrees of freedom it needs, the minimum being one. Programmable robots presumably must be capable of a variety of tasks, especially if an economical number of them is to be manufactured. Beyond this, choice of task for design purposes is difficult. The major variables seem to be payload weight and distance to be moved. For assembly of a small gasoline engine the distances are all small but a factor of 100 or more separates the weight of the lightest and heaviest parts. For an auto instrument panel distances are large but all the parts are in a small size and weight range. Large and heavy parts pose the biggest challenge, especially because conventional fixed automation machinery cannot handle them.

For tasks of a given class, a kinematic analysis can be performed to minimize the size of a given linkage that will reach a specified set of endpoints. It is necessary that the arm not be fully outstretched at such points so that fine motions can occur. See Section IV B.

The time quoted in item 2 must include time for the arm to settle down on the target point. Settling oscillations and overshoot can result from the structure or the servo. Settling time can be approximately related to servo bandwidth (for a rigid arm). For example, if stop to stop motion time is to be one second and settling time is budgeted 10% of that time, then for an effective damping ratio of 0.5, the servo with arm and load must be flat to about 13 hz, a very difficult goal to meet with a large arm. Backlash, if present, can be mitigated by moving the arm very slowly at the end of a gross motion. This strategy makes efforts toward high servo bandwidth somewhat superfluous.

Items 1, 2, and 3 determine to a large degree the actuator torque requirements and the servo bandwidth needed to throw around the arm and load. The capabilities of the actuators need to be balanced (see Section IV A) so that no joint is over or under designed with respect to the others. A number of industrial robots seem to have weak wrists in relation to their elbows and shoulders.

Actuator Type and Location

4. for the torque requirements from above, what type of actuator should be used
5. what sort of transmission should couple the actuators to the arm
6. how much accuracy should the arm have
7. how much resolution should it have

Remarks: Families of actuators can empirically be described rather accurately, relating their peak torque or rotor inertia to their total weight. For a family of DC torque motors all operating at the same supply voltage, relation is

$$\text{mass in kg} = 2.1 \times (\text{torque in nt-m})^{0.875}$$

while for a family of hydraulic rotaryvane actuators, all operating at the same supply pressure, the relation is

$$\text{kg} = 0.235 \times (\text{torque})^{0.55}$$

Comparison of these relations indicates that for these torque motors to compete on a torque to mass basis with these vane actuators, gears of ratio at least 10 or 15 to one will be necessary. Even with vane actuators, the weight of a hydraulically driven arm is mostly actuator weight. One can locate the actuators in the arm's base and transmit power through shafts, cables, tapes or chains, which will save weight but introduce compliance. Gears contribute both compliance and backlash, which decreases accuracy, resolution and servo stability. Hydraulic actuators directly coupled to the joints develop high torque but compliance appears in the fluid, an effect which can be reduced by careful design of the control system. Large hydraulically driven arms with fast gross motion requirements will need large servo valves which in turn have low enough bandwidth to affect settling tim and the speed of fine motions.

Thus, the issue of actuators, their type and location on the arm is a complex one affecting all aspects of design and control. It is not clear

whether there is one clear cut solution suitable for all situations. Technical aspects of this are discussed in Section IV-A. Note that although miniature hydraulic actuators are not commercially available, there does not seem to be any reason in principle why they should not be applicable to mini-robots. Whether they are the right choice is an open question.

Fine Motion Patterns

8. how small must the fine motions be
9. how rapidly must they be performed
10. what and how many arm degrees of freedom must be involved

Remarks: Resolution of the joint sensors, size of the arm, backlash in gears and friction in the actuators or joints all can limit the fineness. If a rotary actuator far from the hand must contribute to the fine motion, then the radius from the joint to the hand times the joint sensor resolution indicates but does not absolutely limit the fineness. (Some types of actuators can be jogged open loop with predictable results.)

The rapidity of fine motions is an issue for industrial arms equipped with touch or force feedback. References 2 and 3 describe a force vector measuring system, located in the wrist, capable of resolving three components of force and three of torque about a chosen point. Such a system can be used to assemble objects in much the same way people do, by making some small deliberate collisions occur and judging from the direction of the resulting contact force how to move next. To avoid large contact forces, the appropriate change in the arm's trajectory must be made quickly. A way of accomplishing this is to interpret the force vector as a servo command. However, contact forces build to large values quickly if arm inertia is large and the objects and their supports, including the arm itself, are stiff. Technical aspects of this are discussed in Section III-D and IV-D.

Any type of low pass cutoff will make rapid fine motions difficult. For hydraulics the crucial items are the servo valve and the compliance represented by the fluid within the actuator. Sizing the arm and valves for rapid gross motions and heavy loads will yield large slow valves and large fluid compliances, inconsistent with rapid fine motions.

Computation time lags and filtering time associated some types of high accuracy joint sensors also add to this problem.

Structural Members

11. for the given kinematic configuration, how strong or thick should the structural members be

12. should the members be sized for static stiffness (an issue related to accuracy in a gravity environment) or dynamic stiffness in conjunction with the arm's masses (related to structural vibration and its interaction with the servos)

Remarks: The links must not only support their own weight and that of the actuators and payload, but should not create, in concert with these masses, structural natural frequencies close to those of the servo because this will make gross and fine motions difficult to accomplish quickly and could prevent using the servo to damp out structural vibrations. These issues are discussed in some detail in Section IV C.

Design Evaluation

Some competing criteria are:

13. how closely does the arm meet the speed, reach, strength and accuracy requirements originally posed

14. how efficiently, in terms of arm weight and power consumption, are these requirements met

Remarks: For industrial arms, the idea of load factor efficiency criterion for item 14 makes sense, where load factor means the ratio of dynamic payload, (usually less than mere lifting capacity since an economic time to move the payload is usually enforced) to the weight of the movable parts of the arm itself. Experience indicates that a load factor of 5% to

10% may be typical and that 20% would be quite an improvement. Substitution of control techniques for structural weight as a vibration supression method could allow increases in load factor.

An allied efficiency criterion is energy consumption. Typical large industrial manipulators use 10 to 30 horsepower. It seems reasonable to compare this to a "payload power" such as (payload) x (reach)/(slew time).

D. Accommodation as a Possible Servo-Sensor Control Stragegy

Accommodation is a basic servo-sensor strategy for making an arm modify its fine motions. Detailed explanations are contained in references (1) and (2). The basic idea is that the arm or a device on the end of the arm or work surface will move slightly in response to forces exerted on it as manipulative actions occur. We may distinguish two basic types of accommodation: passive and active. Passive accommodation is accomplished by mounting the work in a spring-loaded slide or other base. Active accommodation is accomplished by putting a force sensor on the arm or work surface and involving this sensor initimately in the servo control loops of the arm. Both kinds of accommodation are intended to allow small errors of placement or gripping of parts, or small errors in positioning the arm, without the intended actions of the arm being impaired or halted.

Passive accommodation seems best suited to very small errors and when "getting out of the way" is the appropriate strategy for assembling two items. For this to be successful, the force levels needed to push the arm or part into position must not damage the part. The forces can be taken up by guides on the base which holds the parts. This will involve a lot of guides plus the necessity of accurately jigging the part to the base and guide. The forces involved may not be too high if there is some backlash in the arm, but backlash involves problems of its own.

Active accommodation is a more general solution to the error problem because other strategies besides getting out of the way can be used. The extra jigs and guides are eliminated, and less accurate initial

jigging can be tolerated. Larger errors can be tolerated without excessive force buildup because the force sensor informs the servo how to move the arm to reduce the forces. Reference (1) shows how active accommodation can accomplish tasks such as edge following, putting pegs in holes, placing holes over studs, packing items into corners, and so on.

Active accommodation acts by generating velocity commands which are superimposed on the gross motion commands. This will cause the arm to keep moving until all forces exactly reach their desired levels, which can be controlled by the gross motion commands. The dynamic characteristics of the arm's response are determined by the magnitude of velocity command generated per unit of force sensed. These forces are, of course, generated by the arm's motion, so the force feedback loop comprises an extra element in the arm's servo and must be designed with care. This will be discussed in some detail in the next section. Briefly, the issues are these:

- servo stability when the arm is in contact with an object is radically different than when it is not in contact -- the servo must be designed accordingly
- the physical stiffness of the coupling between the arm and its environment influences stability -- a compliant coupling is the most benign -- since force sensors generally are instrumented compliant systems, the physical stiffness of the sensor affects not only its sensitivity but also the dynamic behavior of the arm
- the arm must respond rapidly to force-generated commands, so that any phase lags, caused by servos or computation, must be kept small

- this rapid, continuous response should be distinguished from binary or threshold force tests, which may also be made by an accommodation loop -- binary tests usually involve stop and go motions of the arm, which are inherently slow but require less of the servo
- backlash which occurs between the actuator and the load may be tolerable if good force sensor readings are available -- a lot depends on how much friction there is in the arm and how the servo is designed.

Ref (4) discusses freeing some of an arm's joints as a technique for achieving a kind of accommodation. This is suitable for direct electric drives where true "freeing" can be obtained, but poses problems of friction in gear drives and the need for extra valving to free hydraulic drives. More basic, one cannot "free" an arbitrary axis relevant to a task, but rather one must free a joint of the arm. This lack of generality severely limits the usefulness of this strategy, since often no suitably oriented arm axis exists. Active accommodation overcomes this by finding the right combination of axes to move slightly. The desired effect of freeing occurs but no axis is actually free.

E. Summary

This section posed the assembly problem as one of uncertainty reduction, and qualitatively discussed the factors influencing assembly arms. The next section will go into technical detail on these points and demonstrate the design tools needed to specify an arm which will perform assembly at a given level of accuracy, speed, strength and reliability.

IV. TECHNICAL ASPECTS OF DESIGN METHODS: TOOLS FOR A SCIENTIFIC APPROACH TO ARM DESIGN

This section goes into detail on the technical aspects of arm design and illustrates the use of a number of analytical and computer simulation tools to aid this process, drawing on the results of several parallel research projects.

A. Gross Motion Size, Payload and Speed*

1. Task Influences

The task or range of tasks determine the demands placed on an arm. Its size is determined by the size of objects on which it works and by how far it must reach for parts. The size of the work area it must cover may be influenced by how many such objects it must work on simultaneously, with two to four being a good possibility because of the time saved in tool changing.

Size strongly influences actuator requirements since, for a given mass and angular acceleration, the required torque depends on arm length squared. The weight of parts to be carried plus the live weight of the arm determine the mass which the actuators must accelerate and support against gravity. If the actuators are at the joints (the low compliance design choice) then the weight of the arm may be largely actuator weight. Thus, there is great pressure for actuators which, though light in weight, deliver a lot of torque. The actuation problem is discussed below.

The required accelerations depend on the size of the motions and the speed with which they must be accomplished. Station times on manual assembly lines range from 15 seconds to one minute and usually consist of several tasks. Most of the time on many automobile assembly stations is taken up by gross motions in the form of carrying parts to the assembly point. On appliance lines, a station time of 15 seconds may include three or four small tasks where the person reaches no more than about 20 inches (51 cm) to obtain parts which weigh less than three pounds (1.4 kg). The

* Portions of this part were supported by NSF Grant No. GI-39432X.

heaviest parts weigh over 20 pounds (9 kg) and their size dictates moving them several feet.

These requirements combine to make a difficult design problem, even to produce a high performance gross motion device. It is debatable whether this device should also be capable of fine motions. The issues are these: General gross motion devices and fine motions devices both need six degrees of freedom, the difference being the size of motions. A fine motion device will not be as massive as a gross motion device which supports the same payload since it probably will not have to support its actuators. These actuators will be designed for limited motion range and hence can be lighter for the same torque output. Much less torque is required to produce small angular motions than large ones of the same angular acceleration. Motion sensors can be located closer to the work in a fine motion device (see Error Analysis below), allowing more accurate motions. Some of these advantages of a separate fine motion device are offset by the need then for two motion devices. Furthermore, the gross motion device will have most of the attributes needed for fine motion, including low friction and backlash as well as accurate angle sensors. These are needed so that the arm can position the part properly and participate in the motions even if the fine motions are performed by another device.

2. Technology Influences

a. Introduction

Available technology places limits on the ability of a piece of real hardware to perform certain tasks. Obvious limitations include the fact that the actuators required to move the manipulator are limited in their ability to exert force or torque, thereby limiting the loads and accelerations that can be handled. Other factors, such as friction, quality of workmanship, and number of bits of position sensing will influence the accuracy, repeatability and resolution of the resulting equipment. These qualities determine the fineness of work that the arm is capable of doing as well as influencing the quality of the resulting servo control system.

In practice we must design by choosing between alternatives, each with its own set of technological limitations. For example, in the following discussion it will be shown that hydraulic actuators possess a different set of technological limitations than electric actuators. To make an intelligent decision, we must understand the consequences of the sets of limitations of the technological alternatives.

b. Influences of Choice of Actuators

Once an arm configuration has been chosen the requirements for actuators for moving the manipulator arm can begin to be specified. First, it is necessary to specify the torque requirements for each of the actuators. This torque requirement is influenced by each of the following:

- Arm mass and dimension
- Actuator masses and location
- Desired gross motion trajectory (task)
- Payload mass
- Required gross motion task completion time

The desired gross motion trajectory, or task, and the required task completion time establish the accelerations necessary for completion. These required accelerations plus the net inertia of the manipulator, actuators, and payload determine the torque required of the actuators. The less the alloted task completion time, the greater the required accelerations and so the greater the required torques. It is also clear that the greater the moment of inertia of the mass distribution of the arm, the greater the torques required for the same trajectory.

Besides inertial loading, there is gravitational loading. This is a function of the gross motion trajectory that the arm must execute since each point in the trajectory path has a corresponding set of gravitational moments generated on the actuators. Consequently, gravitational loading is not a function of the speed with which the arm executes the trajectory. The total loading on the actuators at each point of the trajectory is the sum of the inertial and gravitational loadings.

It should be pointed out here that the torques spoken of are only what is ideally required to execute the task in open loop fashion. No control system is assumed. A realistic actuator control system may overlay the ideal torque history with its own dynamic effects, but these perturbations should be small if the control system is properly designed.

The effects of task time and payload can be displayed in a performance curve such as Figure IV-1 taken from reference 2. Specified task time is shown as the abscissa and payload is the ordinate. The curves represent lines of constant peak torque for a specified trajectory for each actuator of a given arm design. (Specific details of the arm and task will be given later.)

The curves represent a boundary on the performance of the arm. Points below the net curve represent task time and payload that are possible for the arm to execute. Points above the curve represent points beyond the ability of the actuators of the arm.

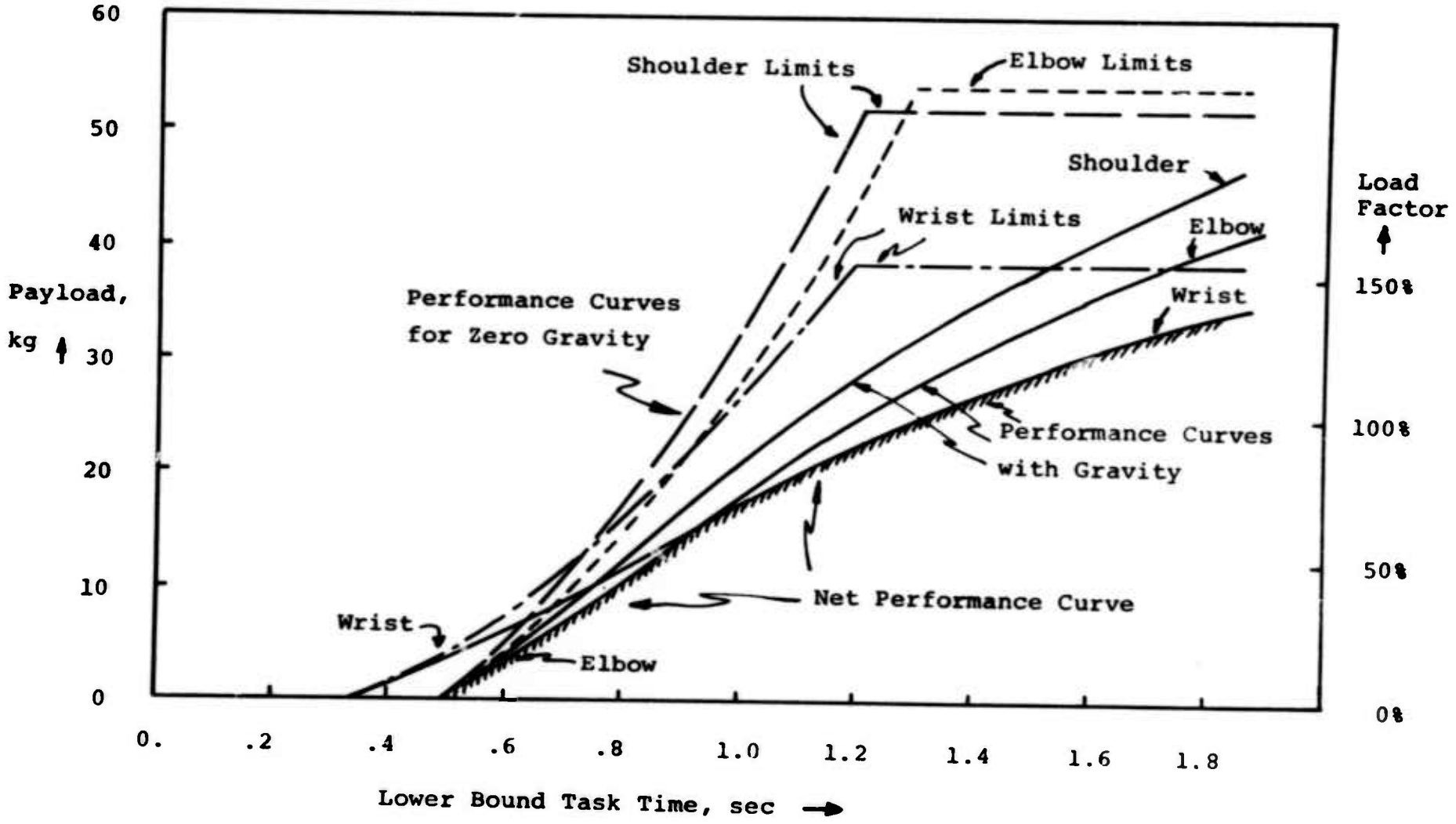

Figure IV-1

Performance Curves for Manipulator Design for the Downsweep Task

Notice that as task time increases, the curves become more horizontal as the influence of inertial loading diminishes and the gravitational loading, independent of speed, predominates. For shorter task times, the inertial loading effect becomes greater until the entire torque capacity of an actuator is necessary to move the arm and actuator mass without payload. This represents the lower theoretical limit on task time for the manipulator.

The performance curve of Figure IV-1 was generated with the aid of a computer simulation program. The program simulates the dynamics of a three joint, three link arm operating in a plane. It can be used to simulate the approximate dynamics of a six degree of freedom manipulator for tasks in which all joints and links remain the the same plane.

The assumptions used for generating the performance curve of Figure IV-1 were that the manipulator have dimensions and mass distribution equivalent to that described in later sections of this report executing a 90° shoulder sweep from straight out horizontal to straight down vertical. Figure IV-2 shows the simulated manipulator in various stages of this trajectory. Also indicated are the masses of the joints and links. Figure IV-3 shows the joint torque histories for the trajectory shown in Figure IV-2. Notice that prior to the start of the trajectory at $t = 0$ each actuator is exerting torque equivalent to the gravitational loading of the starting configuration.

A performance curve exists for each actuator. The net performance curve consists of the segments of the individual performance curves that are limiting over their particular ranges of task time. For example, in Figure IV-1 it is seen that for task times greater than one second the wrist actuator is limiting, but for task times from .6 to 1.0 seconds the elbow actuator is limiting, while for task times for .5 to .6 seconds the shoulder and elbow actuators are almost equally limiting. This is the result of an attempt to obtain a balanced manipulator design in which no one actuator limits performance over the entire range of task times. Had the manipulator actuators been designed to have equal payload

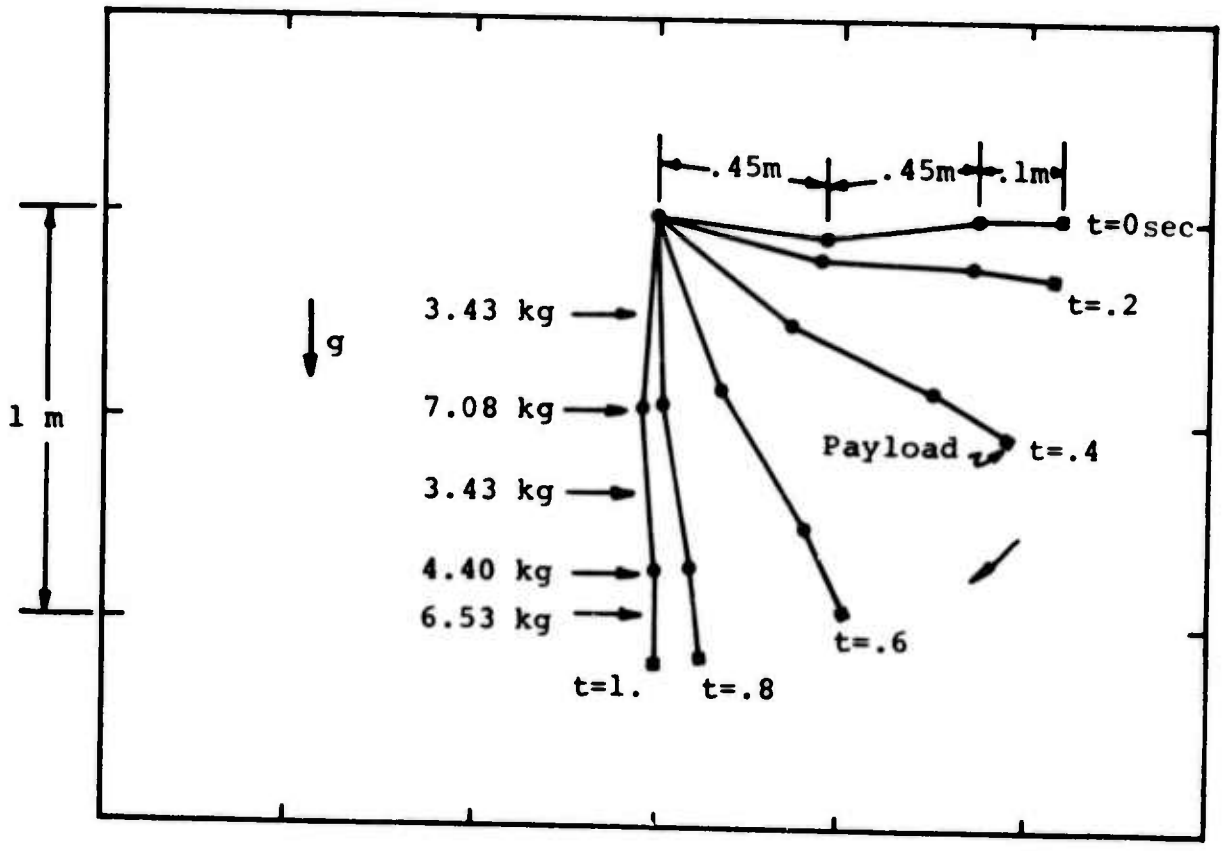

Figure IV-2 Typical Downsweep Task Trajectory

Masses at joints are actuators and associated hardware.

Masses between joints are links.

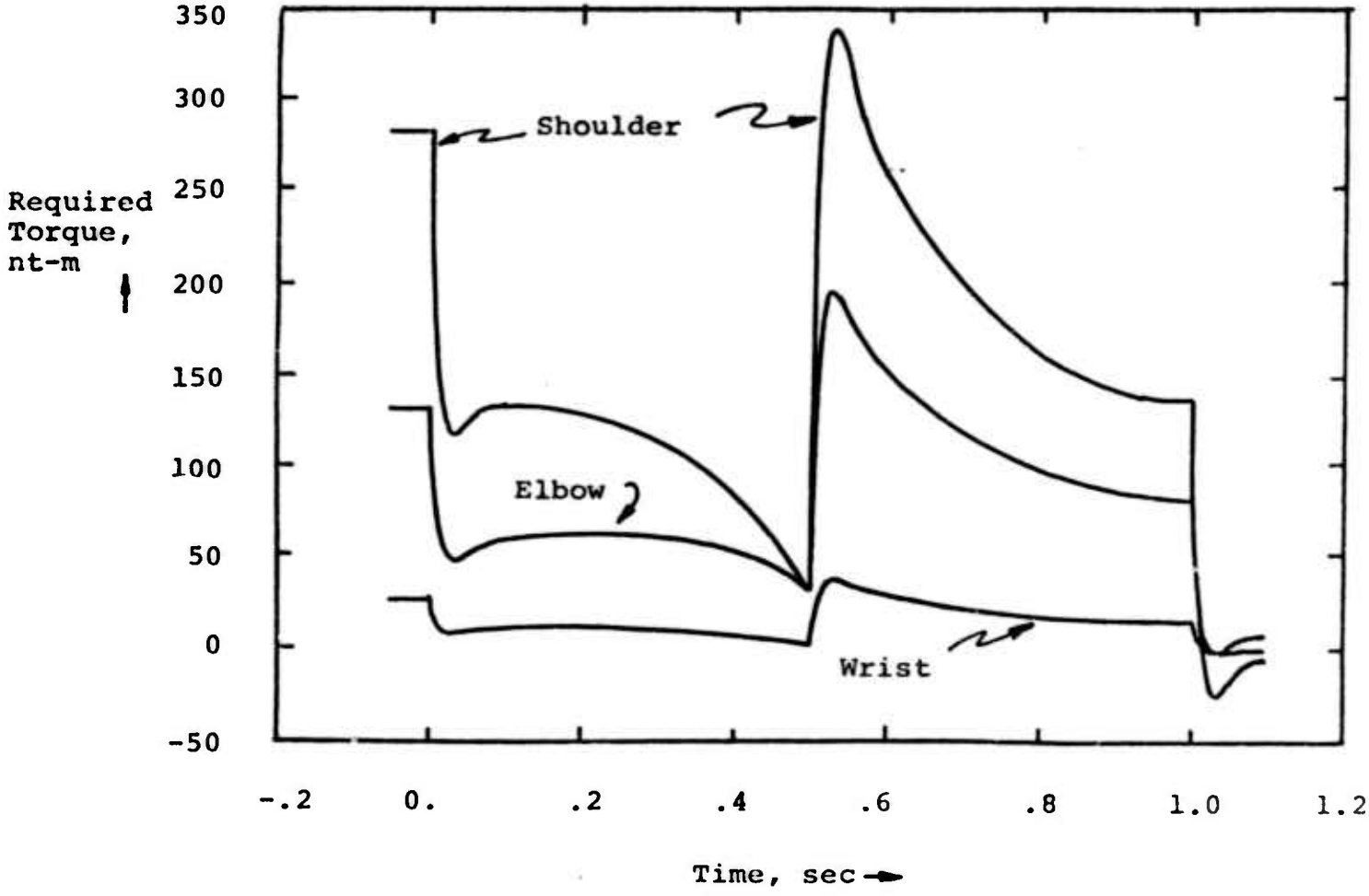

Figure IV-3 Typical Torque History for Downsweep Task Trajectory

capacities at long task times — for essentially pure gravitation loading — then the payload capacities for short task times would have been widely distributed with certain actuators very overdesigned and others under designed. For this particular manipulator design the shoulder would have been much too weak and the wrist much too strong for the shorter task times. An informal survey of commercial manipulators indicates that many have weak wrists, for reasons to be discussed below.

Obviously two important components of the total inertial loading are the actuator masses themselves and the payload. The more massive the outboard actuators are, the more torque is required from the inboard actuators to move them. However, more torque required from an actuator generally means a more massive actuator.

Figure IV-4 shows maximum torque vs. mass for families of hydraulic and electric actuators. It can be seen that torque increases faster than mass for these families of actuators. Hence, it should always be possible to find a set of actuators with sufficient torque to move a certain payload over a trajectory in specified time by choosing sufficiently large actuators, up to reasonable limits. However, the less mass required of a given actuator, the less the torque requirements for the actuators inboard of it and so the less massive they need to be also. Consequently, it is important to choose actuators with as high a torque density as possible, especially for the outboard (elbow and wrist) actuators. Figure IV-4 shows that for a wide variety of hydraulic and electric actuators, the hydraulic ones are about an order of magnitude better in torque density than the electric ones. This means that arms designed for hydraulic actuators will not only have less mass but also will require less torque to move the arm and payload.

c. Gearing on Electric Actuators

The low torque density of electric actuators can be increased by adding appropriate gearing. However, the gearing presents several problems from the control point of view.

- Increased weight of the gears

Figure IV-4: Maximum Torque vs. Mass for Several Hydraulic Actuator and DC Torque Motor Families

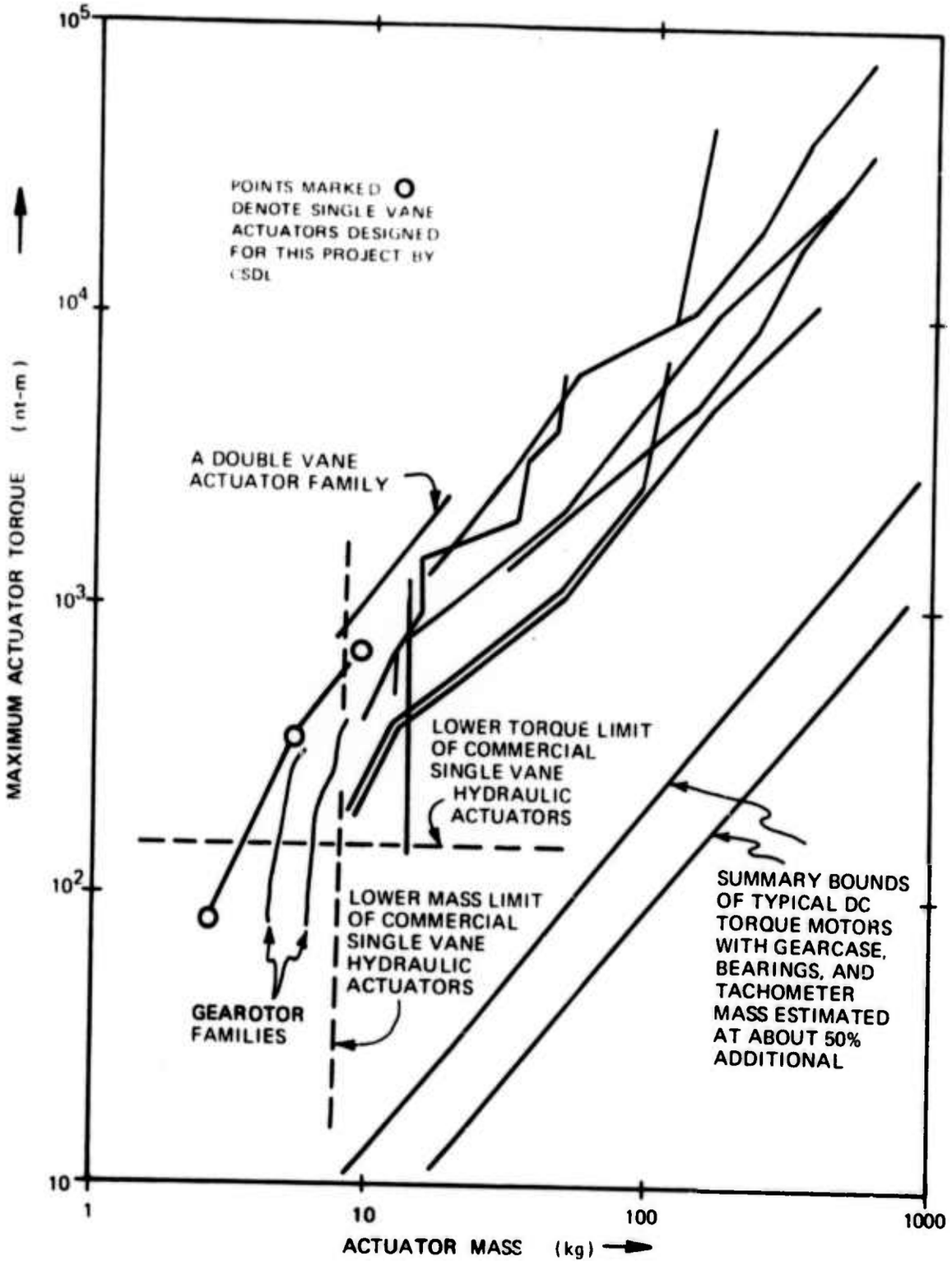

- Backlash between actuator and load
- Additional compliance in drive train as the meshing teeth deflect under load
- Increased apparent inertia of the actuator

These problems degrade the ability of the actuators to perform fine motion servoing — a serious drawback for an assembly machine.

Designers of commercial arms often solve the problem of heavy outboard actuators by utilizing small ones or little if any gears. This saves load on the inboard actuators but results in a weak wrist.

d. Influences on Accuracy, Repeatability, and Resolution

A discussion of the influences of technology on accuracy, repeatability and resolution of a manipulator requires good operational definitions from which to work.

Accuracy is an error measure representing the ability of the manipulator to achieve an arbitrarily selected position in space. The operational definition is as follows:

(1) Choose an a priori endpoint position in space in shoulder coordinates.

(2) Compute the corresponding set of joint angles.

(3) Command the arm to achieve that set of joint angles.

(4) Measure the error between the actual endpoint position and the desired endpoint position in shoulder coordinates.

The resulting measured error represents the accuracy of the manipulator system.

Repeatability is an error measure representing the consistency of operation of the manipulator system. Its operational definition is as follows:

(1) Command the manipulator to execute a particular trajectory, ending with a certain set of joint angles.

(2) Measure the endpoint position in shoulder coordinates.

(3) Command the manipulator to move away and then repeat the same trajectory as above.

(4) Again measure the endpoint position in shoulder coordinates.

(5) Compute the error between the first measurement and the second.

This error represents the repeatability of the system. It is the error to be expected between identical system commands.

Resolution is a measure representing the smallest consistent incremental position change the system can make. An operational definition is as follows:

(1) Command the manipulator to execute a particular trajectory ending with a certain set of joint angles.

(2) Measure the endpoint position in shoulder coordinates.

(3) Choose an incremental direction from the endpoint position in shoulder coordinates and command a small increment in position in that direction.

(4) Measure the new endpoint position in shoulder coordinates.

(5) Compute the difference between the first measurement and the second.

This operation is repeated several times to determine the smallest consistent incremental position change of the actual manipulator for an incremental command. The smallest actual incremental change is the resolution of the system.

Resolution is limited by things such as nonlinear frictional force characteristics. Typically, before a machine with moving parts can begin to move from a standstill, a certain breakaway force or torque must be exerted to overcome the static friction between the parts. After the parts begin to move, they must still face a constant running friction which is usually less than the static friction.

Due to the servo compliance between the desired manipulator position and the actual manipulator position an error between the actual and desired positions causes the servo to exert a restoring force. Hence, there is a certain incremental command error required to generate the breakaway force necessary to overcome the static friction. Now assume that a certain command error existed that provided enough actuator force to just overcome the static friction. Then how far the system travels will depend upon how different the running friction is from the breakaway friction. If the running friction is much less than the breakaway friction, then the system may move a comparatively large increment before the running friction brings it to a stop. However, if the running friction is only a little less than the breakaway friction, than the resulting actual position increment may be rather small.

Consequently, it can be seen that the resulting increments in actual manipulator position, which correspond to the resolution of the manipulator, depend on nonlinear frictional characteristics and servo compliance at least. Also, it is clear that the commanded increment in position does not necessarily equal the resulting actual motion. In

fact, it usually will not. Based on this analysis, the resolution of a manipulator may be improved by increasing servo stiffness (decreasing servo compliance), by reducing friction in general, and by making breakaway friction as close to running friction as possible.

In general, backlash will not affect the resolution as we have defined it. However, it will affect the command errors that must be given to generate the small actual increments. In particular, if a change of direction is involved in executing a particular increment of position, the length of the backlash will have to be added to the required command increment.

If the manipulator control system is based on commands issued from a digital computer, then the quantization of commands may itself determine the resolution of the manipulator. This is entirely dependent on the design of the control system. It follows that a design criterion for the control system would be not to limit the resolution of the device unnecessarily.

The physical processes that lead to repeatability errors are hard to find, but can be assumed to lie in variations of the physical processes themselves and surrounding conditions. Our operational definition of repeatability requires that the test point be approached along the same trajectory. This was done to insure equal processes; for example, that all backlash elements were in the same state from test to test. We may find a different repeatability measure if this condition were relaxed and we allowed the test point to be approached from arbitrary directions. Not only backlash but also other factors, such as friction, may vary with trajectory history, leading to a larger repeatability figure.

Accuracy errors involve a larger part of the system than do resolution and repeatability. Accuracy measures the ability of the system to execute a position command open loop. All of the following will contribute to errors in accuracy:

(1) Structural deflections

(2) Servo compliance

(3) Position sensor error

(4) Backlash in drive train if it is not seen by position sensor

Because the first three factors tend to remain constant from test to test, they do not tend to contribute to errors of repeatability and resolution. But just because they tend to remain constant over many tests, it is theoretically possible to compensate for these errors in the digital computer at the cost of added complexity.

Backlash, however, may not produce the same error from test to test especially if the trajectories leading to the test point differ. This may result in the backlash being in a different state in different tests, contributing to errors in accuracy.

Accuracy is an irrelevant concept to manipulation systems that are "taught" positions by manually guiding them into the desired position and indicating to the supervising system that it should "remember" this particular point. These systems are simply not required to compute a desired position, only to repeat motions that have been taught. Hence, repeatability and resolution are the only appropriate error measures for their motions.

Accuracy is clearly important to the gross motion of machines that must compute their way. This will be the case if they are taught their tasks by symbolic command languages which make reference to items and places in shoulder coordinates, or if they use visual or other information which is obtained in coordinates other than those of the arm's joints. Clearly resolution is important to the ability of the manipulator to execute fine motion because it determines how fine that motion can be. Repeatability is important to both gross and fine motion because it is a a measure of how consistent and reliable those motions can be.

e. Influences on Servo Design

The purpose of the servo system is to control the actuators to produce the desired response in the manipulator system. Goals of the servo design are to produce smooth, stable performance. The actual

motions of the real manipulator hardware must have good fidelity to the ideal motions prescribed by the computer.

There are two broad influences on the design of a servo system. One is the nature of the input commands to the servo system. If the manipulator is expected to accomplish gross motions in .5 sec, then the frequency response, or bandwidth, of the entire controlled system, including payload, certainly ought to be well above 2 Hz in order to reproduce the desired motions. Computer simulations have been used to determine that, for 0.5 sec task completion times, 5 Hz control bandwidth produces adequate performance, but that 10 Hz control bandwidth produces very good performance for a variety of simulated gross motion tasks of the arm shown in Figure IV-2.

The second broad influence on the design of a servo system is the frequency response of the components of the system. Each component of a system has its own dynamic characteristics, some of which may limit the performance of the overall closed loop system. For example, the servo valve controlling the hydraulic actuator cannot open and close instantaneously on command. Typically, it has a frequency response bandwidth of about 100 Hz. The resolvers used to detect angular position and rate (discussed in section VII) are read by a phase locked loop which will probably have a bandwidth of between 60 and 100 Hz. (Conventional angle readouts have little or no bandwidth limitations but do not generate rate information.) There is a possibility that components such as these with similar bandwidth can interact to produce system instabilities and resonances. The control system must be designed to prevent this.

Another component whose frequency response is important to the control system design is the physical manipulator structure. Work by Book (reference 5) and Maizza (reference 6) has shown that the resonance characteristics of the arm structure are intimately related to the servo bandwidth. This relationship is discussed further in section IV-C.

B. Kinematic Configuration

1. Approach

The approach to determining an optimum arm design with respect to its geometrical abilities and properties is basically threefold: number, type, and dimension. The number of freedoms required and their disposition will first be analyzed. Then the types of joints needed to realize these freedoms, e.g. revolute, spherical, cylindric, etc. Finally, dimensional data will be obtained through a generalized synthesis procedure.

The underlying guide for this entire process is with respect to the tasks at hand; thus, the configuration issues treated here bear primarily on the size and dexterity of the moving elements involved in assembly tasks. These elements include:

1. part(s)
2. end effector(s)
3. means of causing relative motion between the above

The size of the parts and subassemblies is determined by comparing a range of tasks in which a need to automate is clearly demonstrated, but where manual assembly is currently employed. Also, it is our aim to select a range that does not materially imply an advance in the state-of-the-art in mechanical design, e.g., a microscopic or gargantuan assembly environment.

Since modern fixed automation techniques have shown competence in handling subassemblies of up to about 10 cm diameter (spherical), the range chosen for our tasks was between half and one order of magnitude greater, viz. 30 cm to 1 m. Once the requirements for dexterity are defined and met, the overall size and geometry of the mobility subsystem can be matched to the task.

2. Disposition of Freedoms

The range of assembly tasks to be attacked has been conceptually limited by size, weight, etc. but not with respect to dexterity. In general, at least 6 degrees of freedom (dof) are required to orient and place a body in space. These freedoms may be divided between two mobility subsystems for binary assembly tasks (those that involve the interfacing of no more than two elements): one system per element. (Figure IV-5)

More freedoms could aid mobility by:

a. increasing range of motion

b. avoiding singularities of motion that occur in practical mechanical design

c. allowing redundant positions of the members for the same end-point position

There is a case where fewer freedoms would be helpful: when fewer than six dof are required, extra freedoms could add position errors and compliance. For example, an assembly task requiring only the insertion of parts from one direction into an accurately positioned subassembly might require less than completely general motion.

Indeed, a prime consideration of this effort is to include mobility to accomplish parts-fetching and jig-holding. For the outset, however, an arm that embodies both gross and fine motion capabilities is desirable. Experiments and evaluation of both modes of operation can proceed while peripheral devices are designed and constructed for the more specific chores.

Moving base design, i.e., a mobile fixture for holding subassemblies, is currently being investigated. A 3 dof platform design (Figure IV-6) featuring x, y, and θ motions of a limited range is being optimized, and a 6 dof platform of limited range has been suggested for

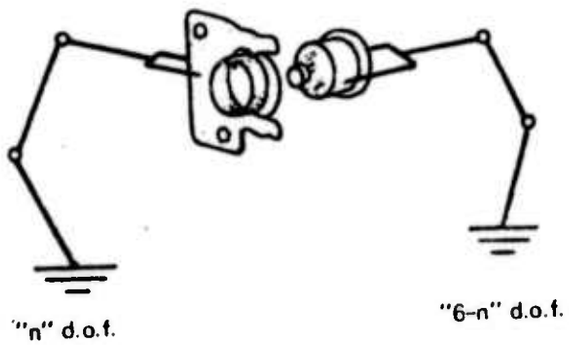

Minimum Freedoms for Binary Assembly

Figure IV-5

use in high speed "accommodation" tasks. (Figure IV-7)

Another system consideration is the ability to interface with existing assembly lines. This may severely limit the dividing up of the mobility subsystem freedoms. Therefore the system under consideration embodies all six dof in one "arm." Additional freedoms can of course be added later. Recall also that for our purposes as a laboratory tool, this system should feature as much flexibility of operation as possible.

To take full advantage of the work volume afforded by the chosen arm configuration, the work should be (conceptually at least) at the center of the ranges of the primary position axes. Since a consideration of the system was "current assembly line techniques," the range of position of the work is quite limited. For an object resting on a table (a most common occurance) the optimal placement of a single arm would be directly above it as shown in Figure IV-8.

An obvious additional freedom now presents itself: vertical traverse, to vary the position of the work volume vertically above the work. This freedom is present in the laboratory system as a series of fixed mounting points along a vertical column.

Since this system will be computer controlled some attention must be paid to the mathematical tractibility of the configuration. The following rules might be observed in picking an arm geometry. These considerations may of course be in conflict with other design goals and should be considered to be of secondary importance.

a. Offsets between joints should be avoided.

b. Successive axes should intersect in angles a multiple of $\pi/2$.

c. Adjacent rotary joint axes should be parallel, i.e., planar geometries are preferred.

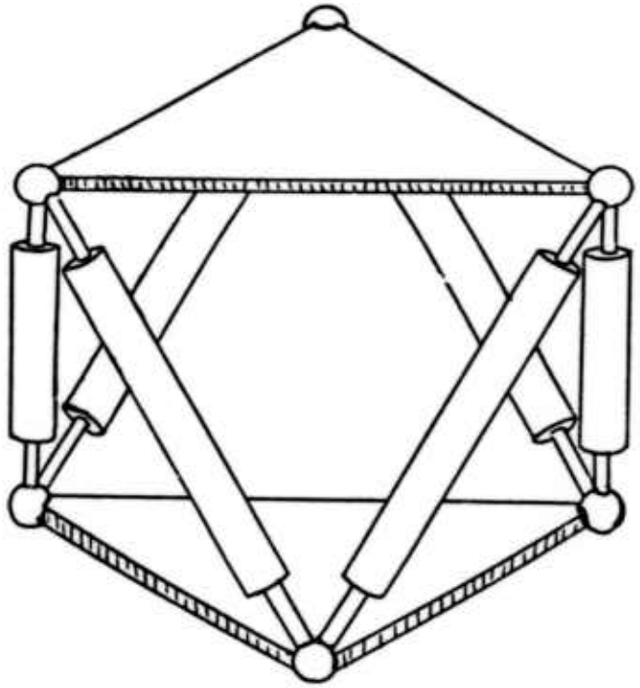

Figure IV-7
Six DOF Moveable Platform

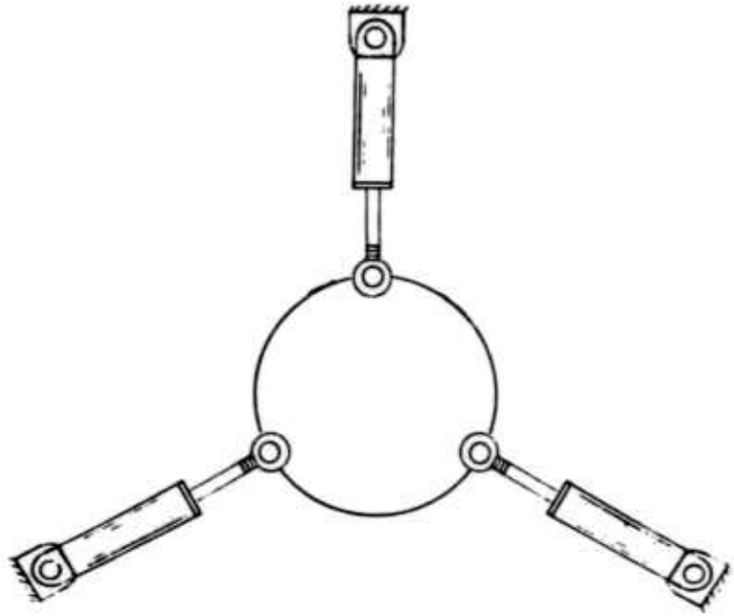

Figure IV-6 Three Degree of Freedom
Moveable Platform

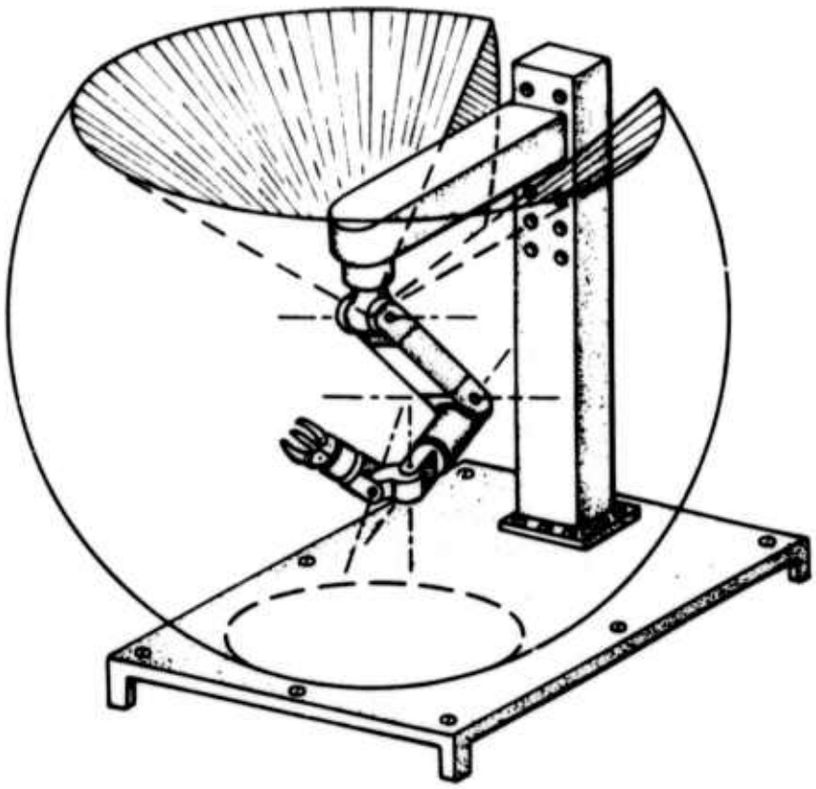

Figure IV-8
Arm Mounting and Work Volume

d. Sliding joints are preferred over rotary.

e. Number of joints should be minimized.

3. Types of Joints

An arm may be divided into two parts of 3 dof each: positioning and orienting. These are not necessarily independent in that one could cause perturbations in the other. Clearly, the latter requires rotational motion, whereas the former can be implemented with a combination of either rotational or telescoping (linear) motions.

Four different configurations for the positioning degrees of freedom can be realized: all three linear degrees of freedom, two linear degrees of freedom and one rotary degree of freedom, two rotary degrees of freedom and one linear degree of freedom, or all three rotary degrees of freedom. These are shown schematically in Figures IV-9 and IV-10. The different configurations have different advantages and disadvantages. The all linear degree of freedom configuration is best for computational purposes as the wrist point can be specified directly in cartesian coordinates. It is probably the best design for stiffness but is the worst design for volume accessed compared to the volume required for the structure. It would also be difficult to use two such arms to work on one assembly. At the other end of the scale, the all rotational degree of freedom arm has the best ratio of volume accessed to volume of structure, particularly if the arm is hung from an overhead structure. This configuration has an additional advantage in that there are two solutions for having the wrist point at a particular point in space. It is, however, the worst design for stiffness and for computation.

As the manipulator was to be used to perform assembly experiments and it was desirable that it be able to interface with existing assembly lines, the all rotational degree of freedom configuration

was chosen. This decision was largely based on the accessibility that this configuration affords with a minimum of structure.

The orienting set of freedoms presents another pair of candidate designs (Figure IV-11). The only functional difference between them is the orientation of the motion singularity: the point at which "you can't get there from here." To illustrate, when type R-P-R is in the "straight out" orientation, the roll axes coincide thereby reducing the number of freedoms by 1: you can roll and pitch, but can't yaw. Similarly, when either joint P or Y in the R-P-Y type is "bent 90^{o}" the roll motion (with respect to the end effector) is impossible, and is extremely difficult within 15^{o} or so of the 90^{o} position.

The RPY design was adopted since the loss of freedom when "bent 90^{o}" was deemed less a problem than when "straight out." Until a truly spherical joint is devised or a 4th freedom added, we'll just have to live with the singularity.

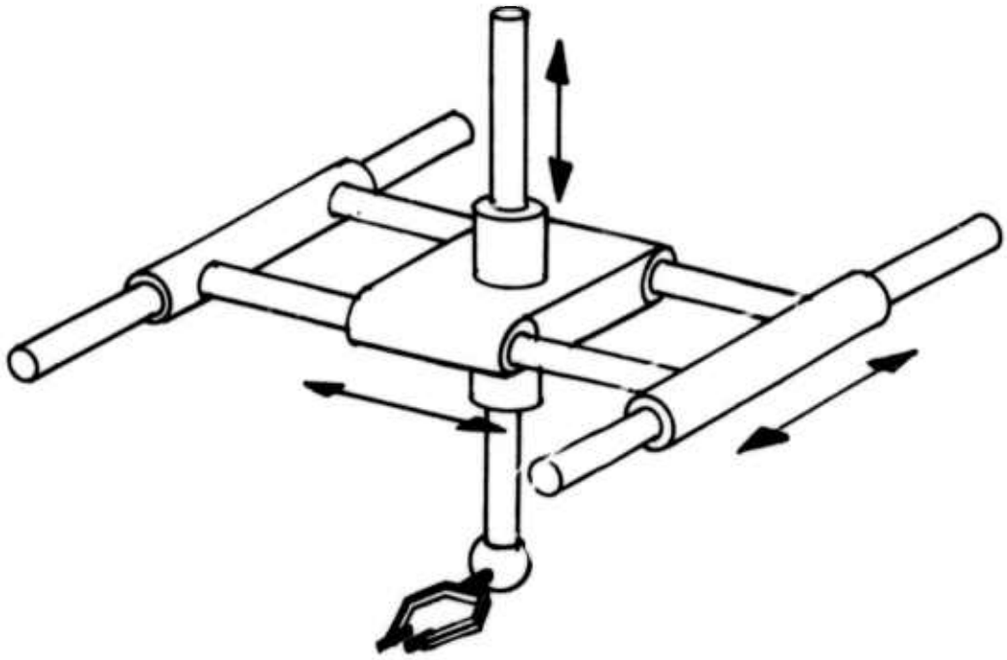

3 PRISMATIC JOINTS

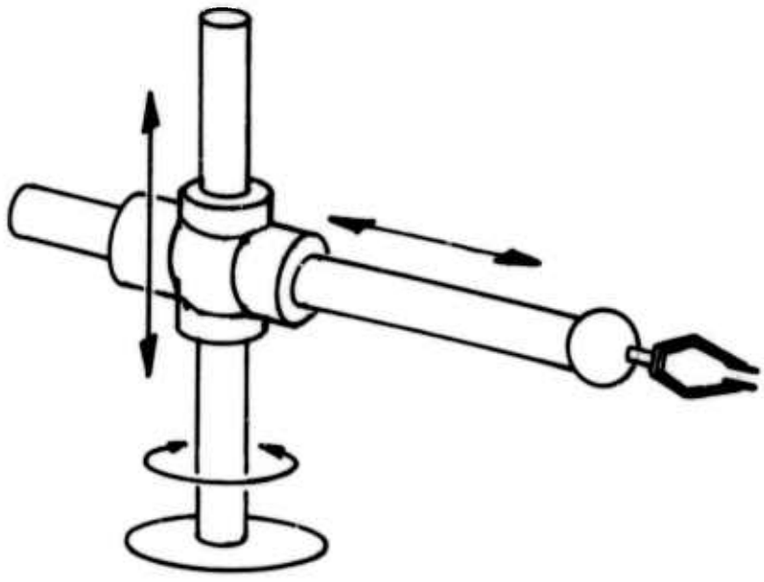

2 PRISMATIC, 1 ROTARY JOINT.

Figure IV-9

Manipulator Arm Configurations

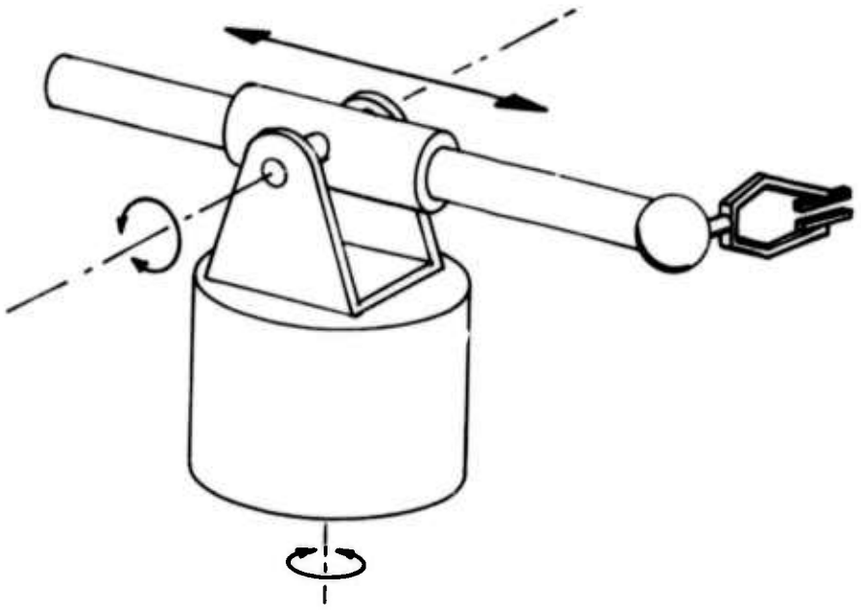

1 PRISMATIC, 2 ROTARY JOINTS

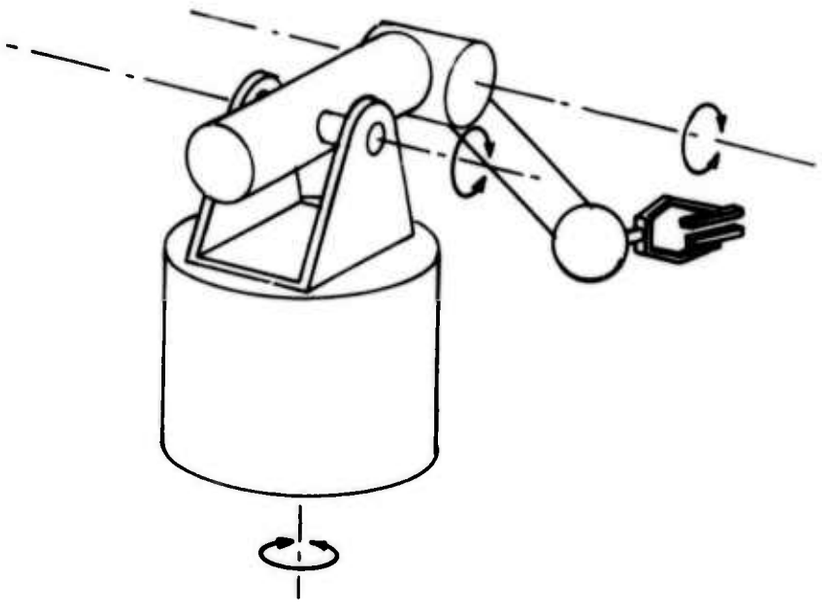

3 ROTARY JOINTS

Figure IV-10
Manipulator Arm Configurations

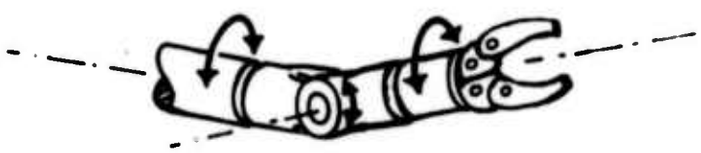

ROLL – PITCH – ROLL

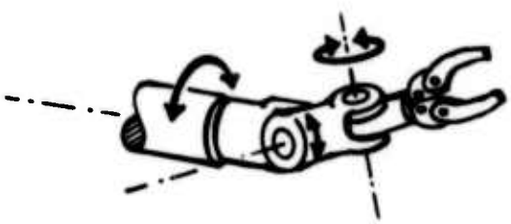

ROLL – PITCH – YAW

Figure IV-11
Candidate Wrist Configurations

4. Optimization of Arm Geometry

A general procedure is outlined here allowing for optimization of arm geometry to a specified task. This procedure requires machine computation and does not readily lend itself to hand calculation or graphical techniques.

Sliding-joint geometries were not considered since empirical data are easily obtained graphically.

Figure IV-12 shows a planar all-revolute arm described by unknown lengths x_1, x_2 and x_3.

One can describe a general "task" requiring the arm to touch n selected points in the workspace with specified orientations. (Interferences are not considered, but may be added with algorithms not treated here.) The points might represent one or more objects, tools, etc., that the arm will be required to interact with.

Figure IV-13 shows such a task definition with the arm in position j. We can express this situation like so:

$$\underline{x}_1 e^{i\theta_j} + \underline{x}_2 e^{i\varphi_j} + \underline{x}_3 e^{i\psi_j} = \underline{Z}_j \qquad \text{IV-1}$$

where $\underline{x}_i$ are complex (unknowns)

ψ_j = orientation of x_3 in position j (given)

$\underline{Z}_j$ = complex location of point j (given)

θ_j and φ_j are to be adjusted by iteration

We wish to optimize x_i for the given task and require (for example) that the arm be as short as possible:

$$\min \left| \underline{x}_1 + \underline{x}_2 + \underline{x}_3 \right| = \left| \underline{Z}_o \right| \qquad \text{IV-2}$$

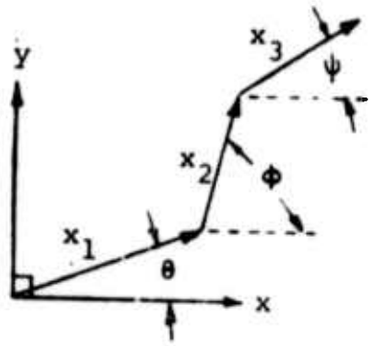

Figure IV-12
Arm Model

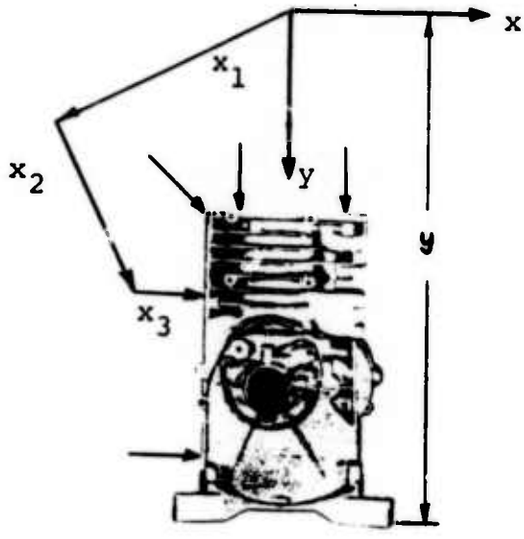

Figure IV-13
Arm with Several Task Vectors

The n + 1 relations may be written out like so:

$$\begin{bmatrix} 1 & 1 & 1 \\ e^{i\theta_1} & e^{i\varphi_1} & e^{i\psi_1} \\ \cdot & \cdot & \cdot \\ \cdot & \cdot & \cdot \\ \cdot & \cdot & \cdot \\ e^{i\theta_n} & e^{i\varphi_n} & e^{i\psi_n} \end{bmatrix} \begin{bmatrix} \underline{x}_1 \\ \underline{x}_2 \\ \underline{x}_3 \end{bmatrix} = \begin{bmatrix} \underline{Z}_o \\ Z_1 \\ \cdot \\ \cdot \\ \cdot \\ \underline{Z}_n \end{bmatrix} \qquad \text{IV-3}$$

or, equivalently:

$$M\underline{x} = \underline{Z}. \qquad \text{IV-4}$$

A root-mean-square solution of (4) for x can be obtained by introducing the complex conjugate of M, viz $\overline{M}^t$:

$$\underline{x} = (\overline{M}^t M)^{-1} \overline{M}^t \underline{Z}. \qquad \text{IV-5}$$

For non-trivial solutions, $(\overline{M}^t M)$ will be invertable.

Convergence error can be given by

$$\underline{E} = M\underline{x} - \underline{Z}. \qquad \text{IV-6}$$

Minimization of $|Z_o|$ can be assumed by including it in the error parameter:

$$\epsilon = K\underline{\overline{E}}^t\underline{E} + \underline{x}^t\underline{x} \qquad \text{IV-7}$$

where K weights convergence error to the same order of magnitude as $|Z_o|$: typically 10^2 or 10^3.

The optimization procedure is now reduced to the adjustment of the 2n quantities θ_j and φ_j. This will be accomplished, with a pattern-search algorithm, with ϵ as the objective parameter.

Good initial estimates may be obtained graphically. A computer program to implement the above procedure has been written and used. Input values depicted a single planar view of the Briggs and Stratton 3 Hp. gasoline engine.

Nine test positions ($\underline{Z}_j$ and ψ_j) were given. The arm was considered directly above the work at a distance y. This distance entered the solution process as a "patch" by adding y (real) to the imaginary parts of $\underline{Z}_j$. An initially large estimate for y was needed to avoid solutions that imply the interference of a vector (arm member) through the implied task boundary. The results are as follows:

Constraints: "elbow" angle $(\varphi_j - \theta_j) < \pm 2.355$ rad (135^o)

Variables: θ_j, φ_j, y

Run 1 results:

x_3 forced to zero, results inconclusive

Run 2:

x_3 constrained = 8 in. (20.3 cm)

Results:

x_1 = 17.9 in (45.4 cm)
x_2 = 17.9 in
y = 33.8 in (mounting distance) (85.8 cm)

Curiously enough, an "arm" with rather anthropomorphic proportions is implied by the procedure: equal lengths of "forearm" and "upperarm". The 8" value for x_3 was picked in consideration of the mechanical outlines of possible end effectors and other tools.

Other tasks of a more complex nature might not indicate such proportions, and one might well conjecture whether this result is due to a product designed with human assembly in mind.

The greater-than-human-size indicated by the procedure is probably due to the immobility of the "shoulder": with only 6 dof allowed,

the mobility subsystem can have "hands," but no "feet."

The final dimensions of the arm reflect the values obtained above and are shown in Figure V-1.

C. Relation Between Servo Bandwidth and Structural Vibration*

Because all structures are flexible and because pressure to reduce structural weight increases the structure's flexibility, one must be cautious about exciting structural vibrations through the action of the control servo. If the arm is moved slowly enough then such vibrations will not be bothersome. This may, however, require intolerably slow motions.

Flexibility may occur in structural members and in drive trains (shafts, gears, bearings, etc.). Gear teeth and long shafts are especially severe sources of flexibility. The stiffness of a long shaft or beam decreases with the cube of its length, so the flexibility problem is much worse for long arms than for short ones. Servo-induced vibrations can arise either during fine motions or during the startup or slowdown phase of controlled gross motions in places where trajectory accuracy is important.

Work on this problem has been conducted on the assumption that each arm joint has its own servo control which acts independently on sensor data derived from that joint alone. Two simplified models have been used, a one-joint arm and a two-joint arm. In the former, the joint is in the middle of the arm, forming a controlled elbow, while the shoulder is locked. In the latter model, the shoulder is also controlled. Reference (5) contains detailed studies. In each model, the joint servo gains are chosen to achieve a natural frequency (undamped) of w_s. Damping is provided by velocity feedback and provides damping ratio ζ relative to w_s. Both w_s and ζ are calculated on the assumption that the structural members are rigid. These members are assumed to be uniform tubes of radius r with wall thickness of r/5. With the joints locked solid the structure will exhibit a lowest frequency w_c of structural vibration. A study was conducted to determine the relationship between w_s and w_c with these results:

* Work supported in part by NASA MSFC Contract NAS8-28055.

- if $w_s < w_c/3$, the structure appears to be essentially rigid
- if $w_c/3 < w_s < w_c/2$, some structural vibration occurs but is well damped
- if $w_s > w_c/2$, insufficient damping is available and structural oscillations will be troublesome or even destructive.

Most arms seem to be designed conservatively, with w_s well below $w_c/3$. This causes the arm to be heavier than it needs to be for the bandwidth it can achieve. The extra weight penalizes gross motion times (for fixed strength actuators) approximately in proportion to w_c. Joint angle resolvers must be located inboard of any joint-related compliances, or else servo instability will occur (ref. 7). This fact is still being discovered empirically by some arm designers.

Additional studies have been performed with more complex servo control schemes. A rigid arm servo design technique is explained in reference (1), consisting of providing sensor data from all joints to the control decision at each joint. The same w_s can now be obtained with lower servo gains, especially at the shoulder, than in the former servo method. The main result with respect to structural vibration is that $w_s \approx w_c$ or more can be achieved with good performance. No commercial manipulator operates with this more complex servo. It would seem, however, that much lighter or faster arms (for the same actuators) would thereby be possible. (See Ref. 6)

In addition to stiffness considerations, one must also pay attention to strength. We find that for many arms, stiffness requirements exceed strength requirements and the latter are automatically satisified if the former are. This is not always the case, as reference (5) shows. For the record, however, it should be clear that plastic deformation in an industrial arm is tantamount to a failure and must be avoided.

One may utilize the torque-speed studies in Section IV. A. 2 to obtain operating torque levels. In Section VII. B it is shown that an arm of adequate stiffness will have an area moment of 5 in^4 at the shoulder, where a torque of 500 ft-lb may be encountered during gross motions. If

r = 3 in, then the stress at the outside edge of the structure is only 3600 lb/in^2, less than 3% of the yield stress for ordinary steel. The bulk of the analysis in Section VII. B therefore deals with stiffness, not strength.

D. Servo Control Methods and Force Feedback

In the previous part of this section, it was noted that servo controls can be synthesized to utilize information from all joints in determining control at each joint. Besides the benefit of better vibration control, other advantages are possible. These are discussed here.

In reference 1 it is shown that the dynamic equations of motion of a rigid arm can be put in the form

$$\begin{bmatrix} \dot{\underline{\theta}} \\ \ddot{\underline{\theta}} \end{bmatrix} = \left[\begin{array}{c|c} O & U \\ \hline O & O \end{array}\right] \begin{bmatrix} \underline{\theta} \\ \dot{\underline{\theta}} \end{bmatrix} + \begin{bmatrix} O \\ I^{-1} \end{bmatrix} \underline{\tau}$$

where $\underline{\theta}$ is a vector of controllable arm degrees of freedom (joints), $\dot{\underline{\theta}}$ is a vector of joint velocities, $\ddot{\underline{\theta}}$ the corresponding accelerations, I is the inertia matrix and $\underline{\tau}$ is a vector of control torques applied at the joints.* This model is linearized but experience with simulations indicates that the nonlinear Coriolis terms usually account for less than 10% of the torque in such maneuvers as those in section IV. A. 2. Reference 1 also shows that a control of the form

$$\underline{\tau} = K_T(\underline{\theta}-\underline{\theta}_c) + K_{TD}(\dot{\underline{\theta}}-\dot{\underline{\theta}}_c)$$

can be used to cause the arm to follow a commanded trajectory described by $\underline{\theta}_c$ and $\dot{\underline{\theta}}_c$. Interesting choices for matrices K_T and K_{TD} will not only place the poles of the overall system at desired places but will cause the system to have characteristic oscillation modes in convenient coordinates and with good damping. One can, for example, make the arm behave as a set of completely independent damped second order systems whose independent axes are those of the hand coordinates of the arm. This is

* U is an identity matrix.

important in the design of accommodation strategies where one needs to have an arm which will respond dynamically only in the desired direction, as indicated by force feedback, with no bothersome dynamic crosstalk into uncommanded directions. Reference 1 gives a general procedure for accomplishing this which will produce the correct K_T and K_{TD} for any configuration of a given arm.

A basic accommodation loop functions by converting force sensor readings into servo commands which modify $\underline{\theta}_c$ and $\underline{\dot{\theta}}_c$. Generalized force/torque vector $\underline{F}$ is measured by a sensor on the arm or work surface. If the sensor is on the arm at the wrist, $\underline{F}$ is in hand coordinates. Accommodation works by generating velocity modification commands $\underline{\dot{x}}_{DM}$ in hand coordinates:

$$\underline{\dot{x}}_{DM} = K_F \underline{F}$$

where K_F is called the accommodation matrix. If this matrix is chosen to be diagonal then simple "get out of the way" strategies will be executed because a force in any hand coordinate will request a velocity modification in that same direction, and will result in a reduction in the felt force. This modification is in the class of fine motions discussed in Section III, and may be superimposed on the gross motion commands, which are also in hand coordinates. The net command is then converted into joint commands $\underline{\theta}_c$ and $\underline{\dot{\theta}}_c$ by means of Resolved Motion Rate Control (reference 8). Note that the resulting motions will cause force $\underline{F}$ to change. Thus a new servo loop has been added. If $\underline{F}$ arises from elastic interactions between the arm and its environment, then a small motion of the hand $\underline{x}$ will cause a force $\underline{F}$ according to

$$\underline{F} = K_E \underline{x}$$

where $\underline{x}$ is measured in hand coordinates and K_E is the stiffness of everything between the force sensor and the "solid" ground relative to which $\underline{x}$ is measured. The resulting equations are third order in matrix form. If K_F is chosen to be other than diagonal or if zero entries are placed strategically on the diagonal, then other interesting tasks can be performed,

involving other strategies besides "get out of the way." See reference 1.

In reference 9 * a detailed study of the behavior of accommodation loops is made for the case of a three joint arm about the size and strength of that described in later sections of this report. It is shown that matrices K_T, K_{TD}, K_F and K_E must all be designed simultaneously, although some latitude is possible. K_E can be "designed" to the extent that it represents sensor stiffness (all force sensors seem to be instrumented compliances) although other compliances, such as the environment contacting the hand or the arm's own structure, are involved. High K_E is good for sensor design since the sensor then introduces little structural distortion, but high K_E makes the design of the rest of the servo more difficult. It can be shown that the product $K_F K_E$ must be smaller than some limit or else oscillations will occur when contact is made.

Reference 9 investigates two manipulation tasks by means of servo design techniques and computer simulation: collision with a boundary and putting a peg in a hole. Experience gained with the first task indicates that good stable response can be obtained. The simulated arm, which is quite strong and large, can be brought to a stop in about 0.3 seconds upon impact, utilizing only the control servo. This indicates that control techniques which need no computer are possible. In the second task, pegs are put in holes with clearance to diameter ratio of 0.001. A fundamental analysis of this task is also made, predicting regions of success or failure in this family of tasks, depending or friction, angular approach error and clearance to diameter ratio. Tasks near the limit of these success regions have been successfully simulated. Figure IV-14 shows a sample plot from such a simulation, where the peg approaches the hole at 10 cm/sec, with 2° misalignment. The coefficient of friction is 3. This is a difficult insertion task. The plot shows the rate of turn of the peg as it aligns itself with the hole. The "desired turn rate" is requested by the accommodation loop. The "actual turn rate" is the peg's response to this request

* work supported by NSF Grant No. GI 39432X and GI 43787.

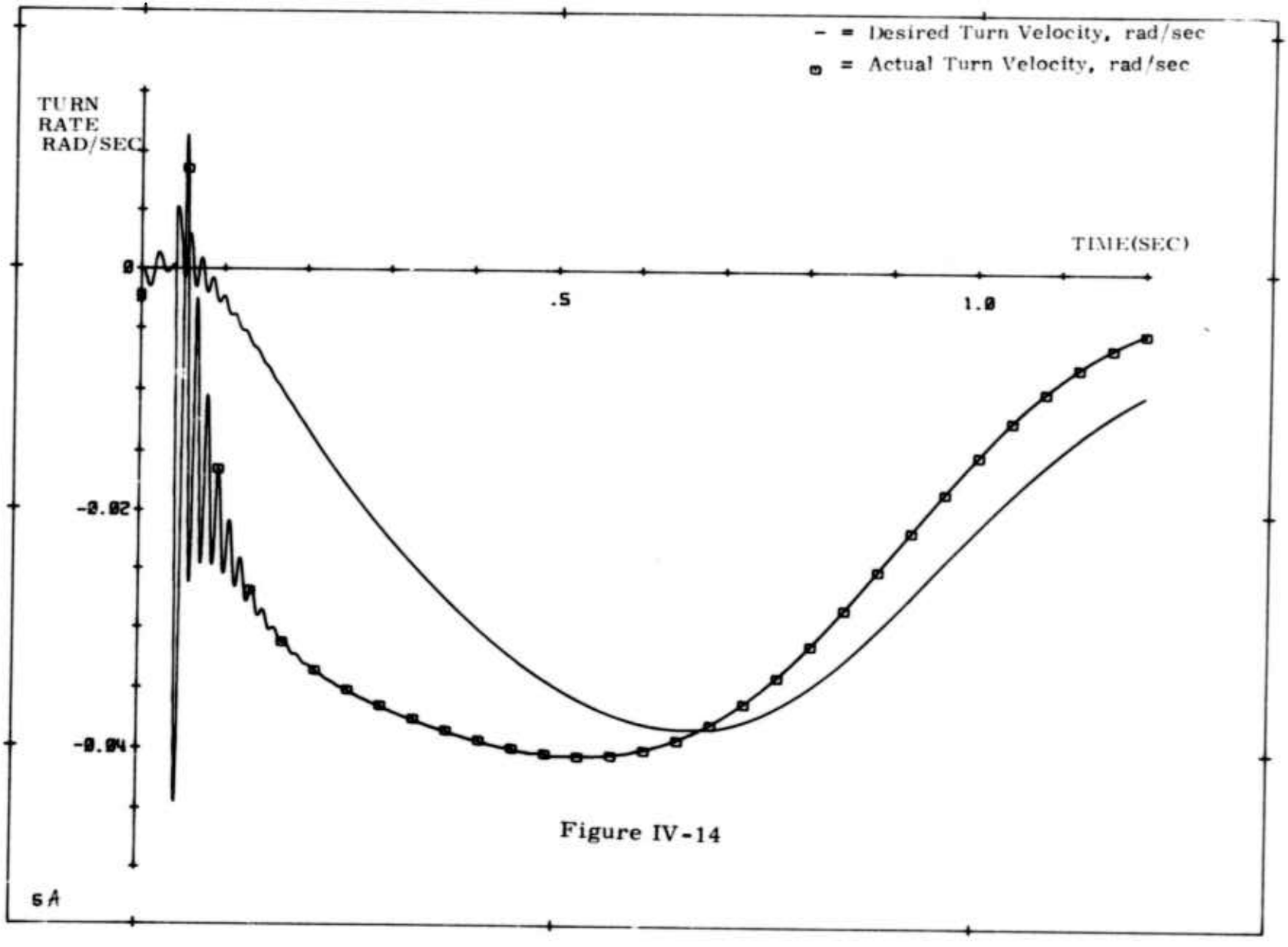
- = Desired Turn Velocity, rad/sec
ω = Actual Turn Velocity, rad/sec
TURN
RATE
RAD/SEC
TIME(SEC)
0
.5
1.0
-0.02
-0.04
SA

Figure IV-14

and to the forces exerted directly on the peg by the hole. As accommodation builds up, these forces die out and the peg goes smoothly into the hole.

A one degree of freedom simulation of the collision task has been set up to investigate the effects of backlash. Backlash can result from gear, chain and spline drives, and can occur in power drive trains or in sensory readout devices. Backlash is not a problem in put-take industrial robots or in devices like auto transmissions, derricks and so on. It causes difficulty in servos or other controlled devices which must reverse direction as they seek a commanded position under tight servo control.

The issues studied here are backlash location and angle readout location. One quickly discovers than an angle readout with internal backlash causes servo oscillations or instabilities. The same occurs if a readout is located on a load which is connected to its drive motor through drive train backlash. If the readout is on the motor, however, then the accommodation loop still functions, although not as effectively. This is illustrated in the next three figures, which show desired and actual velocities of a simple one degree of freedom arm colliding with a barrier. In Figure IV-15 there is no backlash. Curve 1 is the position of the arm's endpoint, curve 2 is its velocity, curve 5 is the desired position and curve 6 is the desired velocity, the latter two being modified sharply by accommodation after the collision occurs at around time = 0.18 sec. Stable behavior occurs and all velocities recede to zero as the arm comes to rest against the barrier. Figure IV-16 shows the effect of adding 0.005 radians of backlash between the motor and the load. The load's speed jumps up suddenly at time = 0.1 seconds when the backlash closes and the motor first begins driving the load. The backlash remains closed during contact and stable behavior results. Figure IV-17 shows the result when the backlash of 0.005 radians is shifted from the load to the angle readout. The high velocity of the load near time = 0.1 is caused by the servo's belief that the load is not moving, since the backlash on the angle readout does not close until around time = 0.07. The ultimate result is instability. This indicates that if, in the previous test, there were

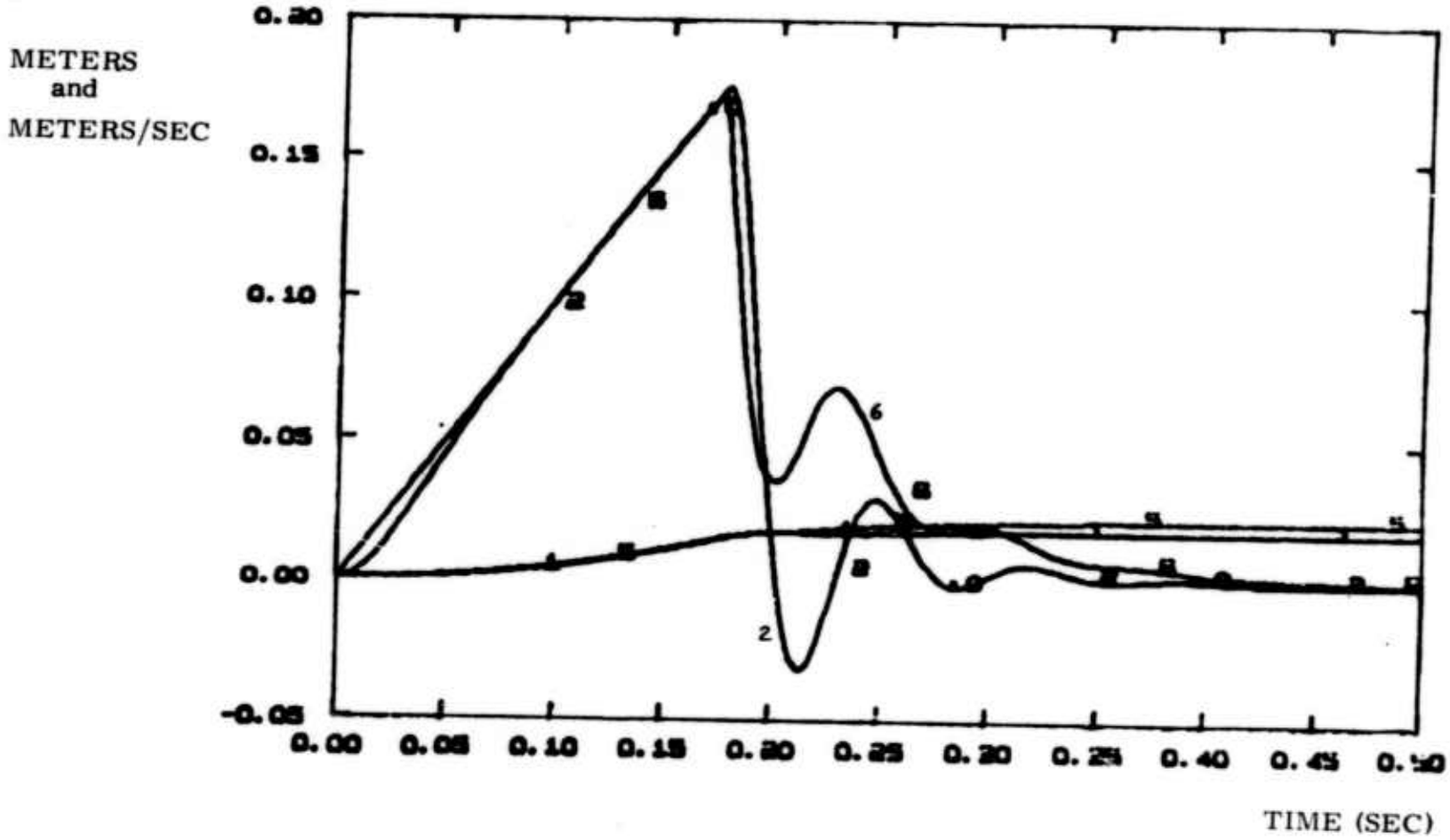
METERS
and
METERS/SEC
0.20
0.15
0.10
0.05
0.00
-0.05
0.00
0.05
0.10
0.15
0.20
0.25
0.30
0.35
0.40
0.45
0.50
TIME (SEC)

Figure IV-15

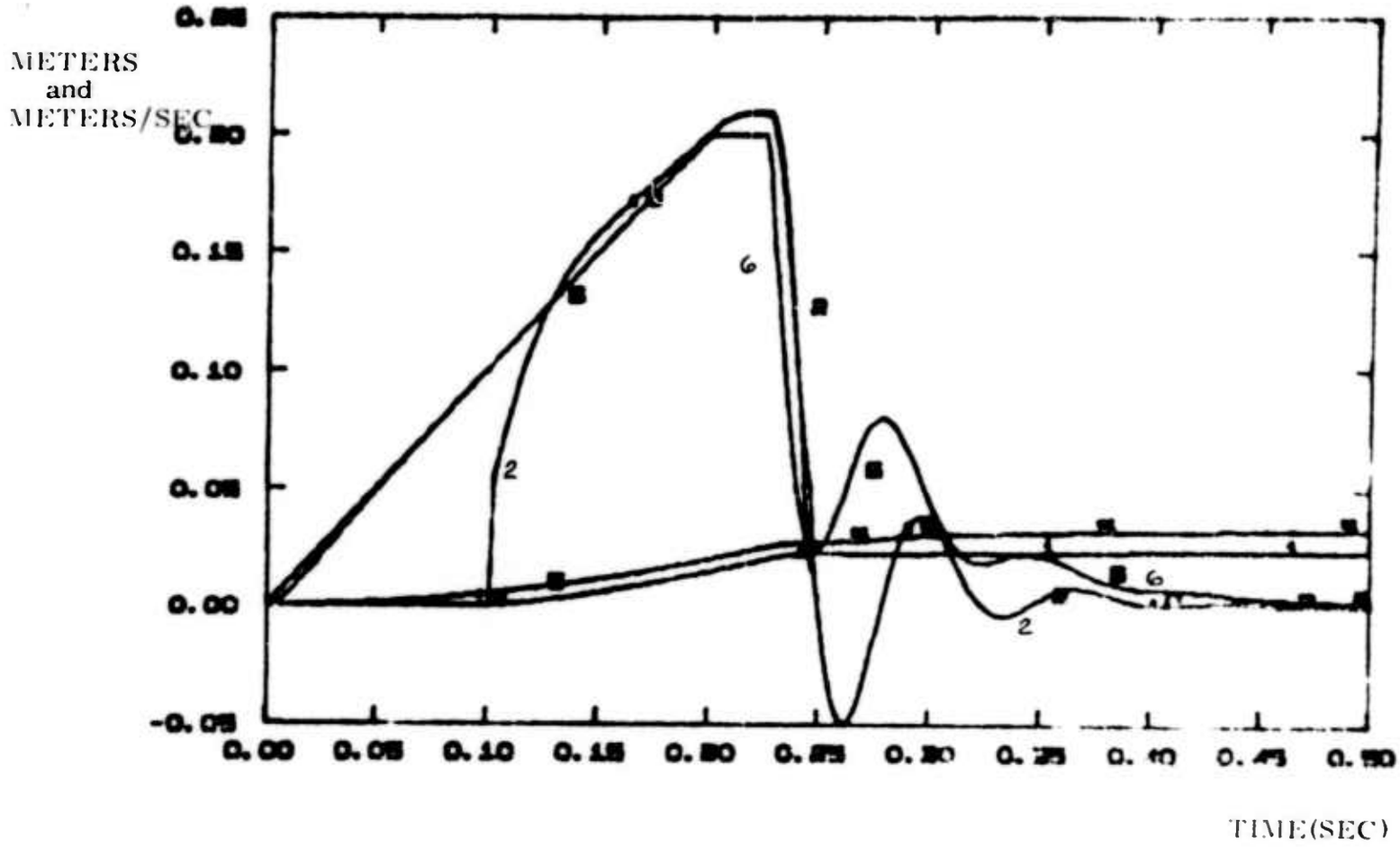
METERS
and
METERS/SEC
0.15
0.10
0.05
0.00
-0.05
0.00
0.05
0.10
0.15
0.20
0.25
0.30
0.35
0.40
0.45
0.50
TIME(SEC)

Figure IV-16

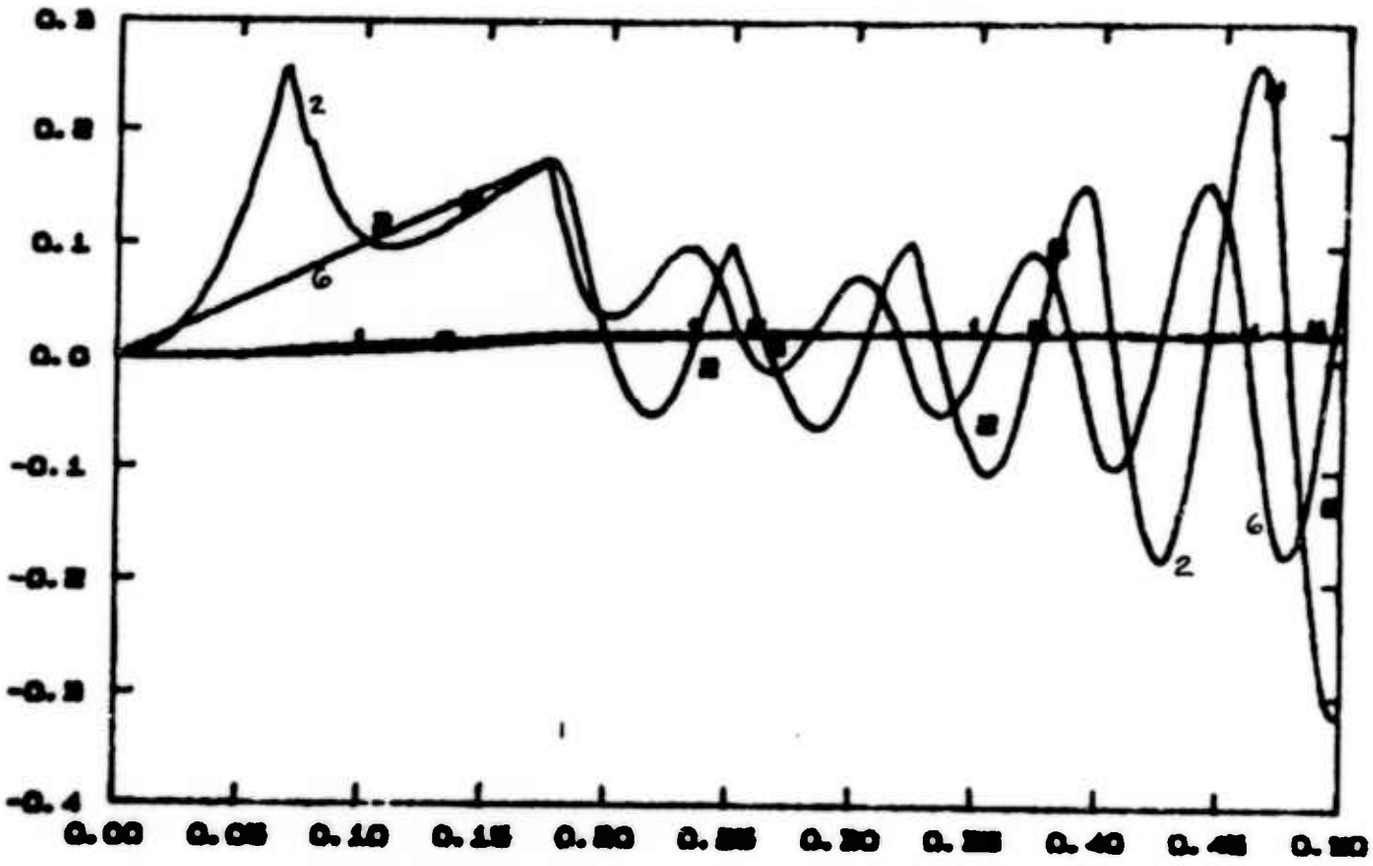

Figure IV-17

additional backlash in the force sensor, the result would be instability. Thus high quality force sensing can make up for sloppy drive trains to some extent, although in some cases it appears that one must pay a penalty in decreased arm speed and increased contact forces between the arm and its environment.

E. Error Analysis

An error analysis is not an exercise in pessimism but is the key to understanding whether a proposed design will in fact perform as intended. It also points out reasons for weak performance and indicates how and where to make improvements. It shows how accurate sensors need to be, for example, or how stiff compliant elements must be made, in order that desired performance goals be met. Error analyses usually do not concern themselves with malfunctions.

Error analyses can be carried out in three areas of assembly arm studies:

- the arm itself
- the objects it interacts with
- the strategies it utilizes for carrying out tasks

A general procedure for determining errors in manipulator arms is discussed in reference 2 . The error sources analyzed are angle sensors, bearing location and eccentricity, structural compliance and thermal expansion. An appropriate arm design should balance these contributions to error so that no one source dominates while effort is expended to reduce the others. Some types of error are predictable and can be compensated while others are random. This analysis method was used in the design of the arm described in Section VII to specify angle readout accuracy and to determine that certain bearings and shafts were too compliant.

Normally one is not interested in the accuracy of an arm itself but rather the combined accuracy of the arm and the items it interacts with. Errors can appear in the objects grasped by the arm, in the exact position of the object in the gripper, and in the position of the assembly into which the grasped object is to be placed. One quickly concludes, for example, that it is fruitless to build ultra-accurate arms to move floppy rubber hoses around (unless special precautions are taken). A conclusion of ongoing assembly task analysis is that automated assembly will involve many gripping tools whose major function is to accurately locate a grasped object with respect to the gripper.

Error analysis of strategies is really an investigation in depth of the strategies themselves. If execution of a strategy requires that a force of no more than 10 newtons be exerted, then success depends on how accurately one can measure the force and how quickly one can cease to increase applied force once the 10 newton level has been reached. Other strategies may call for the determination of the direction in which force is acting. There will be an error in this determination. If success of the strategy depends critically on the accuracy of this direction measurement, the strategy may be failure-prone. Thus we see that hardware and strategies interact; a good strategy on paper may be beyond an arm's capability; shortcomings in an arm may force one to employ additional compensating strategies at a cost in task completion time.

In this vein, we have identified a number of arm design inadequacies which detract from performance in various ways:

- structural compliance (task completion time is lengthened while one waits for vibrations to die out, or the arm must be moved slowly)
- backlash (to ensure repeatibility, the arm must be moved slowly near the end of a gross motion; reversing direction during fine motions leads to errors;

attempts to servo with force feedback may cause instabilities; one may have to adopt a strategy of "grounding" the arm on some solid object just before beginning fine motion in order to guarantee that one knows where the arm is)

- inadequate control servos (task completion time is lengthened due to the need to move the arm slowly; control gains are higher than necessary and vibrations may occur; payload cannot be changed without upsetting the servo)

- unbalanced actuator capability or unbalanced structural rigidity (arms with weak or compliant wrists seem to be common; a compliant shoulder is less common but is worse in that the whole arm can be set into vibration; a prototype arm with this problem exists in a large company's laboratory; both inadequacies result in wasted resources, servo problems, inability to complete tasks or longer task completion times)

F. Summary of Design Tools

The following list comprises tools developed during this and other studies and utilized in specifying the design of the arm described in the following sections:

- TOAD (teleoperator arm design program) - computer programs to write kinematic and dynamic equations of motion for arms

- speed/payload/torque analyses and simulations to size actuators

- actuator technology studies
- servo analysis and simulation of accommodation strategies and other fine motion methods, including effects of compliance and backlash
- structural analysis and its relation to servo control of arms
- servo control techniques for determining dynamic performance
- error analysis to criticize arm designs and strategies for assembly

V. DISCUSSION OF DRAPER LAB ARM DESIGN (POPEYE)

A. Discription of Arm

The Draper Lab arm was designed as a research tool for automatic assembly. The basic requirements were that the device be capable of assembling items as large as a cube one meter on a side, be capable of picking up parts as heavy as 20 kilograms, be capable of slewing 1 1/2 radians in all axes in 0.5 sec unloaded, have an overall absolute accuracy of less than 1 mm (0.04 in) and be capable of quickly interchanging tools or end effectors used for different assembly tasks. Designing to these difficult specifications brings out many problems and solutions applicable to mini-robot arms.

While there are a number of different kinematic configurations that could successfully be used, an overhead hung six degree of freedom elbow type of arm design was selected as it was quite compact for the work volume it could access and was judged to be more easily adaptable to existing assembly lines. A rigid gallows structure that bolts to a work table was designed to suspend the arm (see figure V-1). The horizontal beam of this structure can be set at different heights for different tasks. Eventually this movement was to be powered although not to be used as a high speed degree of freedom. The arm proper had shoulder azimuth and elevation degrees of freedom, an elbow elevation degree of freedom, and wrist roll, pitch, and yaw degrees of freedom. The links between the shoulder and elbow and between the elbow and wrist were idealized as being an equal 0.45 m (~ 17.75 in) in length. However, it was not possible to design a universal joint for the wrist that would allow sufficient movement for both pitch and yaw. Therefore the pitch and yaw axes are separated by 82.5 mm (~ 3.25 in) and the 0.45 m length between the elbow and wrist extends to a point equidistant between the pitch and yaw axis. The idealized load point was considered to be 0.20 m (~ 8 in) from this point. Thus, the overall straightout length of the arm is 1.10 m (~ 43.3 in).

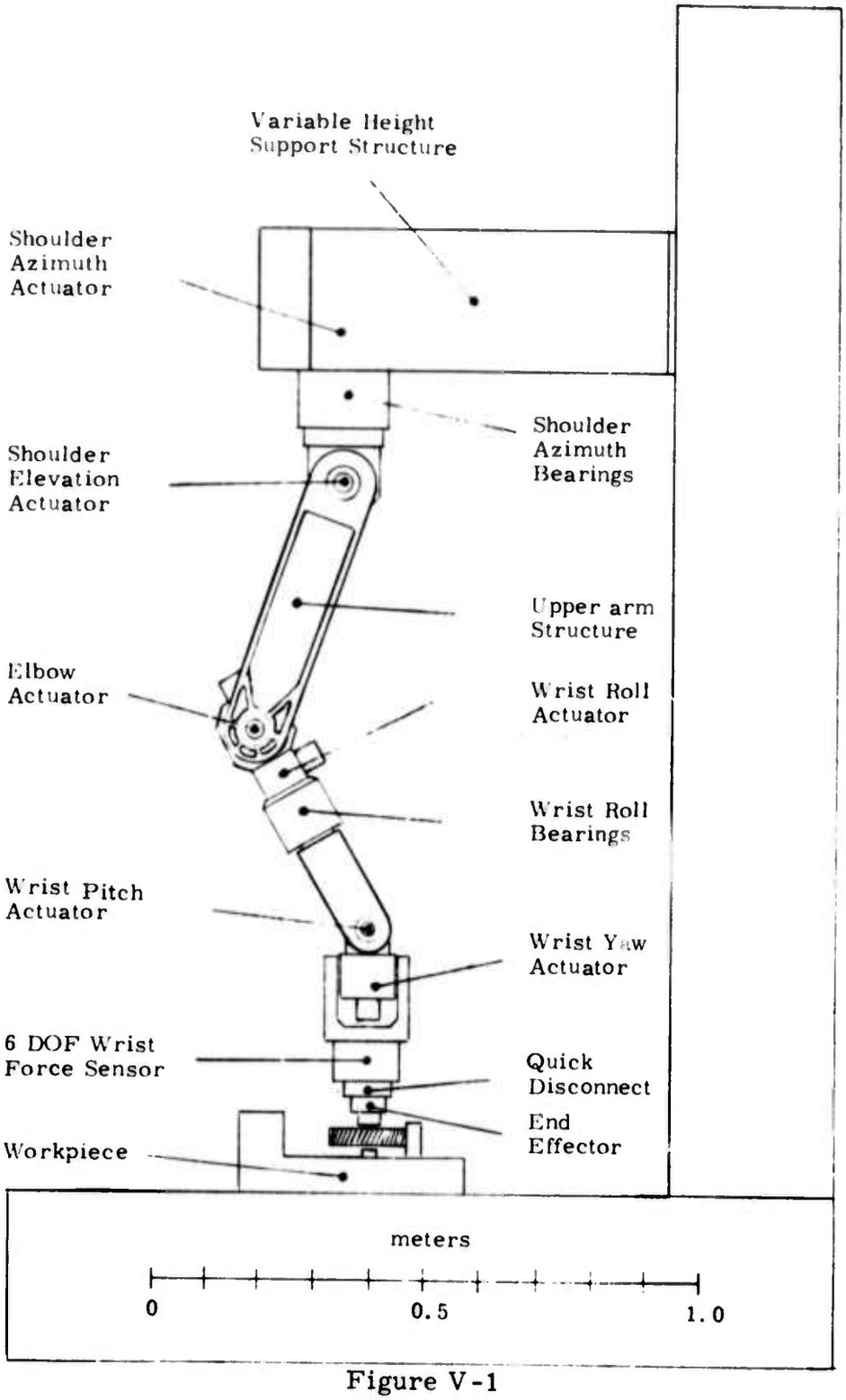

Figure V-1

Side View of Draper Arm, Work Surface, and Support Structure

All of the degrees of freedom are driven by direct coupled single vane hydraulic actuators with a working pressure of 14×10^6 Pascals ($\sim$2000 PSI). At this pressure the shoulder actuators will develop 690 Nt-m ($\sim$ 510 ft lb) of torque; the elbow actuator, 350 Nt-m ($\sim$260 ft lb) of torque and the wrist actuators, 82 Nt-m ($\sim$60 ft-lb) of torque. Except for the shoulder azimuth and the wrist roll, the bearings for the actuators also act as the bearings for the structure. Due to the large moment loads possible on the shoulder azimuth and the wrist roll degrees of freedom, additional larger diameter bearings were incorporated. Where possible the actuator housings form part of the arm structure. The wrist roll actuator is bolted directly to the elbow actuator. The wrist pitch and yaw actuators were designed with a single siamese housing. To avoid backlash, connections between the actuator shafts and structural yokes were made using friction clamps as opposed to keyways or splines. In all degrees of freedom, the position feedback sensor, which is a dual speed pancake resolver (1X and 64X), is designed into the actuator housing and uses the actuator bearings.

B. Critique of POPEYE* as a Research Tool

The POPEYE design reflects the need for a research arm that attempts to meet the research goals as reviewed in Section I of this report. The design reflects the dual attributes of a good pick-and-place arm and an assembler. These attributes are:

For Pick-and-Place

- Speed
- Accuracy
- High Load Capacity
- Large Work Volume

For Assembly

- Accuracy (good positional accuracy)
- Accurate Control of Small Motions (good rate control and high damping)
- Accurate Control of Forces at the Hand (accurate, wide dynamic range, low drift wrist force sensor)
- Versatile Set of Articulations (at least six degrees of freedom with the ability to reach around objects)

1. Advantages of POPEYE Design

Of course the arm could not be designed to optimize all attributes. However, the design does have inovations that should result in an arm that will have excellent kinematic and dynamic behavior. The more important of these design inovations are:

a. Overall kinematics: six degrees-of-freedom, shoulder connected to a stiff overhead beam (see figure V-1), an elbow which allows articulation around five sides of task. The large work volume afforded by this design should also help with the parts feeding problem.

* Because of its husky lower arm, this design has come to be called POPEYE.

b. Loads connected directly to the actuators thus eliminating backlash due to gearing.

c. Position feedback sensors — 1 and 64 speed pancake resolvers wound on the same pole pieces — designed into the motor housing and on the load shaft. This eliminates shaft windup and backlash between the actuator output and the feedback element — often a source of servo instability.

d. The use of the two speed resolvers has many advantages. Among these are:

   (1) 16 bits position accuracy

   (2) 18 bits servo quantization

   (3) A rate signal derived from the Phase Lock Loop method of reading out and digitizing the resolver signals

   (4) The 64 speed winding gives the equivalent of a 64 speed gearup of a tachometer without introducing the extra apparent inertia of real gears, backlash or shaft windup. This in turn results in a sensitive rate signal (approximately 1 volt/rad/sec)

e. The hydraulic vane actuators were designed without internal (vane) seals. This has the advantage of eliminating much of the cause of stiction and also aided in servo damping.

f. The design of a six-degree-of-freedom, wide dynamic range force sensor array. This will be incorporated in the wrist force sensor and used, in conjunction with the control computer, to resolve the forces at the hand into the six components — three rectilinear, and three torque.

2. Disadvantages of POPEYE Design

The principle disadvantage of the POPEYE design is the cost of producing it. The hydraulic motors, motor and bearing houses, arm linkages, force sensor array and housing all had to be designed. The machining of all these parts will be relatively expensive compared to present systems; however, the inherent reliability of its very clean design offers compensating advantages as a research tool.

VI. SUMMARY OF DRAPER LAB ARM SPECIFICATIONS

A. Dexterity

1. Six degrees of freedom exclusive of end effector, based on minimum requirement for general spatial motion. All degrees of freedom are revolute (as opposed to telescoping or prismatic) and are embodied in the arm proper. See Figure V-1 for a general view of the arm.

2. Angular excursions of joints (Constrained by practical joint and actuator design)

Shoulder Azimuth	$\pm 150^{\circ}$
Shoulder Elevation	$\pm 130^{\circ}$
Elbow Elevation	$\pm 135^{\circ}$
Wrist Roll	$\pm 150^{\circ}$
Wrist Pitch	$\pm 135^{\circ}$
Wrist Yaw	$\pm 100^{\circ}$

B. Size

Maximum reach at wrist point	0.90 m (35.4 in)
Minimum reach of wrist point	0.38 m (15.0 in)

As the length of different end effectors and sensors will vary, the wrist point is used as a datum. The wrist point is considered to a point equidistant between the wrist pitch and the wrist yaw axes.

C. Accuracy

A single point-positioning accuracy of better than 1 mm (or 40 mils) was specified. The figures listed below are the result of many factors: size, strength, speed, etc. These worst-case errors are defined statically with the wristpoint as a datum.

1. Basic Resolver Error (±LSB):
   - Elevation* = ±.132 mm (±.0052 in)
   - Azimuth = ±.189 mm (±.0035 in)
2. Repeatability (±1/4 LSB):
   - Elevation* = ±.033 mm (±.0013 in)
   - Azimuth = ±.022 mm (±.0009 in)

* Two resolvers in tandem

3. Structural Error (RMS) = $\pm$.26 mm ($\pm$.0104 in)

4. Vertical Droop (unloaded) = .16 mm (.0062 in)

Accuracy for "fine" motions has not been defined.

D. Performance

Fine-motion operating bandwidth: 10Hz

Gross-motion "task" time: 0.5 sec,

Stiffness (referred to wristpoint):

Arm extended = 1050 Nt/mm (6000 lb/in)
Elbow @ 90° = 1230 Nt/mm (7000 lb/in)

Lowest structural natural frequency = 30 Hz

Inertia @ shoulder with 10 Kg load $\approx$ 22-1/2 Kg-M^2 (200 in-#-sec^2)

The gross motion task referred to above is to move any or all axes of the unloaded arm in a 90° slew motion stop to stop.

E. Subsystem Specifications

1. Actuators

Type:	Hydraulic, single vane, direct acting
Seals:	no internal, shaft seals only
System Press:	17.5 MPa ($\sim$ 2500 PSI)
Displacement:	
Shoulder	51.1 x 10^{-6} m^3/rad (3.12 in^3/rad)
Elbow	25.6 x 10^{-6} m^3/rad (1.56 in^3/rad)
Wrist	6.22 x 10^{-6} m^3/rad (0.38 in^3/rad)

Rated Actuator Torques @ 14.0 MPa ($\sim$ 2000 PSI)

Shoulder Azimuth and Elevation	690 nt M (510 ft #)
Elbow	350 nt M (258 ft #)
All Wrist	82 nt M (61 ft #)

Speed (at rated torque): 6 rad/sec

Valve pressure drop at speed: < 3.5 MPa (500 PSI)

2. Angular Position Transducers

Type:	Two speed, 1X and 64X: wirewound pancake resolvers
Size:	76.3 mm (3 in) O.D. 44.5 mm (1.74 in) I.D.
Excitation:	15V, 1000 Hz 1/2 watt/unit
Transformation Ratio:	1X : 1 to 1 64X : 4 to 1
Accuracy:	1X : 1.5 deg (8 bits) 64X : 20 sec (16 bits)
Speed:	adjustable - a tracking Phase-locked loop is used
Tachometer Output:	Supplied by PLL, analog
Mounting:	Integral with actuators

3. Wrist Force Sensor

Type:	laser interferometer
Degrees of freedom:	6
Full Scale Force:	500 nt (110 lbs)
Overload Force:	5000 nt design goal (1100 lbs)
Displacement:	0.04 mm (0.0016 in) full scale
Resolution:	14 bits or 1:8000

VII. SUBSYSTEMS

A. Actuator Selection and Design

1. Power Source Selection

The major decision in the selection of the actuators for the manipulator arm was whether to use D. C. torque motors or to use either hydraulic motors or hydraulic actuators. Both have their advantages. The main advantage of the electric motors is that they are considerably easier to control than the combination of hydraulic servo valves and hydraulic actuators. In general, it is easier to design for wiring for an electric motor than for hydraulic lines. The hydraulic systems have a potentially serious leakage problem. Noise may be somewhat more of a problem with a hydraulic system. The main disadvantage of a D. C. torque motor is that its torque to weight ratio is much lower than that of a hydraulic motor or actuator. In order to increase the torque to weight ratio of the electric motor, it would probably be necessary to use mechanical gearing of some type. In general, the use of gearing will cause backlash which will in turn cause control problems.

It should be realized that the choice of actuator types is not independent of the assembly machine or assembly arm configuration. If the assembly machine employs linear degrees of motion, preloaded zero backlash ball screws can be used to amplify the force available from an electric motor. Also, if the degrees of freedom can be arranged so that the motor masses do not create large inertias and/or large gravitational forces that must be overcome by other motors, the torque to weight ratio is less important.

For reasons that are detailed in section B on Kinematic Configuration, an elbow type of arm design was chosen with all six degrees of freedom invested in the arm proper. To achieve the necessary drive stiffness and to avoid backlash, remote drive mechanisms were ruled out. Therefore, it is necessary that the shoulder actuators have sufficient torque to overcome the inertia and gravitational loads caused by the elbow and the wrist actuators in addition to those caused by the end effector and load. The

elbow actuator must have sufficient torque to overcome the inertia and gravitational loads caused by the wrist in addition to those of the end effector and load. This causes a pyramiding effect on the required actuator torque which virtually rules out any consideration of using direct drive D.C. torque motors. Thus, if electric motors were to be used they would need to be geared, probably in the range of 10:1 to 20:1. While it might be possible to develop a zero backlash gearing system using preloaded gear pairs or perhaps using all rolling element cycloidal gear reducers or a counter driving double motor arrangement on each axis, it was decided that the more straight-forward approach would be to use either a hydraulic motor or a hydraulic actuator.

2. Hydraulic Motor/Actuator Design

Preliminary design work was done for both a continuous rotation hydraulic motor and for a single vane hydraulic rotary actuator capable of up to 300^{o} of rotation. The hydraulic motor design was for an orbital gerotor type of motor. This motor essentially consists of a rotor with externally cut cycloidal gear teeth that rotates inside a stator with internally cut cycloidal gear teeth. See Figure VII-1, 2. As the stator has one more tooth than the rotor, the rotor will make n_r orbits per rotation where n_r is the number of teeth or lobes on the rotor. If the rotor rotation is used as the shaft output, a planetary gear effect with a ratio of n_r:1 will be achieved without resorting to external gearing. This effective gearing has the same effect as external gearing in raising the apparent torque and stiffness of the hydraulic motor.

While orbital gerotor motors are commercially available from several sources, they do not appear to be suitable for use as servo motors. In the commercial motors, the rotor rotation is picked up with a shaft that has loose fitting balled-over splines at both ends. This shaft is free to wobble which allows the rotor to orbit while preserving the rotation. Unfortunately, this shaft with its loose fitting splines becomes a source of backlash and wear. In our design, the splined shaft was replaced with a pair of freely rotating cranks. The free rotation of the cranks allows the rotor to orbit while the cranks will rotate as a pair

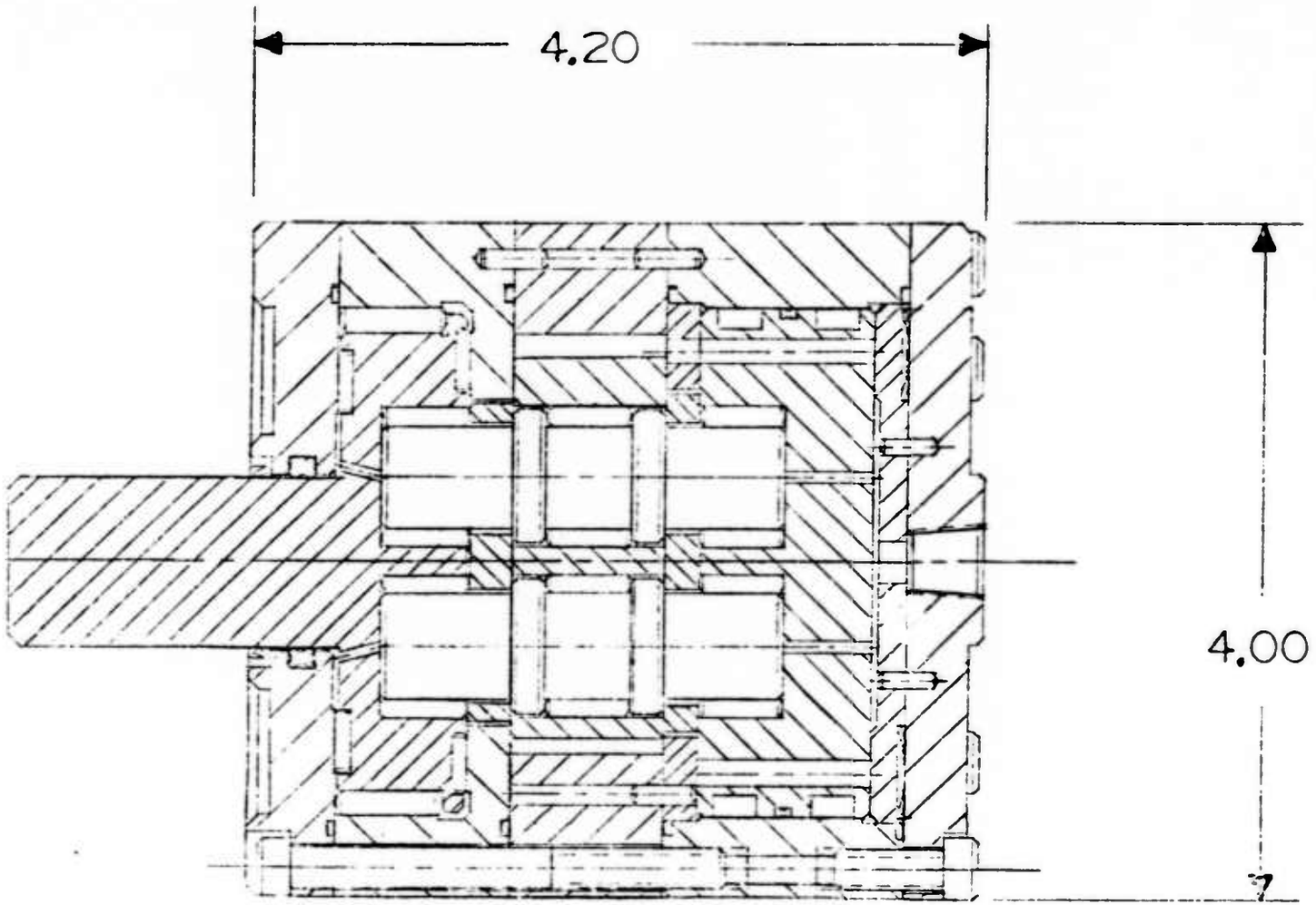

Figure VII-1
Layout of Gerotor Hydraulic Motor

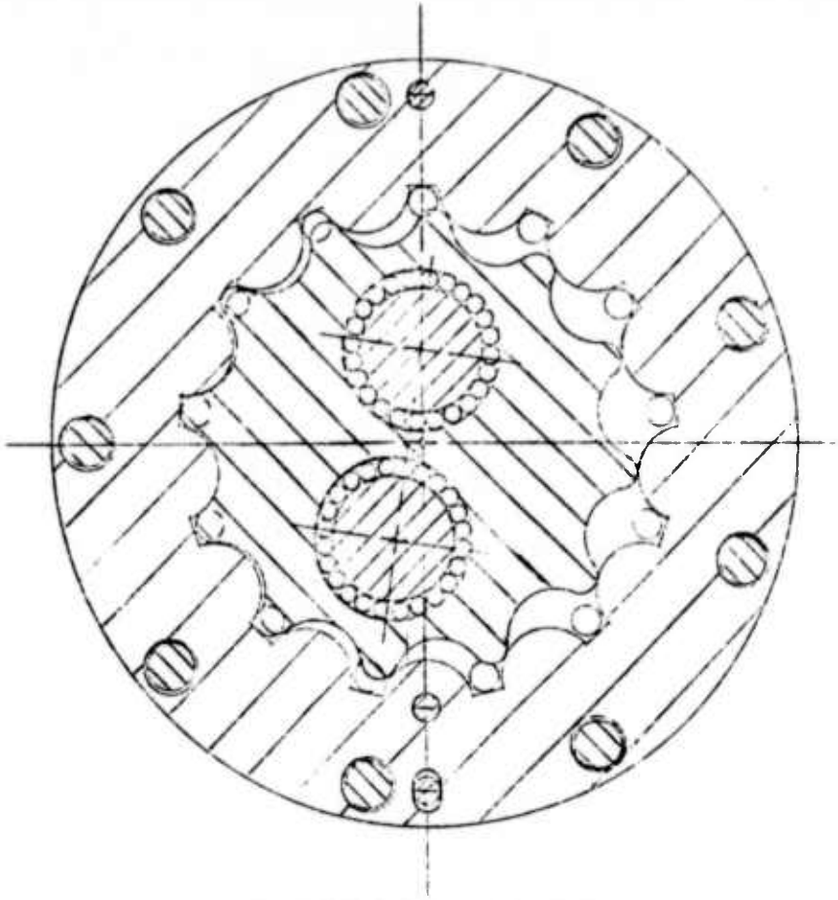

GEROTOR DETAIL

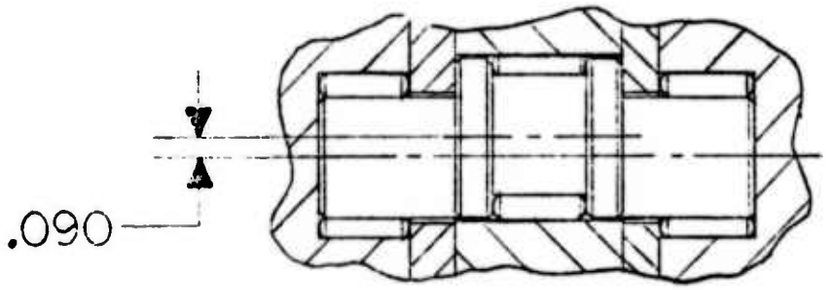

ECCENTRIC CRANK DETAIL

Figure VII-2
Gerotor Hydraulic Motor Details

to preserve the rotation of the rotor. This feature not only eliminates the backlash but also makes the motor mechanically stiffer and more compact.

The initial design was for a motor that would produce approximately 625 Nt-m of torque at a working pressure of 17.5×10^6 Pascals (460 ft-lb_f at 2500 PSI). This estimated torque is found quite easily by multiplying the fluid displacement per radian rotation of the output shaft by the working pressure. The working pressure is the pump pressure minus an estimated pressure drop due to losses in the fluid lines and the servo valve. This pressure drop is proportional in a non-linear manner to the flow rate and the servo valve opening. The other parameter of interest is the actuator stiffness which, along with the arm inertia, is needed to predict the open loop resonant frequency. The compliance of the actuator is largely due to the bulk modulus of the hydraulic fluid. Other factors that may contribute are hydraulic line compliances and output shaft torsional compliance, etc. As the servo valves are mounted directly on the actuators and the shaft stiffness is treated in the section on structural stiffness, only the compliance due to the bulk modulus is treated here. For a piston type hydraulic actuator it can be shown* that the stiffness is

$$K = \frac{2\beta A^2}{V_i}$$

where β is the hydraulic fluid bulk modulus in Pascals (or PSI), A is piston area in square meters (or sq. in.) and V_i is the fluid volume between one side of the piston and the servo when the piston is centered in cubic meters (or cu. in.). For a rotary actuator or a motor, this becomes

$$K = \frac{2\beta D_r^2}{V_i}$$

where D_r is the displacement per radian in cubic meters (or cu. in.).

* See Fluid Power Control by Blackburn, Reethof, and Shearer, M. I. T. Press, 1960, pages 510-516.

For a non-orbital motor V_i becomes πD_r assuming that the non-displaced volume is neglible (this may or may not be a good assumption depending on the motor design). For an orbital type motor

$$V_i = \frac{\pi D_r}{n_r}$$

which again makes the assumption that the non-displaced volume is neglible, a fairly good assumption for the motor that was designed. Thus, the stiffness is given by

$$K = \frac{2\beta n_r D_r}{\pi}$$

For motors of equal displacement per radian and thus equal output torque at a given pressure, the stiffness of the orbital motor will be greater than that of a non-orbital hydraulic motor by a factor of n_r. For a single vane actuator

$$V_i = \frac{RD_r}{2}$$

and

$$K = \frac{4\beta D_r}{R}$$

where R is the maximum rotation of the actuator in radians.

Using 1.5×10^9 Pascals ($\sim$ 220,000 PSI) as the bulk modulus (the actual bulk modulus for phosphate ester is 2.67×10^9 Pascals or 387,000 PSI) and with n_r equal to 12 and D_r equal to 35.7×10^{-6} cubic meters per radian ($\sim$ 2.2 cu in/rad), the open loop stiffness for the designed orbital motor is

$$K = 4.1 \times 10^5 \text{Nt-m/rad} (\sim 3 \times 10^5 \text{ ft-lb/rad})$$

While the orbital hydraulic motor inherently has a much higher torque density (torque to weight ratio) and a much higher stiffness than a non-orbital motor or a rotary actuator, it was decided that there would be less risk in placing the primary emphasis on the design of single vane rotary actuators for the arm. The main design problem with the orbital motor was in determining the tolerances and clearances to allow it

to run smoothly but not leak excessively. Although the orbital motor would have superior performance it would probably require more of a development effort. A further problem was that there was only one source for the precision gerotor elements and they would not promise quick delivery on anything not normally stocked even though the tooling existed.

The design of the single vane hydraulic actuator is similar in principle to that of the commercially available vane actuators. However, as commercial actuators designed for high pressure hydraulics were not available in a range of sizes suitable for use as wrist actuators, it was necessary to design our own vane actuators. Also by designing special actuators, several very important advantages could be realized. The most important functional difference is that our design has no seals except for low pressure seals on the output shafts, and relies on close tolerances between the vane and the housing to maintain low leakage rates. Eliminating the seals eliminates the principal source of friction in the actuator and will allow smoother control. The other important functional difference is that the position transducer - a pancake resolver with a single speed and 64 speed winding - is built into the actuator. By designing our own actuators it was also possible to use the actuator cases as part of the arm structure and to use the actuator bearings as the arm bearings in four of the axes (in all cases the actuator bearings also serve as the resolvers' bearings). By accurately sizing the actuators to meet the desired performance specifications it was possible to minimize their weight and overall size. It was also possible to design the servo valve manifold, the cross-over pressure relief valves, the pressure transducer ports and the low pressure drain relief valve and manifolding into the case. See Figure VII-3a and b.

3. Vane Actuator Design Specifications

The specific sizes of the actuators for the different axes were found by computer simulation. See Section IV-B. A somewhat arbitrary performance specification on slew time was used as basis for this simulation as it was believed that the ability to slew rapidly in order to change end effectors or tools and to fetch parts was an important function. The initial specification was that

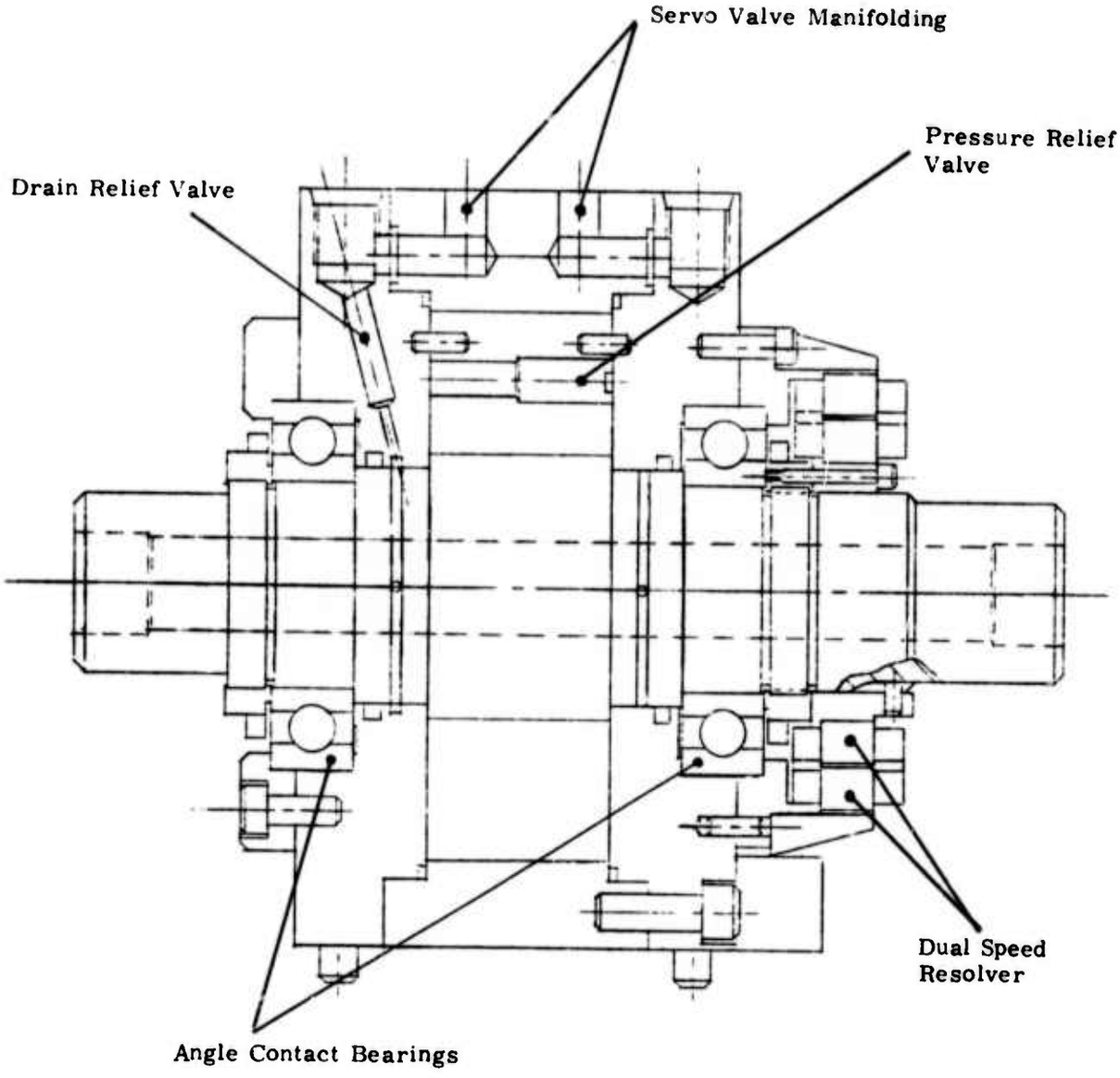

Figure VII-3a Elbow Actuator Layout (sideview)

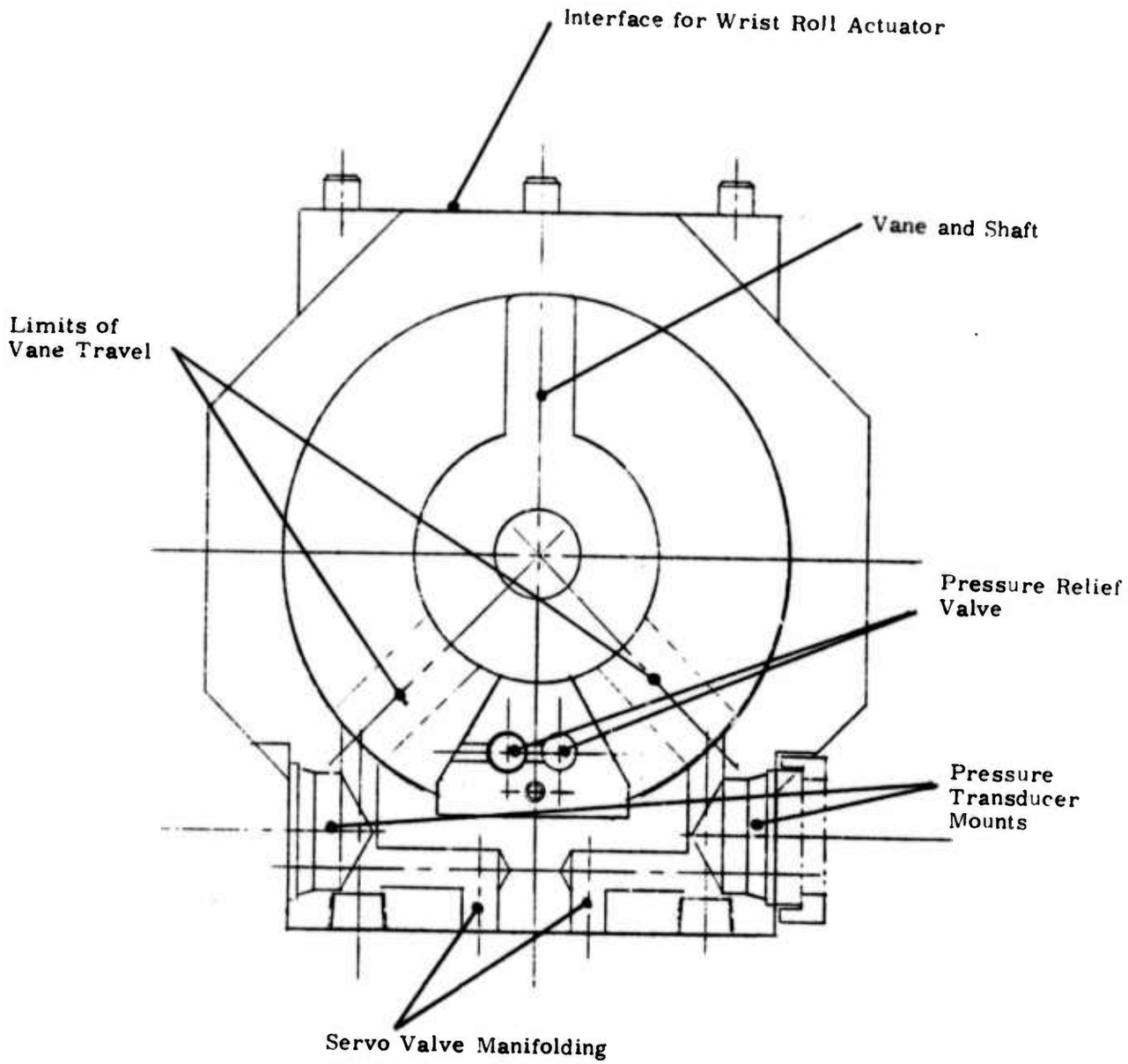

Figure VII-3b Elbow Actuator Layout (endview)

all axes be capable of slewing 1 1/2 radians (~ 90 degrees) in one second with a 10 kilogram load. As the arm would probably slew much more frequently with either no load (to change the end effector or to fetch a new part) or with a light load, the performance specification was changed so all axes would be capable of slewing 1 1/2 radians in 1/2 second with no load. This is a somewhat more stringent requirement for the elbow and shoulder actuators. See Figure IV-1. A model for the mass and inertia was developed, working from the wrist requirements back by estimating the mass for the end effector and wrist structure. This yielded a torque requirement for the wrist actuators. From this, the actuator could be sized and the mass estimated. This, along with the required structure and the previous estimated masses for the end effector and wrist structure, determines the torque requirement for the elbow actuator. Then, knowing the size of the elbow actuator, the torque requirements for the shoulder actuator can be determined. See figure VII-4 for the discrete mass model used for the simulation. The simulation yielded torque requirements of 82 Nt-m (~ 60 ft-lb) for the wrist actuators, 350 Nt-m(~ 260 ft-lb) for the elbow actuator and 690 Nt-m(~510 ft-lb) for the shoulder actuator. For a single vane actuator the torque is given by

$$T = P\ell\left(\frac{r_1^2 - r_2^2}{2}\right)$$

where P is the working pressure (pump pressure minus an allowance for losses), ℓ is the length of the vane, r_1 is the outer radius of the vane and r_2 is the inner radius of the vane. The working pressure was set to 14×10^6 Pascals (~ 2000 PSI) with a pump pressure of 17.5×10^6 Pascals (~ 2500 PSI). The actual dimensions of the shoulder and elbow actuators were set by using the largest possible bearing size (largest bore) consistent with mounting the pancake resolver as both the output shaft torsional stiffness and the bearing radial stiffness were critical. A single pair of 35 mm extra light angle contact bearings (ABEC 7) were used in the elbow actuator and two duplex pairs were used in the shoulder actuators. The inner radius of the vane, r_2, was set at ~2.22 cm (~0.875 in), the outer radius, r_1, was set at ~ 4.60 cm(~ 1.812 in) and the length of the vane for the shoulder actuator was set at ~ 6.34 cm(~2.50 in) while the length of the vane for the

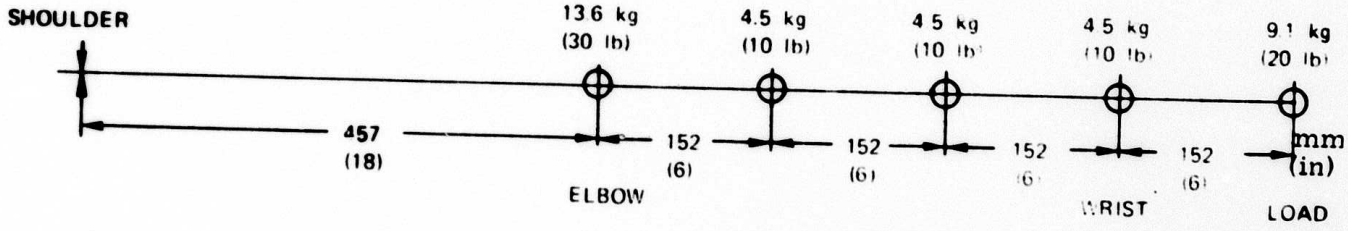

Figure VII-4

Approximate Loading Distribution of
Arm and Load

elbow actuator was set at ~ 3.17 cm(~ 1.25 in). The wrist actuators were designed around a single pair of 25 mm bore extra light angle contact bearings. The inner vane radius, r_2, was set to ~ 1.90 cm (~ 0.75 in), the outer vane radius, r_1, was set to ~ 3.17 cm (~1.25 in), and the vane length was set to ~ 1.90 cm (~ 0.75 in). In order to minimize leakage, the clearances between the vane and the housing were designed to be between 0.008 mm (0.0003 in) and 0.018 mm (0.0007 in). The hydraulic leakage around the vane and through other clearances is given by

$$Q = \frac{wb^3}{12\mu L}(P_1 - P_2)$$

where b is the clearance, w is the total width of the leakage path and L is the length of the leakage path along the flow direction, μ is the absolute viscosity, and $(P_1 - P_2)$ is the pressure difference across the vane. The important parameter is b, as the leakage flow is proportional to the third power of the clearance, i.e., doubling the allowed clearance will increase the leakage eight-fold.

The required servo valve size is determined by the flow rate at the maximum rotation velocity plus the leakage flow. This total flow rate should not cause a pressure drop across the servo valve greater than the pump pressure minus the working pressure or in this case ~ 3.5×10^6 Pascals (~ 500 PSI). If the actuator traverses 1.5 radians in 0.5 seconds, the maximum velocity, assuming a triangular velocity profile, is 6 radians/sec. For the shoulder actuators, the required flow rate is ~0.3×10^{-3} m^3/sec with an allowed pressure drop of 3.5×10^6 Pascals across the servo valve (~ 18 CIS @ 500 PSI pressure drop). A conservative servo valve choice, allowing for a leakage flow with clearances of 0.025 mm (~ 0.001 in) and a hydraulic fluid temperature of 52°C (125°F), is the stock Moog series 34 aerospace servo valve. A Moog series 32 servo valve was specified for the elbow actuator and Moog series 31 servo valves were specified for the wrist actuators. The aerospace valves were selected for their small size and mass at a given flow performance. There is a price penalty but it is not that significant for small quantities (the quantity discount is much higher for the so-called commercial valves).

B. Structure

1. Mechanical Properties

a. Requirements and Materials

The design of the load-carrying members both movable and stationary is constrained by a few important (and interrelated) requirements necessary to achieve the stated system goals. Among these are:

(1) minimum weight
(2) maximum stiffness
(3) sufficient strength and fatigue life
(4) lowest resonance to be above 25 to 30 Hz

The minimum weight property reduces power requirements insofar as the arm is a significant fraction of the total mass. Lower mass means that servo gains can be relaxed somewhat and still obtain reasonable positional accuracy. Lower gain requirements in turn enhance gain and phase margins.

We desire maximum stiffness so we can know where the hand is under varying load conditions. It is desirable to know this without relying on external devices (wrist-trackers) and compensating routines in the software. A stiff arm allows accurate position data with only the use of good encoders or resolvers at the joints.

Sufficient strength is available from a wide variety of materials. Considering the loads we have in mind and the endpoint tolerances, stress is less a problem than strain.

The 25 Hz requirement stems from the relation between servo bandwidth and structural vibration. This is discussed at length in Section IVC.

Table I lists a few candidate materials. To choose on the basis of weight and stiffness, the stiffness/weight ratio is included. On this basis alone, the best material is Beryllium. Without digressing into all the specific problems inherent in the use of Beryllium, one should realize that toxicity, stress-corrosion, cost and reluctance to fabrication are all severe compared to the other candidate materials.

TABLE I - SOME MATERIAL PROPERTIES

Material	Density		Modulus		Yield Strength		Modulus / Density	
	nt/cc	#/in^3	GPa	10^6psi	GPa	10^3psi	m	in
601 Steel	.079	.284	216	30.8	0.70	100	2.56	101
Titanium (6%Al-4%V)	.045	.160	112	16.0	0.84	120	2.54	100
7075-T6 Aluminum	.028	.101	73	10.4	0.51	73	2.64	104
Lockalloy (62%Be-38%Al)	.021	.076	196	28	-	-	9.36	369
Beryllium	.019	.067	294	42	0.28	40	15.9	626
ZK60A-T5 Magnesium	.018	.066	45	6.5	0.28	40	2.48	98
Graphite-Epoxy 45° x 45° layup	.014	.052	98	14	-	-	6.86	270

An important question is whether there is an upper bound to the stiffness requirement independent of materials selection. Other components will incur a certain amount of positional error by themselves, among them: bearing and encoder eccentricity, bearing play and elasticity under load.

We do not need to worry too much about the stiffness of the actuators themselves as long as there is feedback of some kind to compensate for it, and the stored energy component is small.

The thermal properties of the arm should be considered in any serious design effort since changes in temperature can add yet another degree of uncertainty to the structure. Significant heat sources can be realized in electric and hydraulic actuators under high cyclic loading conditions.

Low coefficient of thermal expansion should be a desirable property. For our 90 cm arm made out of, say, aluminum alloy, a 50^{o} C range of uniform arm temperature results in a 3/4 mm length change. More significantly, non-uniform heating of the members can cause greater distortions over smaller temperature changes.

The material finally selected is steel for all load-carrying members, owing to its cost, ease of fabrication, and stiffness. The thin wall sections possible with steel allow potentially greater design freedom for internal components: valves and plumbing. For non-load-bearing parts, aluminum or brass (for fittings) will be used.

b. Structure Design

To meet the 30 Hz resonance requirement, assumptions were made concerning mass distribution and end-point loading. Figure VII-4 illustrates these assumptions. The inertia seen from the shoulder (with the 91 nt [20 #] load) is approximately 21.4 Kg-m^2 (184 in # sec^2). An equivalent inertia can be modeled as a point mass of 25.5 Kg (56.1 #) at the wrist-point, 91 cm (36 in) from the shoulder. This point mass approximation is actually conservative since most of the distributed mass is inboard of the wrist-point.

A 30 Hz natural frequency (f_n) is predicted from a point mass load. The required stiffness,

$$K = m\omega^2 = 900 \text{ nt/mm } (5030 \text{ \#/in})$$

where m = endpoint mass

and ω = angular frequency

With no load present, the inertia drops to 11.1 Kg-m^2 (95 in # sec^2), and f_n = 42 Hz. It is assumed that all vibrational energy is caused by small linear motions of the load. This value of K can be built-in easily by considering an equal-stiffness model of the arm in two sections: upperarm and forearm (Figure VII-5).

Consider the relation between deflexions and area-moments:

$$\text{Total deflexion} = \delta_{1\text{-SHEAR}} + \delta_{2\text{-SHEAR}} + \ell\alpha_{2\text{-SHEAR}} + \delta_{2\text{-MOMENT}} + \ell\alpha_{2\text{-MOMENT}}$$

$$\delta_T = \frac{P\ell^3}{E}\left[\frac{1}{3I_1} + \frac{1}{3I_2} + \frac{1}{2I_2} + \frac{1}{2I_2} + \frac{1}{I_2}\right]$$

$$= \frac{P\ell^3}{E}\left[\frac{1}{3I_1} + \frac{7}{3I_2}\right]$$

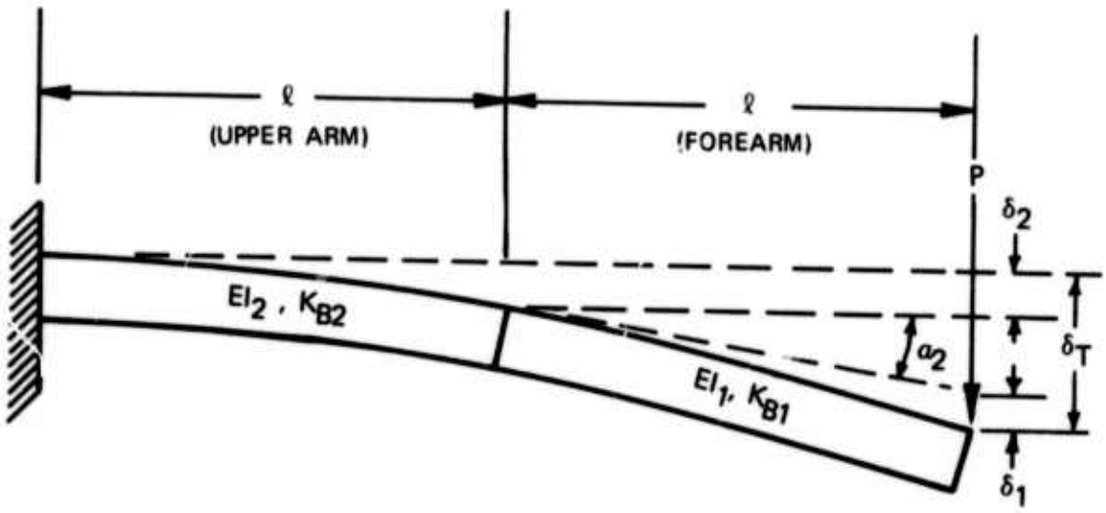

Figure VII-5
Two Part Distributed Stiffness Model of Arm
NOTE: Deflexions shown greatly exaggerated

If we let each section of the beam be equally stiff with respect to the wrist-point,

$$I_2 = 7I_1$$

Values for I_1 and I_2 which satisfy the overall stiffness requirement of 900 nt/mm (5030 #/in) are

$$I_1 = 26.6 \text{ cm}^4 \ (0.65 \text{ in}^4),$$

and

$$I_2 = 187. \text{ cm}^4 \ (4.55 \text{ in}^4).$$

If all sections of the arm structure meet this criterion, we are assured adequate stiffness (in that bending mode at least).

An analogous criterion for torsional stiffness does not exist, since arm payloads and performance have not been defined for rotational (moment) loads. However, one case can be analyzed: when the elbow is cocked 90°, the upper arm is subject to a torsional load caused by payload and arm weight. An equivalent torsional stiffness is now calculated, based on the required lateral stiffness.

When the elbow is bent 90° and a simple load is applied to the wristpoint, three sources of deflextion exist: bending of the forearm, bending of the upper arm, and torsion of the upper arm due to the moment loads that previously applied to bending. Since the upper arm is much stiffer than the forearm, we will ignore this source of deflexion. The stiffness of the forearm alone is just twice the overall bending stiffness (since the deflexions of each member in bending were set equal to each other). The effective lateral stiffness at the wristpoint due to torsional rigidity of the upperarm is just

$$K = K_t/\ell^2 = 1800 \text{ nt/mm } (10.6 \text{ \#/mil})$$

We can solve for the required polar moment of inertia of the upper arm like so:

$$I_p = \frac{K_t \ell}{G} = 252 \text{ cm}^4 \ (6.15 \text{ in}^4)$$

where G = shear modulus, 70GPa (10^7 psi),
and ℓ = upperarm length = forearm length.

For reasonable cross sections, $I_p \approx I_{xx} + I_{yy}$, thus insuring us of adequate torsional stiffness if the lateral criterion is met.

An additional bending mode requires treatment, however, parallel bending of yoke-type elements pictured in Figure VII-6. These elements appear at every joint except azimuth and wrist roll (joints 1 and 4, counting from the shoulder). While these elements are stiff with respect to lateral bending, they are not necessarily adequate in parallel bending. To assure sufficient stiffness we require that the sum of the parallel compliance and lateral compliance of the separate sections be less than or equal to the required lateral compliance assumed adequate:

$$Y_{TL} \geq Y_L + Y_1$$

or

$$\frac{\ell^3}{3EI} \geq \frac{(\ell - y)^3}{3EI} + \frac{y^3}{24EI_1}$$

$$I_1 \geq \frac{I \quad y^3}{8(y^3 - 3\ell y^2 + 3\ell^2 y)}$$

where ℓ = total beam length, forearm or upperarm
y = yoke length
I = sufficient lateral area-moment
I_1 = required parallel area-moment of one yoke side

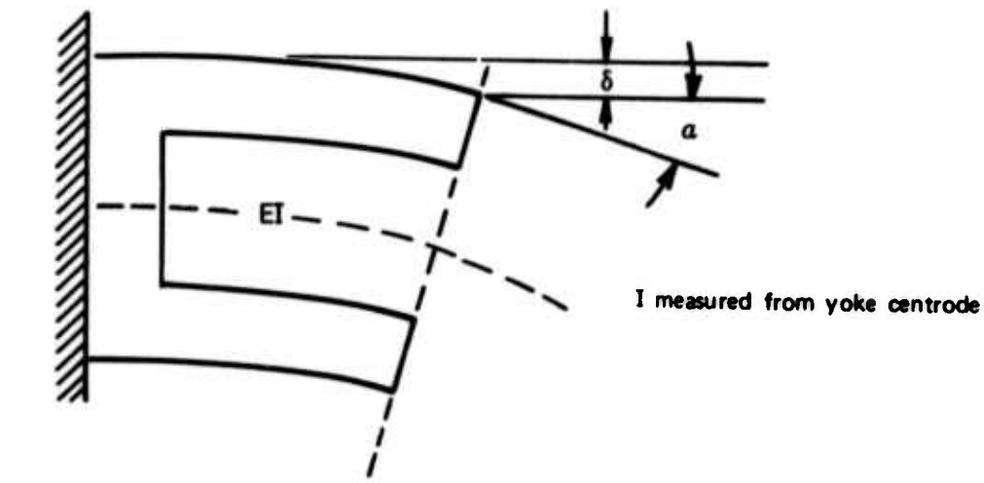

LATERAL BENDING

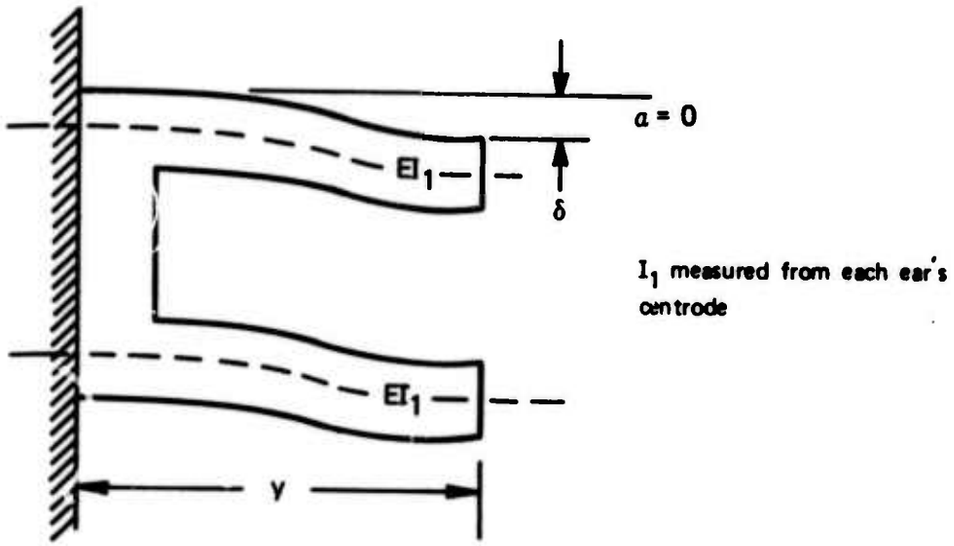

PARALLEL BENDING

Figure VII-6
Lateral and Parallel Bending Modes of Yokes

A similar expression can be derived for sections with more than one yoke.

For the dimensions typical of this arm,

$$I_1 \approx I/150,$$

and this requirement is easily met by the designer.

In addition to the above, the torsional stiffness of the yokes must be checked against that derived for the upper arm member. Referring to figure VII- 7 , torsion of a yoke may be divided into axial twist along each ear plus bending along its "stiff" axis, thus:

$$K_t \geq Kr^2$$

r = radial distance to ear centrode, since the ears are relatively weak in axial twist. To obtain an adequate K_t as noted above, $r^2 \geq 51$ mm (2 in). For all proposed yokes, this condition is automatically met.

c. Support & Worktable

In the section on "Configuration" (IV B) an over-the-work type mounting arrangement was indicated. A straightforward support for the arm was designed as shown in Figure IV- 8 . The rigidity of the members was determined by the > 30 Hz vibration criterion, and the assumption that the support should be "overbuilt" in that respect.

The inertial load seen by the horizontal members is approximately 750 in#sec^2; for a 100 Hz f_n, a stiffness, K_t, of 3 x 10^8 in#/rad is indicated. Since

$$I = \frac{K_t \ell}{3E},$$

we require an area moment of at least 80 in^4. This is easily obtained with a 10" square by 1/2" wall welded steel box beam.

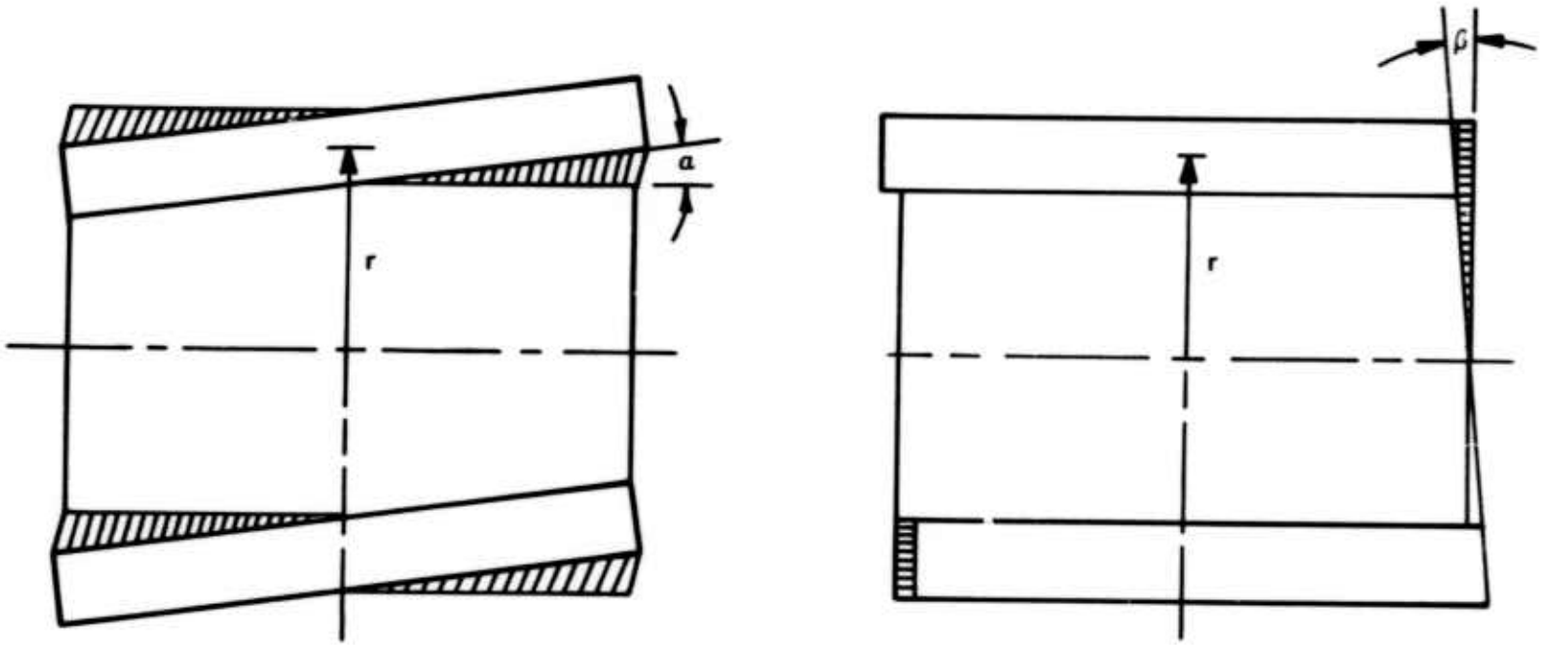

AXIAL TWIST
(end view)

LATERAL BENDING
(end view)

Figure VII-7

Components of Torsional Bending
of Yoke

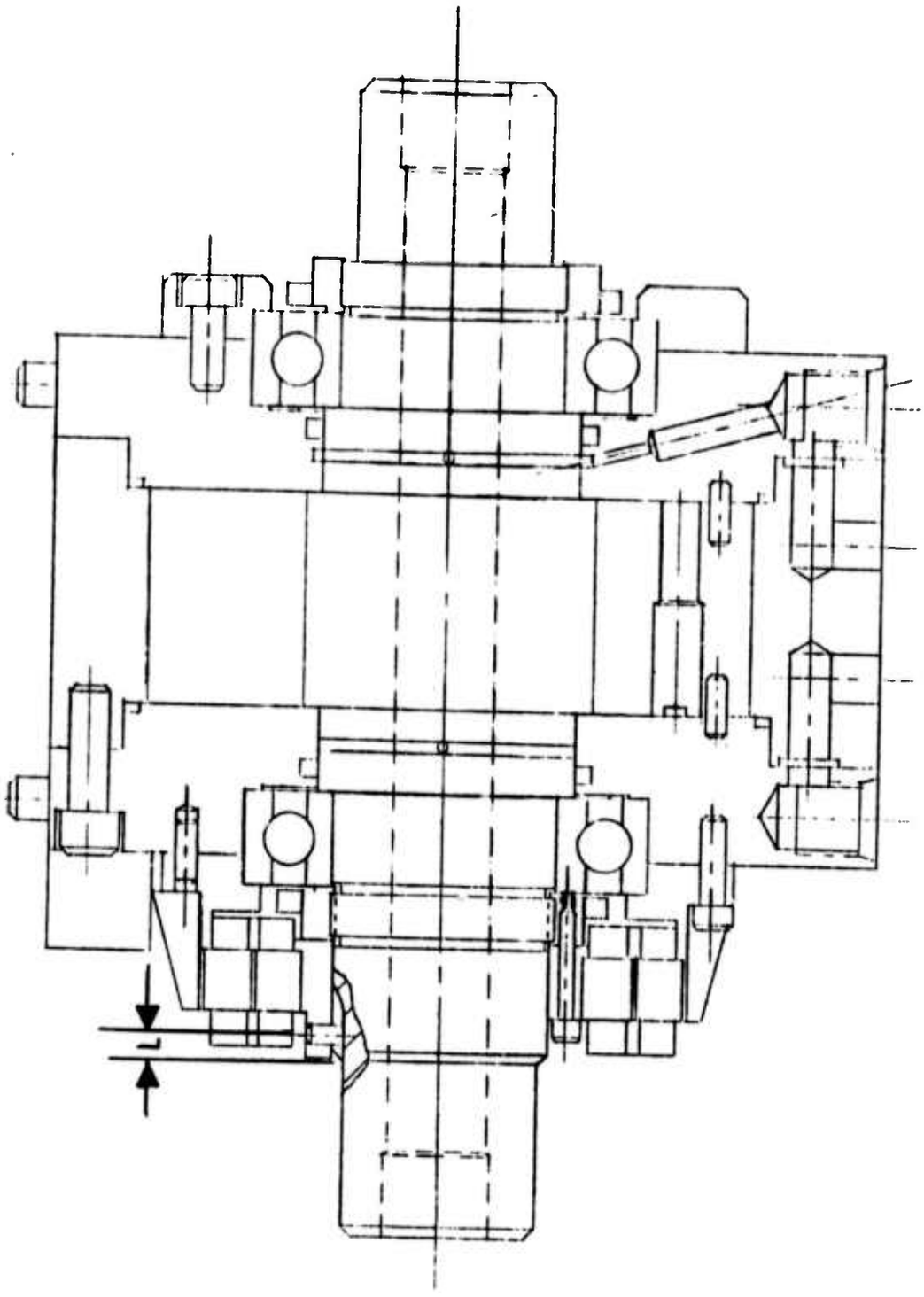

Figure VII-8
Schematic Actuator Design Showing Resolver Mounting

Similarly, the load seen by the vertical member (in bending) is approximately 5300 in#sec^2, where at 100 Hz, $K_t = 21 \times 10^8$ in#/rad. Thus, I must be at least 150 in^4. This is easily obtained with a 12" square x 1/2" wall box beam.

Checking the torsional loading, the inertia seen by the vertical member $\approx$ 810 in#sec^2. Over a length of 60", a stiffness of about 2×10^8 in#/radian is present, thus making ω_n = 500 rad/sec, or about 80 Hz. It is important for the users to consider (1) additional loads that the vertical beam will see in torsion, (2) resonant length of the beam caused by changes in mounting distance.

The worktable upon which the support is mounted may also be a significant source of compliance. As originally ordered, the table consisted of a 48" x 60" x 1" steel plate supported in a thin (1/4" thick) sheet steel frame. The inertial load seen at the base of the upright column is approximately 3400 in#sec^2 without the arm present.

The frame contributed little stiffness to the ensemble and thus several bending (vibrational) modes of the table top (due to the mounted support) were observed:

(1) Bending, lateral axis; $K_x = 4 \times 10^6$ in#/rad, $I_{xx} = 4$ in^4, $f_n = 10$ Hz.

(2) Bending, longitudinal axis; $K_y = 15 \times 10^6$ in#/rad, $I_{yy} = 5$ in^4, $f_n = 10$ Hz.

(3) Torsion, longitudinal axis; $K_t = 2.6 \times 10^6$ in#/rad, $f_n = 4$ Hz, applicable only if table lifts off floor.

Additional stiffeners have been designed, and once installed (under the table-top) the lateral and longitudinal frequencies will each be up to about 100 Hz.

d. Shafts & Couplings

Throughout the discussion on stiffness and natural frequency so far we have been considering the "locked joint" compliances. This is an idealization based on the design of servo controls for the system. More precisely, the term "locked joint compliance" refers to non-instrumented compliances: those not measurable by the angle readout sensors. To illustrate several of these we will consider a typical actuator assembly, Figure VII-8.

Readout sensors (pancake resolvers in this case) are mounted concentrically about the actuator shaft; they are denoted "S" for stator, "R" for rotor. A yoke is coupled to the protruding ends of the shaft, while the motor case is mounted to an arm member. Under loading, the resolver will read the shaft angle, but this will differ from the yoke angle by the small twist due to windup of the shaft between the yoke and rotor. In terms of the compliances we have been considering, we require that the shaft windup be small compared to arm deflexions, or:

$$\frac{\ell}{2GI_p} << \frac{1}{Kr^2}$$

where I_p = polar moment of inertia of shaft

ℓ = length of shaft between yoke and rotor

G = shear modulus

K = required arm stiffness, #/in

r = distance from shaft to wristpoint

For the elbow actuator,

$$\frac{\ell}{I_p} << 12.4 \text{ in}^3$$

The actuator features $I_p \approx 0.2$ in^4, and $\ell \approx 0.2$ in; thus, $I_p/\ell \approx 1$, and the constraint is reasonably well satisfied. Similar requirements exist at the other joints, and the shaft sizes and mounting distances reflect this.

Other compliances exist beyond the scope of measurement by the resolvers, e.g., axial and radial bearing compliance. Choice of bearings effects overall stiffness considerably, and the ideal 5000#/in figure will be degraded to some extent. An analysis of this situation revealed that the bearings chosen (practically the largest possible given the present actuator design) contribute large concentrated compliances. The overall effect can be (very) conservatively estimated by summing the compliances of each bearing set and the structural compliance. The result indicates a natural frequency of about 19 Hz, when the arm is loaded with 9.1 Kg (20 #). Unloaded, the estimate is 27 Hz.

A more detailed treatment of this problem appears in Section III of Ref. (2).

Several requirements were enumerated for the shaft couplings that tie the actuators to the arm members:

(1) must transmit required torque safely
(2) must have short axial dimension
(3) must be rigid
(4) should be easily installed, aligned, disassembled

Tapers, press-fit splines, expanding keys and other possibilities were investigated. The device adopted was an expandable locking ring assembly manufactured in a wide range of standard sizes. (Figure VII-9).

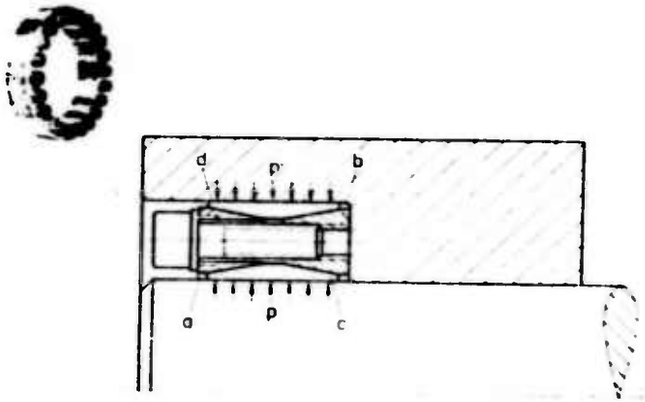

As the socket head cap screws of the LOCKING ASSEMBLY are tightened by a torque wrench, the double tapered thrust rings (a, b) are pulled towards each other, thus exerting predetermined radial clamping pressures (p) on the slit inner (c) and outer (d) rings. These clamping pressures then create a positive frictional connection. Whenever you decide to disassemble or adjust this connection, unscrew the cap screws and the parts can be then removed or adjusted.

Figure VII-9

RINGFEDER® System LOCKING ASSEMBLIES

C. Sensors

1. Angle Sensors

The position of the assembler arm is determined by the measurement of the six joint angles and a knowledge of the geometry of the arm. The measurement devices that were chosen are dual speed resolvers. The decision to use resolvers was made after comparisons with other kinds of angle sensors, including potentiometers and optical encoders.

Among the criteria considered were:

Accuracy - 1 part in 2^{16} desired (20 arc seconds)
Resolution - could motions smaller than $1/2^{16}$ be detected?
Analog or Digital Output
Absolute or Incremental Output
Physical Configuration
Mechanical Coupling - no form of gearing was considered acceptable
Cost and Delivery
Future Technological Prospects
Slew Speed
Environmental Sensitivity

Potentiometers:

Advantages

Potentiometers offer the advantages of low cost, availability, theoretically unlimited resolution, and convenient interfacing (requiring an A/D convertor).

Disadvantages

The major disadvantages are limited life due to contact wear, and an accuracy of only one part in 2^{10} to 2^{12} (10 to 12 binary bits). On the basis of accuracy, potentiometers were eliminated.

Absolute Optical Encoders:

Advantages

From the viewpoint of interfacing to a computer, absolute optical encoders are the most convenient choice. The output is in binary form and requires the simplest of interfaces. Units with an accuracy of 16 bits are available.

Disadvantages

The physical configuration is awkward to use, especially at the wrist joints. Typically, such encoders are cylindrical with a diameter of about 3", and a length of more than 5". Another negative factor is susceptibility to noise, which could be a severe problem in an industrial environment. The decisive factor, however, which eliminated absolute optical encoders from further consideration, was their prohibitive cost. For full 16 bit encoders, with no internal mechanical gearing, the price quoted was $5500 per axis. Furthermore, it does not appear likely that technological improvements will lower this price significantly in the future.

Incremental Optical Encoders:

Advantages

Incremental optical encoders offer the same accuracy as absolute types at a fraction of their cost ($1600 for a 16 bit unit). The only conversion electronics necessary are Up/Down counters to receive the digital output pulses.

Disadvantages

As with the absolute type, the encoder package is bulky. Noise immunity is an even greater problem. Missed count pulses, or glitches causing extra pulses cause errors that carry over to all subsequent readings, until the system is reinitialized. Large errors can quickly accumulate in this manner. A momentary loss of power results in total loss of angle information, which could be catastrophic in this application.

Resolvers:

Advantages

Resolvers, like potentiometers, have infinite resolution. Accuracy of single speed units is limited to about 13 or 14 bits, but multispeed resolvers (a form of electrical "gearing") can easily obtain accuracies of 16 bits and better. Cost is generally less than incremental optical encoders, especially in production quantities. Shaft mounting is extremely convenient, with resolvers that come in the "pancake" type package.

The technological prospects for resolvers are also very good. A recent development is the printed pattern resolver, which appears to be promising for multispeed units. Formerly, printed pattern resolvers suffered from poor transformation ratios — ratio of output signal to input voltage. Improvements in design, however, have resulted in a very acceptable ratio of .7/1. The advantages of printed pattern resolvers are very low cost, small size, and the possibility of making the resolver an integral part of the actuator shaft.

Disadvantages

Of all the angle sensors considered, resolvers are the most difficult to interface to a computer. Complex convertors are needed to derive a digital value from the resolver outputs. The cost of commercially available convertors can exceed the cost of the resolver. Several resolvers can be multiplexed to a single convertor, but only at the expense of the information update rate.

An additional problem with mult speed resolvers is an ambiguity in the output. A 64x resolver, for example, has an output that goes through 64 electrical cycles for each shaft revolution. A particular output can therefore correspond to any of 64 different shaft angles. One method of resolving this ambiguity is to count the cycles as the shaft rotates. This is essentially an incremental method, and suffers from some of the drawbacks of incremental measurements. More reliable is the addition

of a single speed resolver for the coarse measurement, leaving fine measurement to the multispeed resolver. The penalty of this method is the extra cost for the additional resolver and convertor electronics.

After much consideration of the above factors, a decision was reached to use dual speed resolvers, each consisting of a single speed and a 64x resolver mounted in a single pancake shaped package. The 1x resolver provides the 6 most significant bits of angle measurement, while the 64x unit measures an additional 12 bits. Of the total 18 bits, 16 are read by the computer.

Each resolver has a separate resolver/digital convertor, allowing frequent position updates and the tracking of high speed slewing motions. The convertors are not commercial units, but rather a special in house design. Cost is under $100 per axis. The six dual speed resolvers are $1250 each in small quantities. This would drop to $450 each in lots of 100.

2. Phase-Locked Loop Resolver to Digital Convertor

The decision to use dual speed resolvers for angular measurement was based in part upon the ability to build the resolver to digital convertors in house. Commercially available convertors are generally complex, and, as noted above, even more expensive than the resolvers. At the C. S. Draper Laboratory, however, research and development in phase-locked loop circuitry has resulted in the design of a PLL resolver to digital convertor. This convertor circuit is simpler, and less expensive than conventional methods, and will often have better performance.

The basic operation of the convertor is shown in Figure VII-10. The inputs are the resolver modulated signals, $\cos\theta \cos(wt)$ and $\sin\theta \cos(wt)$. θ is the shaft angle, and the cos (wt) carrier term is the resolver excitation, a 1 kilohertz sine wave. The purpose of the convertor is to generate the arc tangent of the ratio of the two inputs.

$$\theta = \text{arc tangent}\left(\frac{\sin\theta \cos wt}{\cos\theta \cos wt}\right)$$

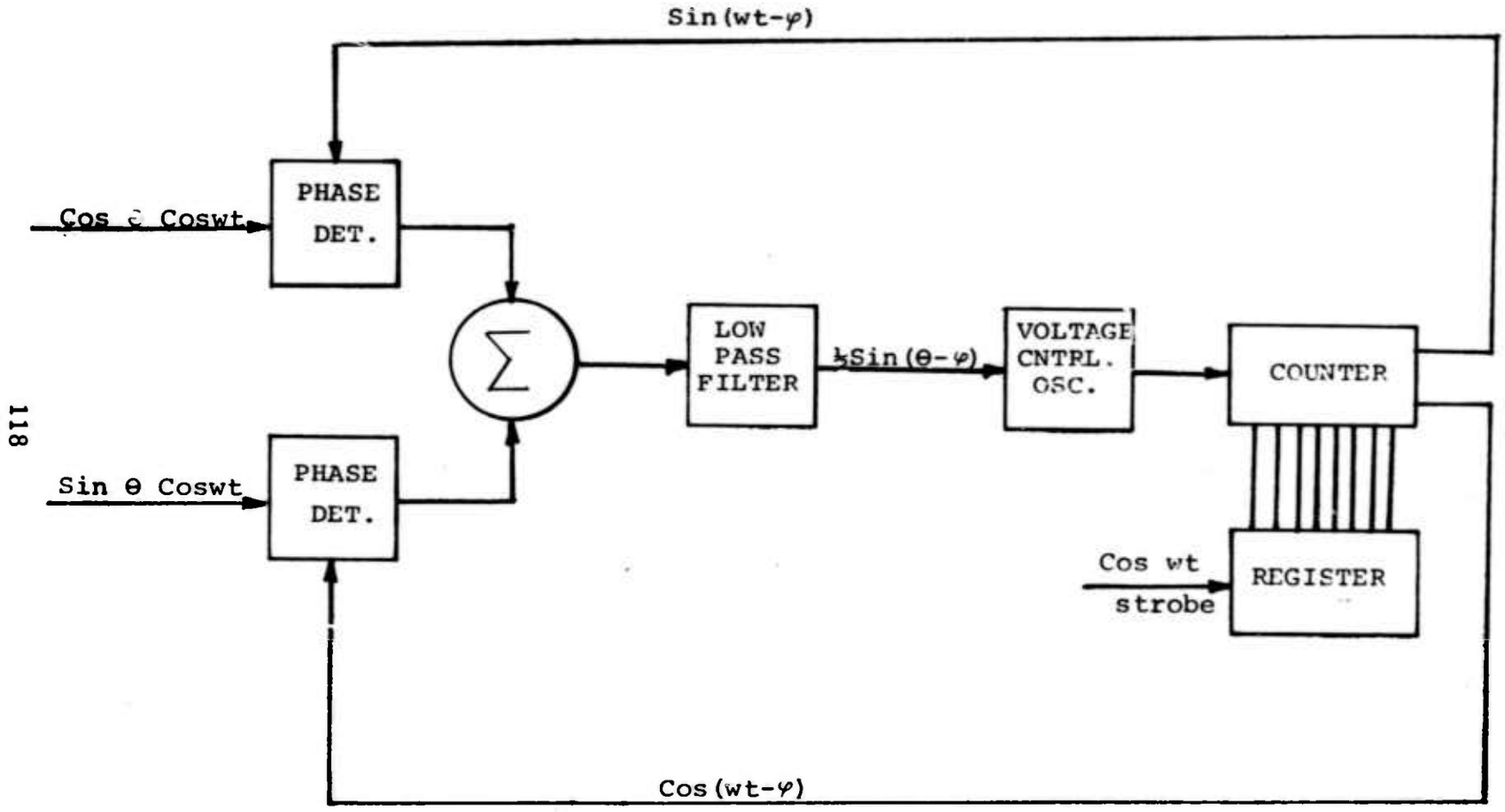

Figure VII-10
Phase-locked Loop Convertor

The novel feature of this phase-locked loop circuit is the use of two phase detectors and two feedback loops. The output of the phase detectors is the product of their inputs, cos (wt) [cos θ sin(wt-φ)] and cos (wt) [sin θ cos(wt-φ)]. These are summed to produce:

$$1/2 \sin(2wt+\theta-\varphi) + 1/2 \sin(\theta-\varphi)$$

The filter passes only the D. C. term, $1/2 \sin(\theta-\varphi)$. This is the error signal in the loop, which controls the VCO output phase and frequency. The servo action of the loop drives the error term to zero by making φ, the loop phase shift, equal to θ, the resolver shaft angle. The phase to digital conversion of φ is then performed by a standard technique of inserting a counter in the feedback loop, and strobing its contents into a register when the reference, cos(wt), has a phase of zero.

By including an integrator in the filter network, a type II servo is created. This enables the tracking of both constant positions and constant velocities with negligible loop error. An extra bonus is the fact that the loop error signal is proportional to $d\theta/dt$, making it equivalent to a tachometer signal. This tach signal can be used in analog compensation networks for controlling the hydraulic actuators.

One feature of this circuit that is characteristic of all phase-locked loops is that there is a filtering effect upon the signal. This is partly desirable, since it reduces the level of noise. The narrower the bandwidth the greater the noise attenuation. This results in a design trade-off, however, since a wide bandwidth is necessary for a fast response to changing inputs. Through testing, a suitable compromise value was achieved. The convertor's characteristics are similar to that of a second order low pass system, with a break frequency of about 60 hertz, damping of .7, and a 40 db/decade high frequency roll off. This size bandwidth is wide compared to the assembler's, yet is sufficiently narrow to filter out most noise.

Each of the six dual speed requires two PLL convertors. The convertor for the 64X resolver has a 12 bit output, while the 1X unit produces 7 bits, of which the least significant is an overlap bit for the MSB of the 64X section. Additional logic combines the two outputs into a single 18 bit word. The 16 most significant of these are available to the computer.

3. Force Sensors

a. System Considerations

One device which is being studied in the current research is a six degree of freedom force sensor. This device can be used between the arm and the hand of a manipulator/assembler, or it may be used in a pedestal form as part of the work mounting. The following analysis covers some of the general considerations of the use of this type of device.

General Case

Suppose that forces, pressures, and moments are applied to a rigid body mounted on a force sensor. This corresponds to the case of a pedestal force sensor. These forces, pressures, and moments can be summed (or integrated) to find a resultant applied moment Ma plus a resultant applied force Fa. There is also a gravitationally induced force mg, acting downward and located at the center of mass:

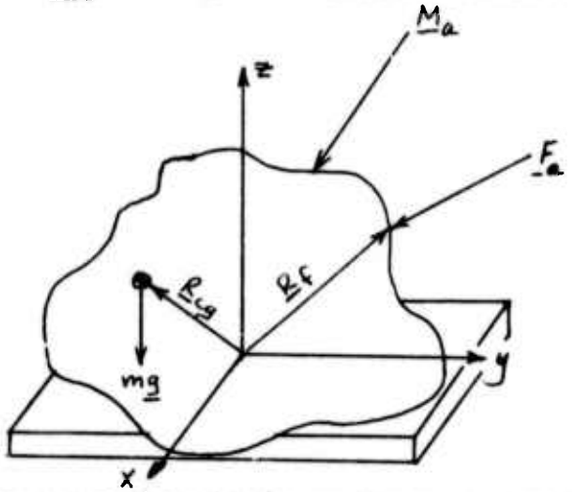

Figure VII-11
Work Object Mounted on a Force Sensor

Now suppose that the force sensor is instrumented in a coordinate system, xyz, and that the sensed forces and moments are read as Fs and Ms. Also, define the location vector of the center of mass as Rcg, and the location vector of the resultant applied force as Rf. We then have:

$$Fs = mg + Fa \qquad \text{VII-1}$$

and

$$Ms = mg \times Rcg + Fa \times Rf + Ma \qquad \text{VII-2}$$

Obviously the vectors in VII-1 and VII-2 have dimensionality 3.

It is possible to evaluate the terms in mg, by letting Fa and Ma go to zero. This corresponds to removing the arm from contact with the body. We then have:

$$\underline{Fs} = \underline{mg} \qquad \text{VII-3}$$

$$\underline{Ms} = \underline{mg} \times \underline{Rcg} \qquad \text{VII-4}$$

VII-3 and VII-4 can be combined into VII-1 and VII-2, moving the known quantities to the right hand side of the equations, and the quantities to be determined to the left. The result is:

$$\underline{Fa} = \underline{Fs} - \underline{mg} \qquad \text{VII-5}$$

and

$$\underline{Ma} + \underline{Fa} \times \underline{Rf} = \underline{Ms} - \underline{mg} \times \underline{Rcg} \qquad \text{VII-6}$$

VII-5 and VII-6 can be coordinatized in xyz to obtain

$$\begin{bmatrix} Fax \\ Fay \\ Faz \end{bmatrix} = \begin{bmatrix} Fsx \\ Fsy \\ Fsz - mg \end{bmatrix} \qquad \text{VII-7}$$

$$\begin{bmatrix} Max \\ May \\ Maz \end{bmatrix} + \begin{bmatrix} -Faz\ Rfy + Fay\ Rfz \\ Faz\ Rfx - Fax\ Rfz \\ -Fay\ Rfx + Fax\ Rfy \end{bmatrix} = \begin{bmatrix} Msx \\ Msy \\ Msz \end{bmatrix} - \begin{bmatrix} -mg\ Rcgy \\ mg\ Rcgx \\ 0 \end{bmatrix} \qquad \text{VII-8}$$

VII-7 and VII-8 show that Fa can be evaluated in all cases. However, Ma cannot be evaluated without additional information since Eq. VII-8 is insufficiently specified. We can substitute the three components of Fa as found from VII-7 into Eq. VII-8, and are left with three equations in six unknowns. (The unknowns are Max, May, Maz, and Rfx, Rfy, and Rfz.) No solution can be obtained, which is tantamount to saying that the location of the applied force and the applied moment vector are both indeterminate unless additional information besides the output of the force sensor is available. Some possible cases which allow a complete solution are:

Zero Applied Moment

The nature of the contact applied to the body may be such that only a force is induced. In this case, the sensed moment arises from the applied force. In this case, the appropriate equations are:

$$\begin{bmatrix} 0 & -Faz & Fay \\ Faz & 0 & -Fax \\ -Fay & Fax & 0 \end{bmatrix} \begin{bmatrix} Rfx \\ Rfy \\ Rfz \end{bmatrix} = \begin{bmatrix} Msx - mg\ Rcgy \\ Msy - mg\ Rcgx \\ 0 \end{bmatrix} \qquad \text{VII-9}$$

This is to be solved for the Rf vector, but the coefficient matrix is singular. However, physical consideration shows that a line on which the point of action of the force lies can be determined, since the moment and the force are both known.

Force Application Point Known

It may be that the point of force application is known, either from the body/arm geometry, or from measurements of the joint angles. If this is true, it is possible to specify something about both the applied force and the applied moment. Under these conditions the equations become:

$$\begin{bmatrix} Max \\ May \\ Maz \end{bmatrix} = \begin{bmatrix} \text{known} \\ \text{quantities} \\ \text{from VII-8} \end{bmatrix} \qquad \text{VII-10}$$

Response to Gravitation

It is instructive to coordinatize VII-3 and VII-4. The result is

$$\begin{bmatrix} Fsx \\ Fsy \\ Fsz \end{bmatrix} = \begin{bmatrix} 0 \\ 0 \\ -mg \end{bmatrix} \qquad \text{VII-11}$$

$$\begin{bmatrix} Msx \\ Msy \\ Msz \end{bmatrix} = \begin{bmatrix} -mg\ Rcgy \\ mg\ Rcgx \\ 0 \end{bmatrix} \qquad \text{VII-12}$$

Note that no information is given about Rcgz. This is to be expected since the sensed moment is independent of the vertical location.

Conclusion

The above equations indicate the amount of information available from a force sensor. The analysis is similar, independent of whether the sensor is mounted on a pedestal or on a wrist, but the coordinatization and the orientation of the mg term are different in the two cases. It is also true that in the case of the wrist sensor, in general the application point is on or near the z axis of the sensor, with corresponding effects on the components which appear in the equations. However, in the wrist case, the orientation of the mg vector is arbitrary, as contrasted with the pedestal case, in which the orientation of the mg vector is known to be in the sensor z direction.

b. Arm Force Sensing by Joint Torque Measurement

Description of the Method

If the torques in the arm joints can be sensed, it is possible to calculate the hand contact forces using the analysis in the following sections. The advantage of doing this is that the necessity for a separate sensor no longer exists, and the cost and space requirements are saved. The disadvantage is that the available sensitivity may be less, since the desired forces have to be separated from the friction forces which are unwanted. In order to perform this separation, the desired forces should be sufficiently large to permit easy separation. The exact force levels which can be measured in this system will have to be determined by experiments, but it may be possible to make a partial analytic prediction. The joint torque system is especially adapted to the Draper Laboratory arm, because the Draper Lab arm is designed to use low friction hydraulic actuators, since the vane motors are designed to be used with non-contacting vanes, permitting a slight leakage between the vanes and the housings. Under these conditions, the torque developed is given quite closely by the pressure differential between the two sides of the vane. It is then possible to measure the forces/torques developed on

the work by the following analysis.

Calculation of the Hand Forces

The problem is the determination of an arm joint torque vector which will give rise to a specified force (and torque) vector at the hand. A simple and direct derivation follows: Let $\underline{dx}$ be a small motion of the hand, expressed in hand coordinates, $\underline{d\theta}$ the corresponding joint motions, and $\underline{J}$ the Jacobian matrix of the arm. If the arm structure is sufficiently stiff, then

$$\underline{dx} = \underline{J}\,\underline{d\theta} \qquad \text{VII-13}$$

If this displacement is the result of a force vector applied to the hand, the energy developed must go into the joint drivers, thus:

$$\underline{f}^t\,\underline{J}\,\underline{d\theta} = \underline{T}^t\,\underline{d\theta} \qquad \text{VII-14}$$

Since the angular displacement vector $d\theta$ is independent, it follows that

$$\underline{f}^t\,\underline{J} = \underline{T}^t \qquad \text{VII-15}$$

which can be transposed to

$$\underline{J}^t\,\underline{f} = \underline{T} \qquad \text{VII-16}$$

the desired result.

Note that the present derivation implies linearity. This means that it can only be applied if the arm stiffness is sufficiently great that $\underline{J}$ is essentially constant under the application of the force and torque vectors $\underline{f}$ and $\underline{T}$.

Now suppose that the arm joints are instrumented to read their torques as vector $\underline{T}$. In the case of hydraulic actuators, the torque can be measured as a pressure difference, while in the case of electric motors, the torque may be measured as a current. Then, considering equation VII-15 we can postmultiply by $\underline{J}^{-1}$ to obtain the applied force

$$\underline{f}^t = \underline{T}^t\,\underline{J}^{-1} \qquad \text{VII-17}$$

* See Ref. 8.

J^{-1} is available since it is computed to obtain desired effects in hand coordinates. Since T is hypothesized to be instrumented, the simple multiplication in VII-17 is all that is required to obtain the desired force vector. Also note that if $\underline{T}$ is contaminated by an error $\underline{E}_t$ the corresponding error in the computed force is given by

$$\underline{E}_f^t = \underline{E}_t^t \underline{J}^{-1} \qquad \text{VII-18}$$

In the presence of gravity, the above equations apply to deviations from the nominal forces and torques due to gravity.

Engineering Considerations

If pressure sensors are applied to the two sides of a vane-type or other hydraulic actuator, it is possible to define the torque as

$$T_n = K_n(P_{2n} - P_{1n}) \qquad \text{VII-19}$$

Errors in the torques are primarily caused by errors in the pressure sensors, and also by friction in the joint. The joint friction can be resolved into components proportional to the various force components applied to the joints, plus any stick effects which may coexist.

A friction coefficient matrix for any actual proposed joint can be measured or calculated from specs. Once this matrix is known it is simple to predict the expected error in the force.

It appears obvious that a reasonably good force measurement is available without any instrumentation. In any event it is easy to test this proposal since only the relevant software need be generated, and the force calculation may be tested by applying known forces to the hand and comparing the calculated forces as derived from the pressure sensors. This may be expressed conveniently as the relevant error ellipsoid.

c. Pedestal Force Sensors*

* Summary of work sponsored by NSF grant no. ATA74-18173 A01.

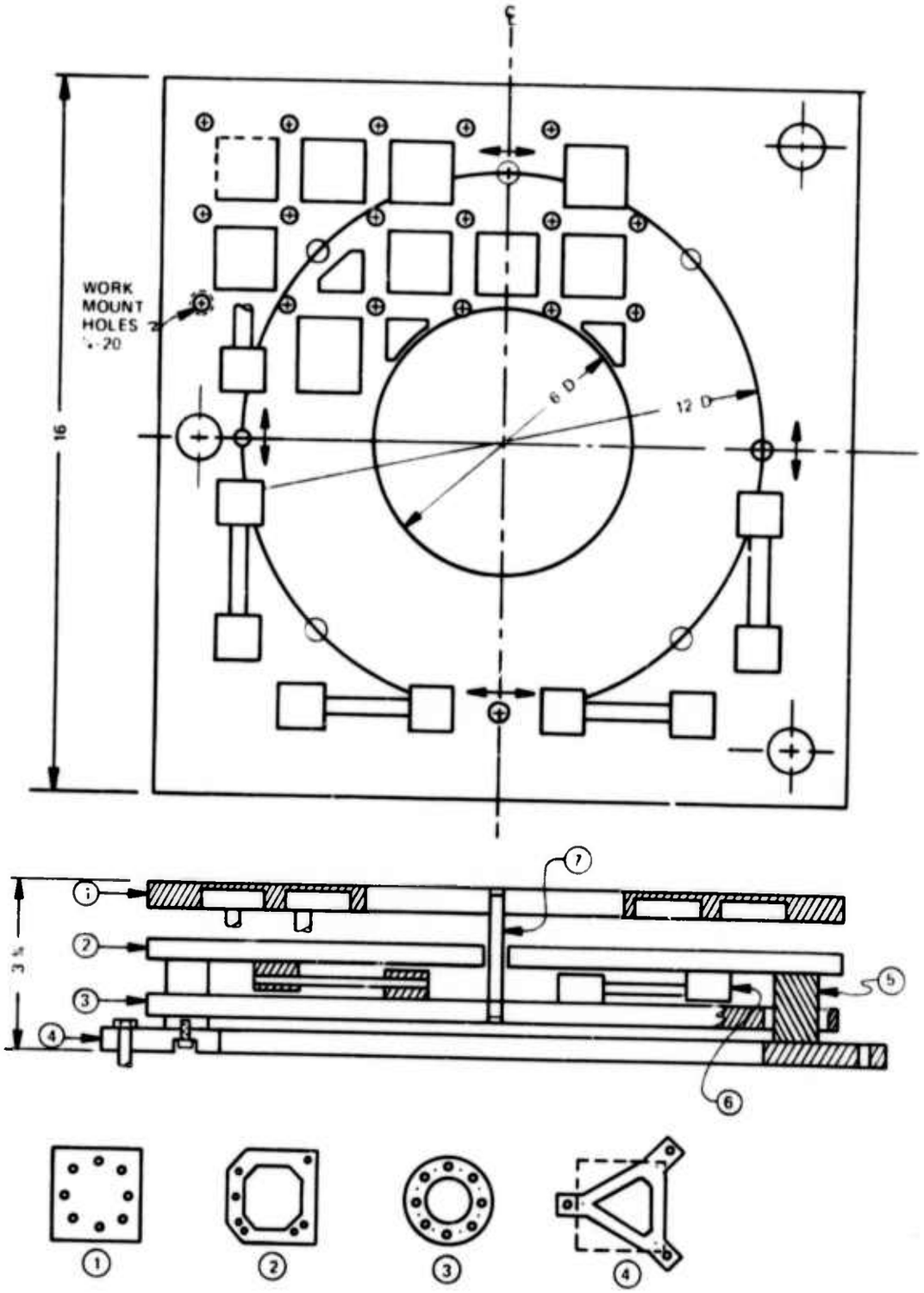

Figure VII-12
Six Degree of Freedom Pedestal Force Sensor

A Strain Gauge Pedestal Force Sensor

A strain gauge type pedestal force sensor has been designed and is currently under construction. The general layout of this design is shown in Figure VII-12. This is a three layer design adapted from the wrist force sensor concept previously described. The sensing elements are to consist of load beams, assuming satisfactory performance of the sample load beam which is currently being awaited.

A BLH product exists which has capacities directly applicable to some of our sensor problems. This is called a load beam, and is a beam and strain gauge assembly. The attached data sheet shows some of its features. Sheets are also attached describing platform transducers, which illustrate technology directly applicable to some of the force components to be sensed. (Tables VII-1, 2)

A Laser Pedestal Force Sensor

The sensor structure of c is to be designed to accept laser instrumentation as soon as this becomes available. In order to expedite the actual construction, it is proposed to order two sets of structural components, one of which will be instrumented with strain gauges, and the other with the laser system.

d. Wrist Force Sensors

Draper Arm Wrist Force Sensors

A preliminary structural concept of this sensor has been devised and is shown in Figure VII-13. This design can also be instrumented with either laser displacement detectors or strain gauges.

e. Laser Force Sensor Specifications

The current specifications are shown in Table VII-3 for the Draper Arm Wrist Force Sensor. Figures VII-14 and VII-15 use sin and cos functions, to avoid the discontinuities which might be encountered if an attempt were made to use the arc tangent function. The functions are guaranteed to be well behaved, and to be monotonic under the presence of a certain amount of distortion in the input waves.

TYPE LBP1

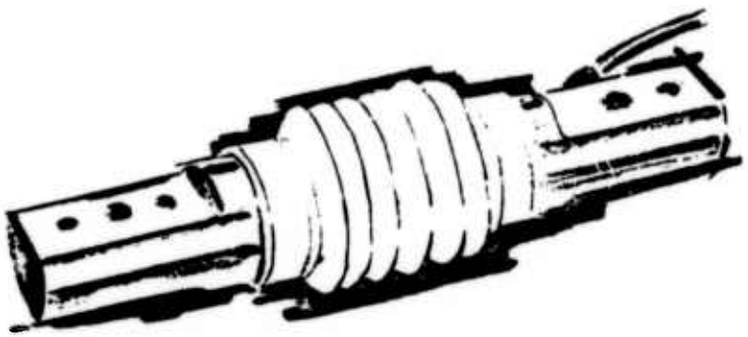

PRECISION ACCURACY

RESISTS SIDE, ECCENTRIC AND THRUST LOADS

LOW PROFILE

ADAPTABLE TO A WIDE VARIETY OF APPLICATIONS, INCLUDING ON-LINE PROCESS WEIGHING

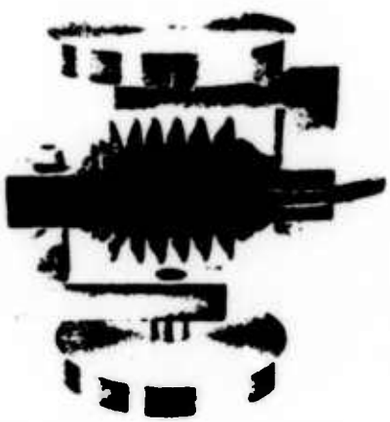

"L" brackets convert LBP1 to low-cost load cell.

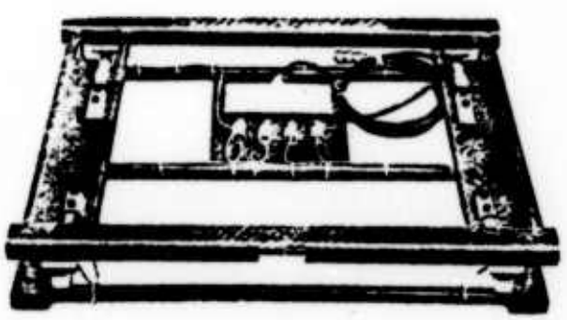

Internal view of platform scale built with LBP1 transducers clearly illustrates clean design and total absence of moving parts.

SUGGESTED METHOD OF INSTALLATION

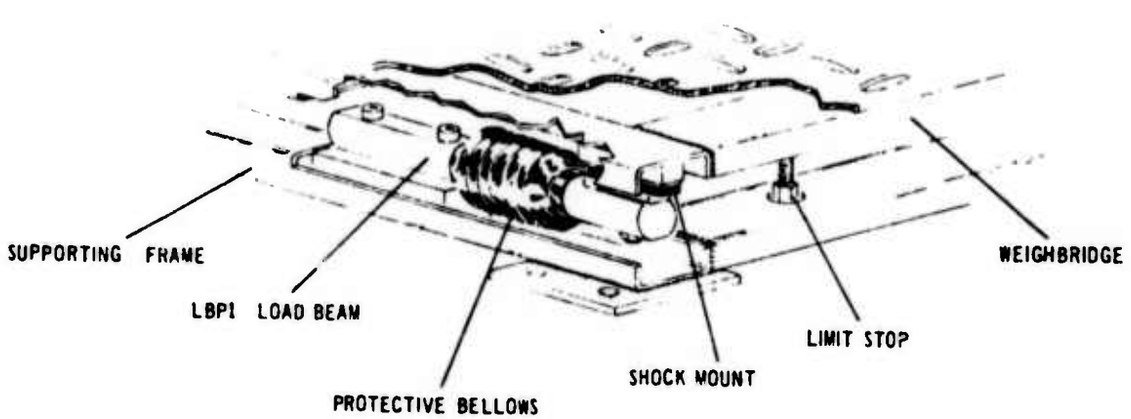

Table VII-1

SPECIFICATIONS

Performance

CAPACITY:	50 to 5000 pounds
RATED OUTPUT:	2 mV/V
CALIBRATION ACCURACY:	0.25% If required, 0.10% of Rated Output;
NONLINEARITY:	0.03% R.O.
HYSTERESIS:	0.02% R.O.
REPEATABILITY:	0.01% R.O.
OVERLOAD CAPACITY:	200% R.O.
APPROXIMATE DEFLECTION:	.010 to .040 inches depending on capacity. Highest deflection for higher capacity units.
CREEP:	Less than 0.01% in 15 minutes. This is an asymptotic value (greater than 90% of final value.)
UNIVERSAL LOAD EFFECT (TOGGLE):	Less than 0.03% R.O. zero shift with full load reversal.
MAXIMUM THRUST WITHOUT FAILURE:	100% of capacity.
MAXIMUM SIDE LOAD WITHOUT FAILURE:	50% of capacity.

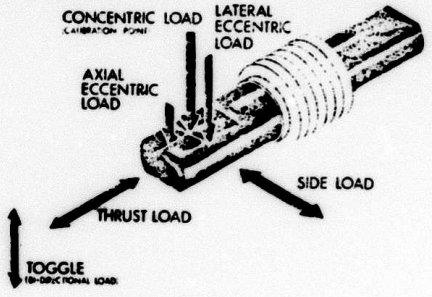

ECCENTRIC LOAD EFFECTS:	
a. Axial Direction	Less than 0.05% change in span with 50% change in moment arm.
b. Lateral Direction:	Less than 0.1% change with 1/8 inch to 1/4 inch off-center load. Distance proportional to capacity.

Electrical

TERMINAL RESISTANCE:	Input 375 ±15 ohms. Output 350 ± 5 ohms.
BRIDGE CIRCUIT SYMMETRY:	Within 2 ohms.
EXCITATION VOLTAGE:	15 volts maximum
APPROXIMATE NATURAL FREQUENCY:	350 to 500 cps
ELECTRICAL CONNECTION:	5 ft. cable.

Environmental

SAFE TEMPERATURE RANGE:	15°F to 115°F
TEMPERATURE EFFECT ON ZERO BALANCE:	Less than ±.0015% R.O./°F.
TEMPERATURE EFFECT ON SPAN:	Less than ±.0008% R.O./°F.
BAROMETRIC EFFECT:	None.

ELECTRICAL TERMINATION	
CABLE COLOR CODE	
INPUT	OUTPUT
Black (−)	Red (−)
Green (+)	White (+)

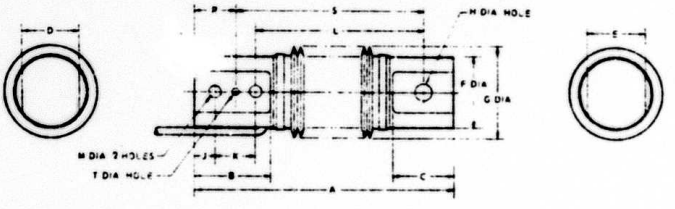

CAPACITY (Pounds)	CATALOG NO.	A	B	C	D	E	F DIA.	G DIA.	H HOLE	J	K	L	M 2 HOLES	R	S	T HOLE
50	420268	4	15/16	15/16	5/8	5/8	1	1⅛	9/32	—	—	—	—	1/2	3	9/32
250	420270															
500	420271	7⅛	2	1½	1½	1½	1⅝	2⅛	3/4-16UNF-2B	1/2	1.000	5.375	13/32	—	—	—
1000	420272															
2500	420273	12	3	3	1⅞	1½	2	3	41/64	1/2	1.750	8.250	1/2-20UNF-2B	—	—	—
5000	420274	12⅛	3⅛	3	2⅛	2⅛	3½	4½	25/32	1	2.000	8.250	5/8-11UNC-2B	—	—	—
7500	420275	12⅛	3⅛	3	2⅛	2⅛	3½	4½	3/4-16UNF-2B	1	2.000	8.250	49/64	—	—	—

129

Table VII-2

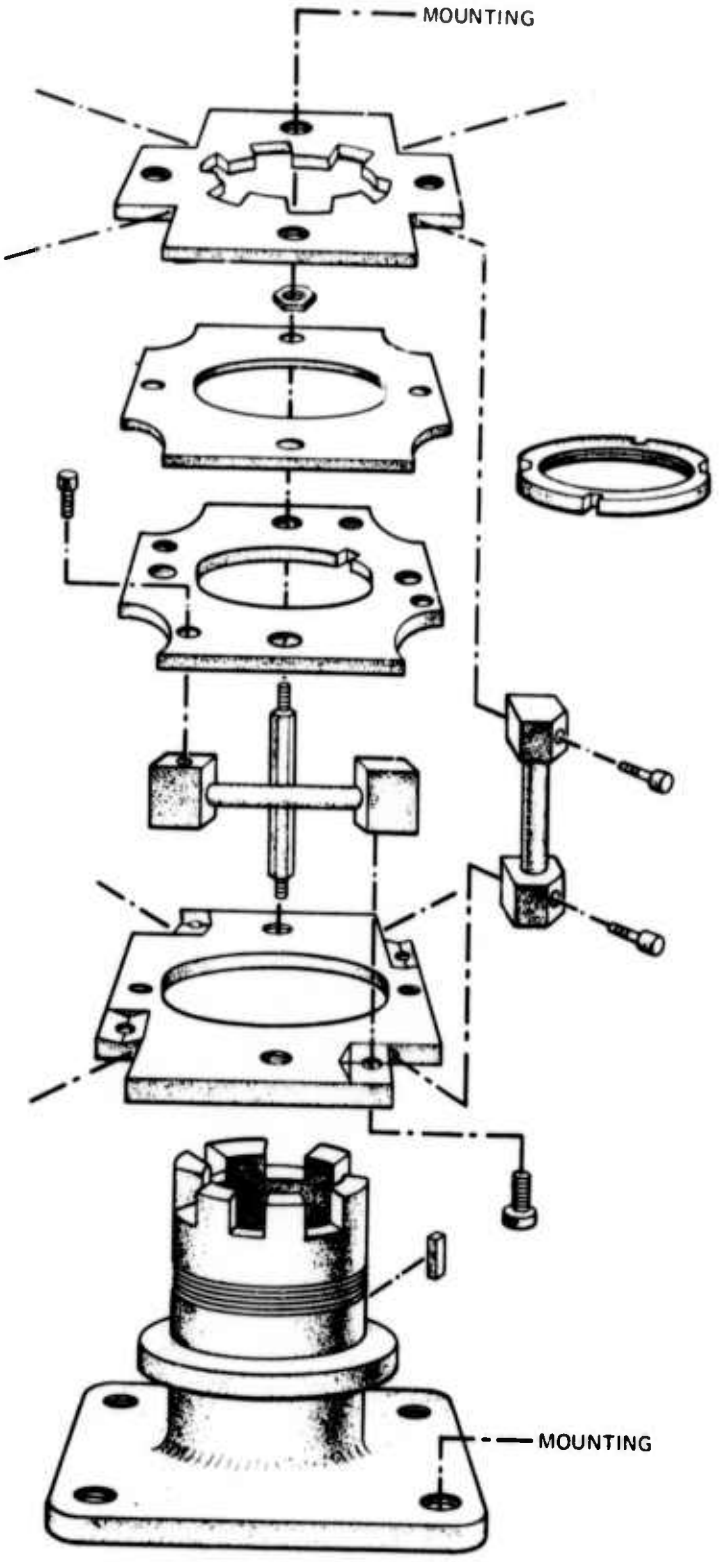

Figure VII-13
Six Degree of Freedom Wrist Force Sensor Concept

f. Other Sensors

Consideration is being given to the incorporation of proximity sensors as a fault hazard avoidance device. These sensors would shut down the arm motion in case any obstacle/object was detected in a location not expected by the computer.

	Newtons at Pick-up	Displacement	He-Ne Wavelengths	Cycles	Counts @ 4/Cycle
Yield Point	4400*	+178 u	-	+564	-
Full Scale Force & Full Scale Torque	1000	+40.5 u	64	+128	512
Full Scale Force	500	+20.3 u	32	+ 64	256
Zero	0	0	0	0	0
- Full Scale Force	-500	-20.3	-32	- 64	-256
- Full Scale Force & (- Full Scale Torque)	-1000	-40.5	-64	-128	-512
- Yield Point	-4400*	-178 u	-	-564	-

Working radius = 6.9×10^{-2} m

Table VII-3

Six Degree of Freedom Laser Force Sensor
Tentative Performance Specifications

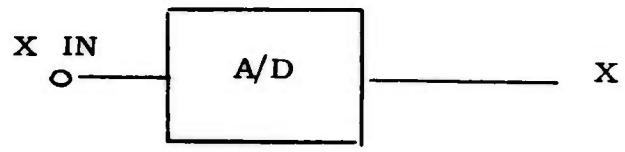

$$R = (X^2 + Y^2)^{\frac{1}{2}}$$

$$\theta = \cos^{-1}(X/R)$$

$$\theta = \sin^{-1}(Y/R)$$

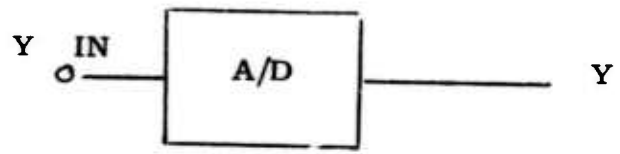

Figure VII-14

Software Cycle Dissection

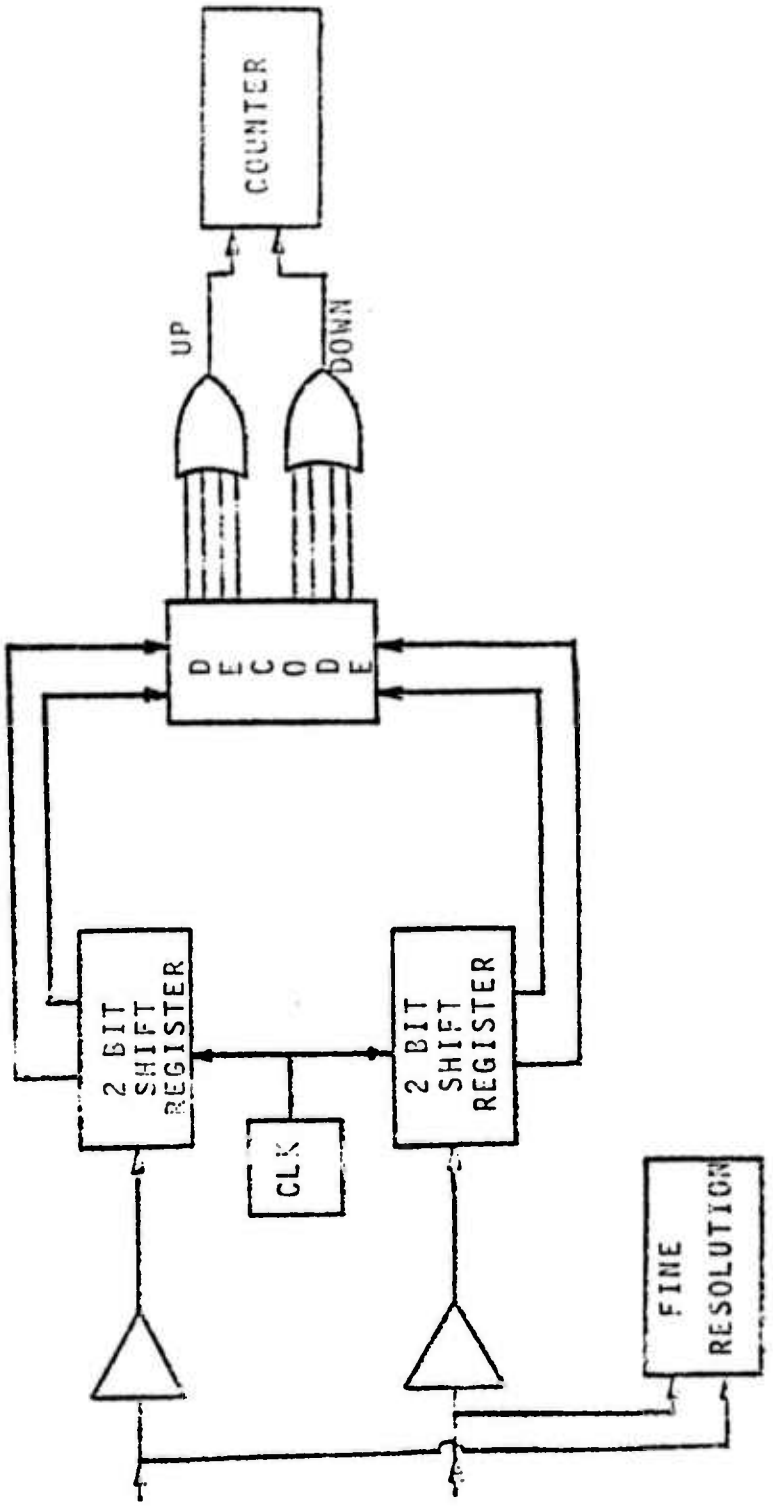

FORCE SENSOR ELECTRONICS

Figure VII-15

D. Hydraulic Control

1. Introduction

The choice of hydraulic actuators for the manipulator brings with it a particular set of control problems that must be dealt with by the hydraulic control system. This system must take commands issued by the computer and then control the actuators to produce the desired performance. The problems that complicate the job of the hydraulic servo include the non-linear behavior of certain hydraulic elements, compliance of the hydraulic fluid, and the dynamic effects of several components in the control loop. The desired performance of the control system includes basic stability, smooth motions of the manipulator structure, and graceful failure of the control system should the computer fail to function properly.

2. Analytical Development

The overall plan of analysis began with formulation of the non-linear equations of motion of the system consisting of the hydraulic actuator and load. Then a computer program to simulate this system was written and debugged. Next, hydraulic control systems were formulated and added to the basic simulation. The performance of the combined system was then tested through simulation. Usually, in order to design the various control systems a simplified, linearized form of the non-linear hydraulic equations was assumed for the purpose of analysis. The resulting designs were then tried on the simulated non-linear system.

In the modeling process decisions had to be made concerning which effects or properties were sufficiently important to include in the system model and which were not. The following are effects that were included:

a. Fluid compliance in the chambers on both sides of the hydraulic actuator vane.

b. Non-linear valve characteristics.

c. Fluid viscosity in the actuator leakage from one side of the vane to the other.

d. Hydraulic valve dynamics between the input electric current and the valve opening size.

e. Inertial load on the actuator.

f. Dynamic effects of the angle reading resolver circuitry.

Among the effects not included were the following:

a. Inertial effects of the fluid between the valve and the actuator. These effects should be small because the valves are mounted on the actuators and so the relevant fluid mass is small.

b. Inertial effects of the fluid between the pump accumulator and the valve. These effects should be small because of the sufficiently large diameter of the hose which causes slower fluid velocities.

c. Friction in the actuator. Friction is designed to be minimized by the lack of seals between the vane and the outer wall of these actuators. Hence, there is no rubbing contact. The only friction should be the low friction in the shaft bearings.

The non-linear model of the hydraulic system with inertial load is illustrated in Figure VII-16. Table VII-4 is a list of variable definitions used in the formulation. The derivation of the equations is carried out in Appendix II . The final non-linear equations are repeated

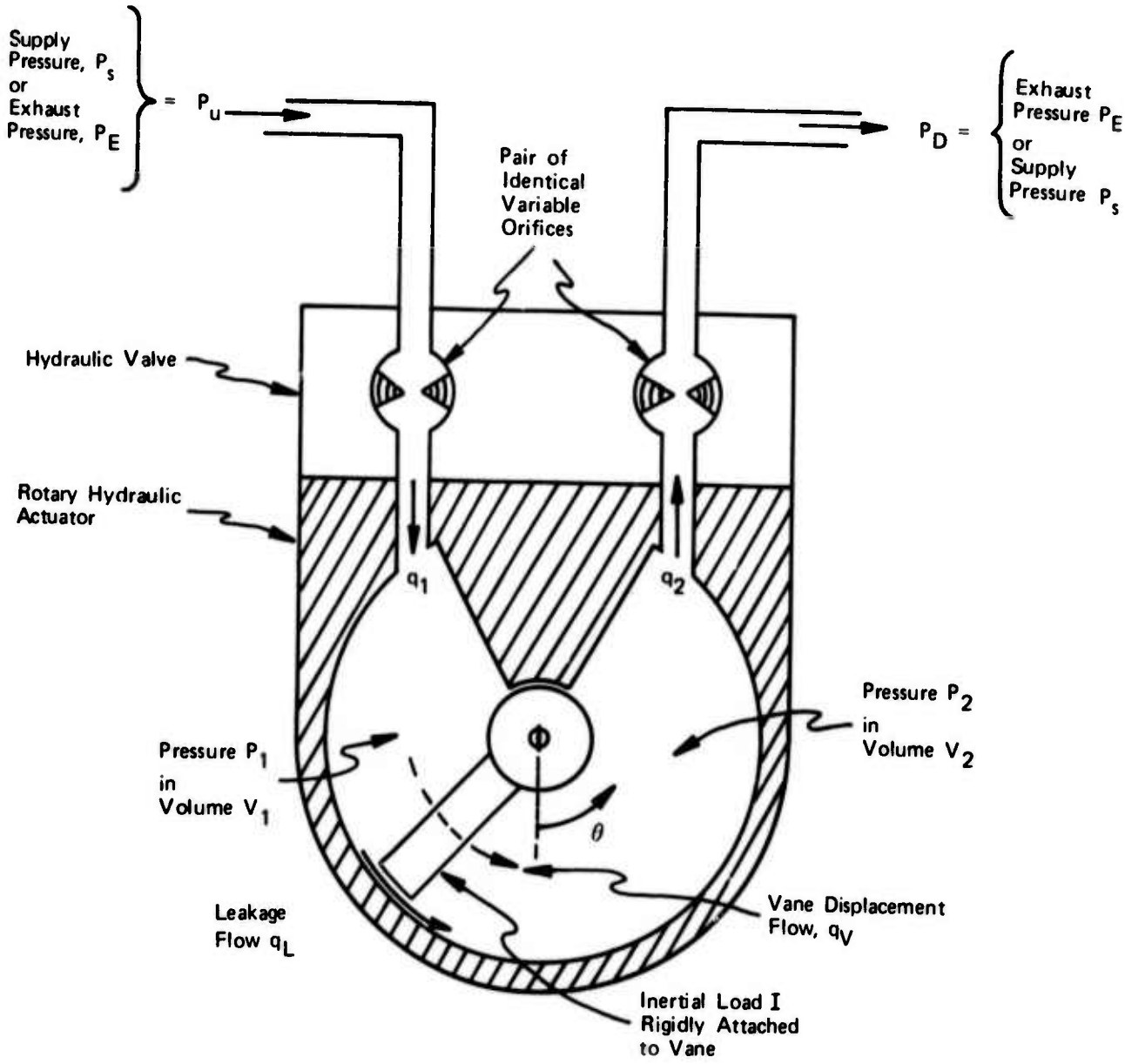

Figure VII-16
Hydraulic System Schematic

Table VII-4 Variable Definitions

θ	angular position of vane, rad
ω	angular rate of vane, rad/sec
P_s	supply pressure, psi
P_E	exhaust pressure, psi
P_1	pressure in left actuator chamber, psi
P_2	pressure in right actuator chamber, psi
$V_1 = V_1(\theta)$	volume of left chamber, in^3
$V_2 = V_2(\theta)$	volume of right chamber, in^3
q_1	flow through left orifice, cis(= in^3/sec)
q_2	flow through right orifice, cis
D	displacement of vane rotation, in^3/rad
q_L	leakage flow past vane, cis
q_v	"flow" due to displacement of actuator vane, cis
β	effective bulk modulus of fluid, psi
$C_1 = V_1/\beta$	fluid capacitance of volume V_1, in^3/psi
$C_2 = V_2/\beta$	fluid capacitance of volume V_2, in^3/psi
P_u	pressure upstream of orifice 1 on left, psi(= P_s or P_E)
P_D	pressure downstream of orifice 2 on right, psi(= P_E or P_s)
x_s	valve spool position
I	inertia of load, $in\text{-}lbf\text{-}sec^2$

here.

$$\frac{dP_1}{dt} = \frac{1}{C_1(\theta)}\left[-\left(\frac{P_1-P_2}{R_L}\right) - D\omega + f_q(x_s,\ P_u-P_1)\right]$$

$$\frac{dP_2}{dt} = \frac{1}{C_2(\theta)}\left[+ D\omega + \frac{P_1-P_2}{R} - f_q(x_s,\ P_2-P_D)\right] \qquad \text{VII-20}$$

$$\frac{d\omega}{dt} = \frac{D}{I}(P_1-P_2)$$

$$\frac{d\theta}{dt} = \omega$$

where

$$\left.\begin{aligned} P_u &= P_s \\ P_D &= P_E \end{aligned}\right\} \text{ if } x_s \geq 0$$

VII-21

$$\left.\begin{aligned} P_u &= P_E \\ P_D &= P_s \end{aligned}\right\} \text{ if } x_s < 0$$

The first of equations VII-20 expresses the rate of change of pressure in the left hand chamber of the actuator in Figure VII-16 as the sum of the flows into the chamber divided by the capacitance (compliance) $C_1(\theta)$ of the total fluid in the chamber. As indicated in Table VII-4 , this compliance is a function of the fluid modulus β and the volume of the fluid chamber, which itself is a function of angular position θ. The second equation is like the first but for the other fluid chamber. The third equation is Newton's equation for a rotary load, and the last equation just defines angular rate ω. The function $f_q(\bullet\ ,\ \bullet)$ is short hand for the quadratic flow function of an orifice:

$$q = f_q(x_s,\ \Delta P) = \begin{cases} K_V x_s \sqrt{|\Delta P|} & \text{for } \Delta P \geq 0 \\ -K_V x_s \sqrt{|\Delta P|} & \text{for } \Delta P < 0 \end{cases} \qquad \text{VII-22}$$

where

ΔP = pressure drop across orifice
x_s = valve spool position
K_V = valve orifice gain
q = flow through orifice

For a single orifice x_s is considered only positive or zero. Hence, the flow through the orifice as defined by the above function is always in the direction of the pressure drop. In a standard fourway hydraulic valve a negative spool position corresponds to a reversal of the connections of supply pressure and exhaust pressure to the hydraulic actuator. This is so actuators may be driven in both directions. This switch in supply and exhaust pressure is the purpose of equations (VII-21) since they define which orifice is connected to exhaust and which to supply.

The non-linear equations (VII-20) were implemented in the computer program that was used in subsequent simulation testing. For the purpose of ease of analysis, however, it is useful to simplify these equations as much as possible. The following assumptions were used to make these simplifications:

a. $C_1(\theta) = C_2(\theta) = C$; that is, that the fluid capacitance is relatively constant and equal on both sides of the vane. This means that the vane is assumed to remain essentially near the center of its range of motion.

b. We assume linearization of the flow functions f_q for the valve orifices as follows:

$$f_q(x_s, \Delta P) \simeq q_o + k_s(x_s - x_{so}) + k_p(\Delta P - \Delta P_o) \qquad \text{VII-23}$$

where x_{so} = valve spool linearization position
ΔP_o = pressure drop linearization value
k_s = spool position gain = $\partial f_q / \partial x_s$
k_p = pressure drop gain = $\partial f_q / \partial \Delta P$

c. We further assume that the pressure drop across both orifices in the valve is about the same, i.e., both $\Delta P_o \cong P_s/2$, assuming exhaust pressure $P_E = 0$. These

assumptions combine to make k_p approximately equal for both orifices.

d. Assume that $x_{so} = 0$. This means that the valve is operating about its closed position and further implies that $q_o = 0$ and $k_p = 0$.

e. Assume that k_s is the same for both orifices This is a safe assumption because hydraulic servo valves are almost invariably designed with matched orifices.

Working with these assumptions as shown in Appendix II gives us the following simplified, linearized equations:

$$\Delta P = P_1 - P_2$$

$$\begin{bmatrix} \dot{\Delta P} \\ \dot{\omega} \end{bmatrix} = \begin{bmatrix} -\frac{2}{R_L C} & -\frac{2D}{C} \\ \frac{D}{I} & 0 \end{bmatrix} \begin{bmatrix} \Delta P \\ \omega \end{bmatrix} + \begin{bmatrix} \frac{2k_s}{C} \\ 0 \end{bmatrix} x_s$$

VII-24

Figure VII-17 shows these equations in block diagram form.

3. Modeling Types of Hydraulic Control Systems

The purpose of the hydraulic control system is to convert the commands from the computer into the desired actions of the arm and load. This control system will physically reside in the interface equipment connected between the computer and the manipulator. Digital words corresponding to computer commands will be fed into the interface from the computer. The output of the interface is a properly modulated analog electric current which will control the valve orifice openings. Actually, since there will be six hydraulic actuators to control, there will be six such hydraulic control circuits in the system interface.

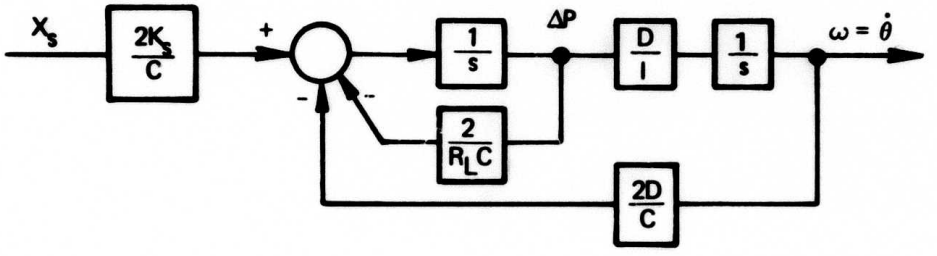

or

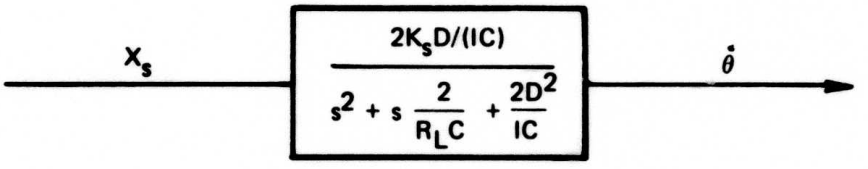

Figure VII-17
Linear Simplified Hydraulic Load Model

The hydraulic control circuits must still function if the computer does not. This is the concept of "graceful failure": the computer must not be so vital to the operation of the system that it goes unstable if the computer fails or if there is a program error and the computer stops. This will put requirements on the control system configuration. The criteria by which the control system is judged are that the performance of the manipulator must be stable, smooth, and sufficently fast.

The control system design process will be to use the simplified linear model of the hydraulic and load system to design alternative control systems. These alternative control designs will be tested by simulating them with the non-linear hydraulic simulation. There are four types of control systems tested:

a. Pure position feedback

b. Position feedback with rate feedback

c. Position feedback with lead filter on rate feedback

d. Position feedback, rate feedback, and actuator load pressure feedback

The simulated system includes additional effects that will not be used in the simplified analysis. For example, the simulated hydraulic control system includes the dynamic effects of the hydraulic valve and the angle reading resolver circuitry. The bandwidths of both of these components are well above the hydraulic resonance frequency and so were excluded from the simplified analysis.

a. Position error control

Position error control is illustrated in Figure VII-18 by a block diagram. The basic idea here is that the electric current through the hydraulic valve is made proportional to the error between desired position and actual position. A root locus diagram for this system, assuming the simplified linear equations, is also shown in Figure VII-18.

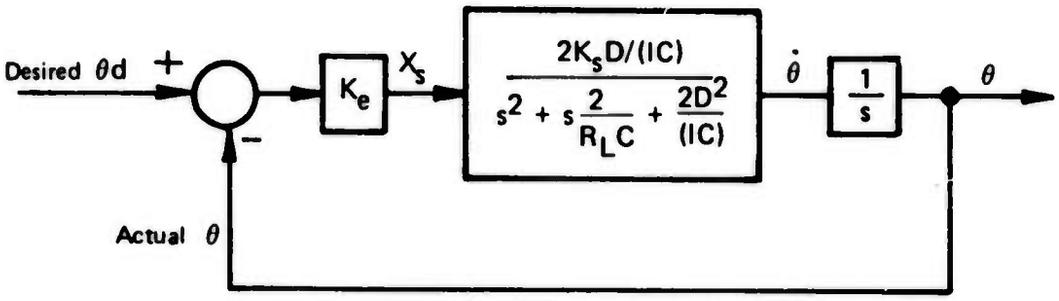

(a) Block Diagram.

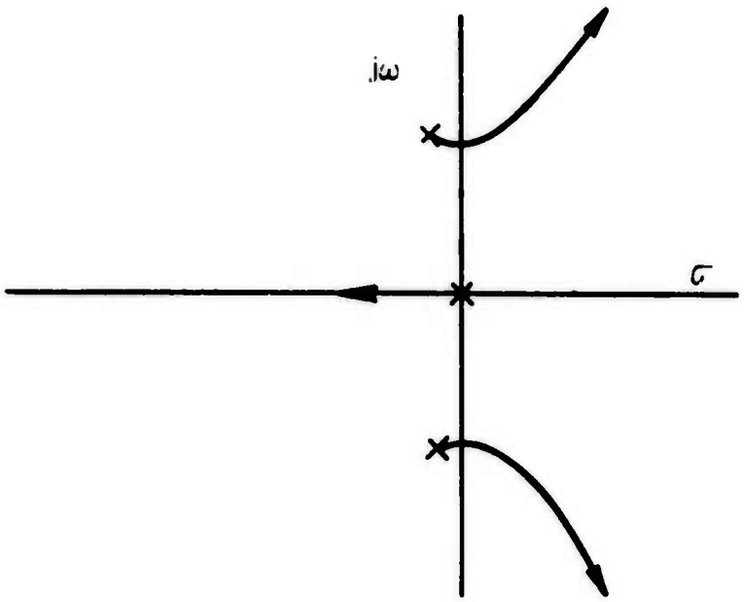

(b) Root Locus of Closed Loop Poles for Increasing K_e.

Figure VII-18
Position Error Control

The locus of the poles of the closed loop system is shown for increasing values of position error gain K_e.

Notice that as the position error gain K_e is increased, the pole pair associated with the hydraulic/load resonance is driven unstable. Qualitatively what is happening is the following: At the resonant frequency of any complex pole pair, their phase lag is 90°. The integrator in the system possesses an additional 90° phase lag. Obviously, these two elements together in the open loop possess a total of 180° phase lag at the resonant frequency of the load resonance poles. Consequently, sufficient error gain will simply drive the system unstable. Also, a look at the root locus shows that pure position error control will not damp the resonant poles. Figure VII-19 shows the results of a simulation of pure position feedback on the non-linear system using component values corresponding to the shoulder actuator of the manipulator design. Clearly the resonant poles have not been damped.

Position error control cannot be abandoned completely. After all, to control the manipulator position there must be a position error loop somewhere in the control system. And, some position loop closure must occur in the interface to insure graceful failure when the computer is not functioning.

b. Position and rate feedback

The addition of rate feedback is a common cure for oscillatory position servo systems. Figure VII-20 contains a block diagram of the system with the additional rate feedback. Also shown is a root locus diagram showing the pole motion of the closed rate loop system for increasing values of rate feedback gain K_r. In this case a particular value of position error gain K_e is assumed and held constant. Hence, the initial pole positions in the root locus of Figure VII-20 correspond to the poles for a certain value of position error feedback.

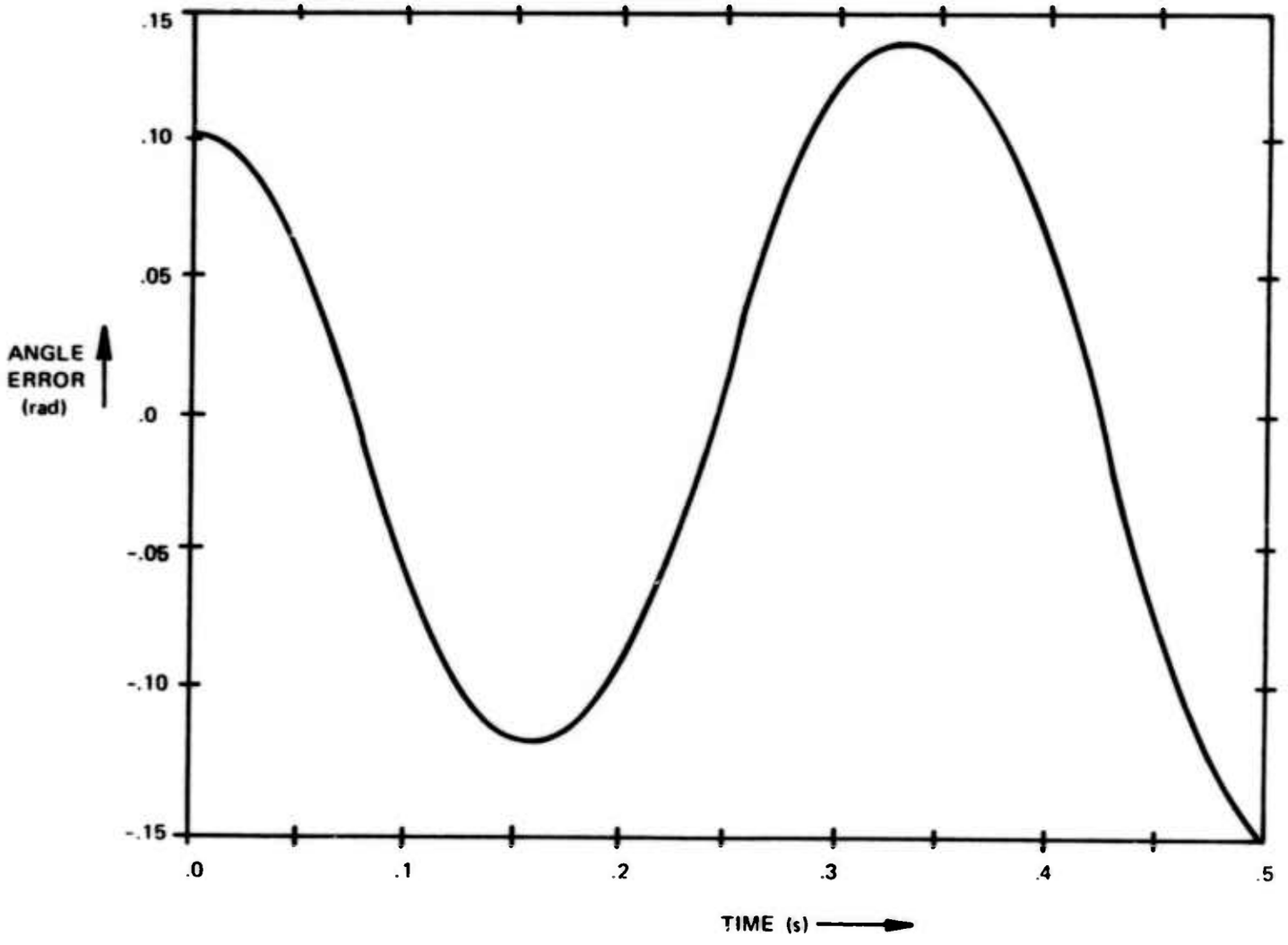

Figure VII-19

Simulation of Step Response of
Nonlinear Hydraulic System Using
Pure Position Feedback

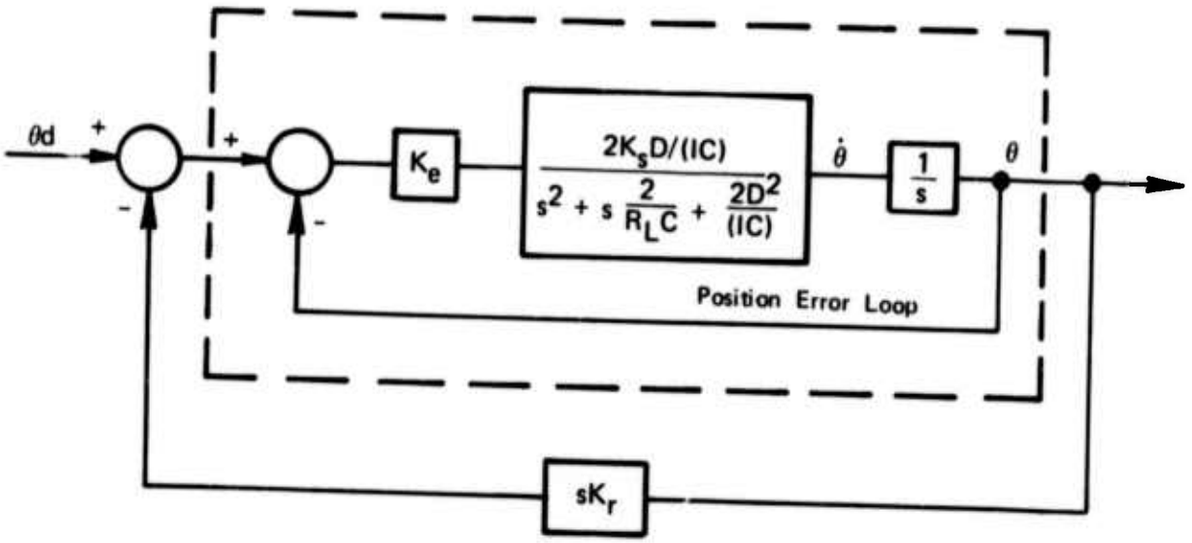

(a) Block Diagram

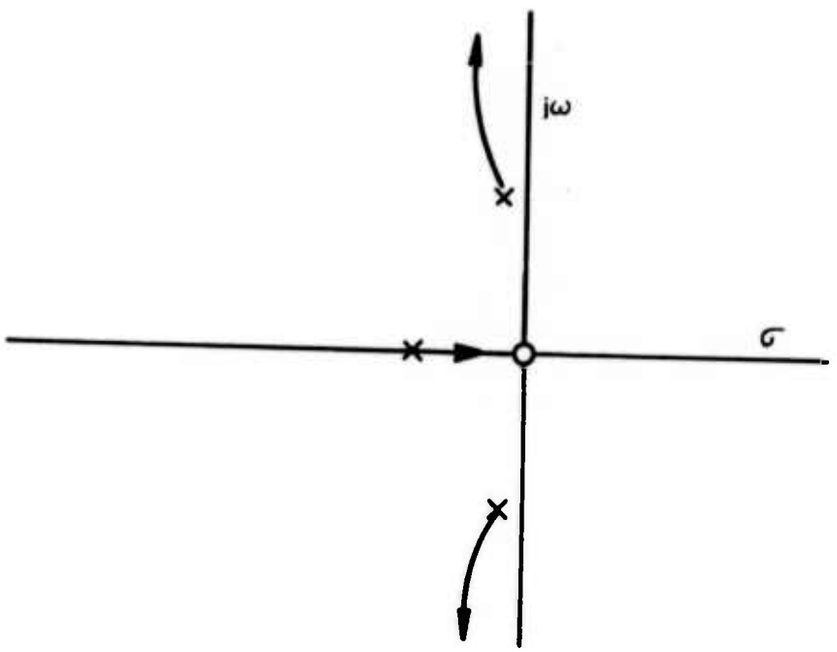

(b) Root Locus of Closed Loop Poles for Increasing Rate Feedback gain K_r.

Figure VII-20
Position and Rate Feedback

As can be seen from the root locus diagram, as the rate feedback gain K_r increases the frequency of the resonant poles increases and the frequency, or speed, of the dominant real pole decreases. This means that for high values of rate, or "tach", feedback the overall system performance becomes sluggish (the real pole) but with high frequency ringing overlaying the basic response. Figure VII-21 shows the result of a simulation of the step response of a typical system with excessively high rate feedback. The simulation used the position and rate feedback scheme on the non-linear model of the hydraulics and load.

c. Position feedback with lead filter on rate feedback

The high frequency ringing apparent in the previous section occurs because at the frequency of the ringing the total phase lag of the open loop system is almost 180° with nearly too much gain. One possible way to eliminate the ringing is to reduce the phase lag in the rate loop at that frequency by introducing a lead filter.

Alternatively, one can imagine the ringing problem arising from the two resonant poles. These poles occur in the transfer relationship between hydraulic valve electric current (spool position x_s) and $\dot{\theta}$, angular rate. Since the output variable is $\dot{\theta}$, rate in this case, the poles may be damped by the addition of feedback of the output derivative, $\ddot{\theta}$, or acceleration. By adding lead compensation to the rate feedback, we obtain the effect of differentiation, resulting in an acceleration feedback signal.

A block diagram of this control scheme is shown in Figure VII-22. The form of the lead compensation is

$$\frac{1 + s/\omega_d}{1 + s/\omega_g}$$

where ω_d = lead frequency, rad/sec

ω_g = lag frequency, rad/sec

$\omega_d < \omega_g$

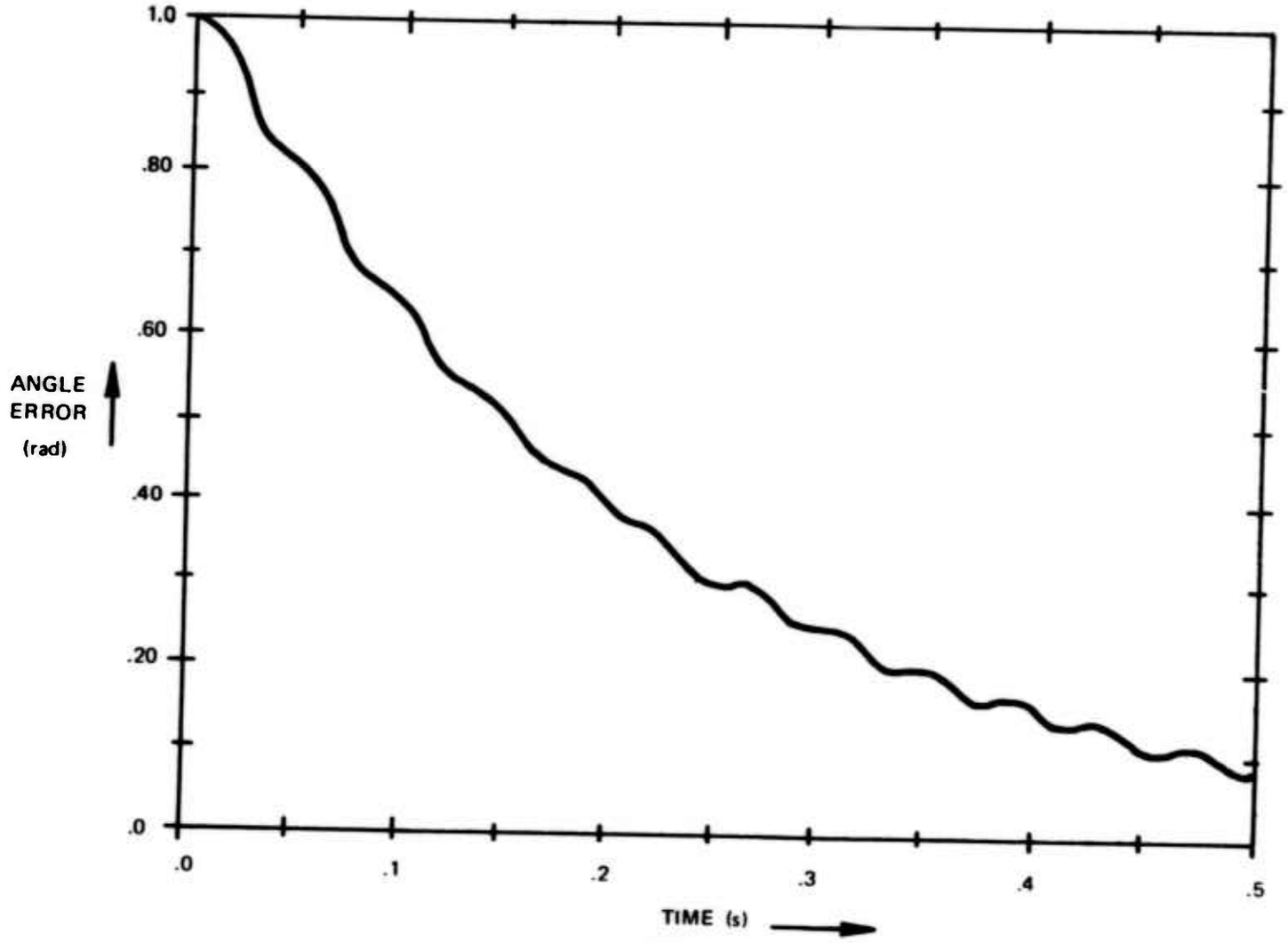

Figure VII-21

Simulated Step Response Using
Position Feedback and Excessive
Rate Feedback

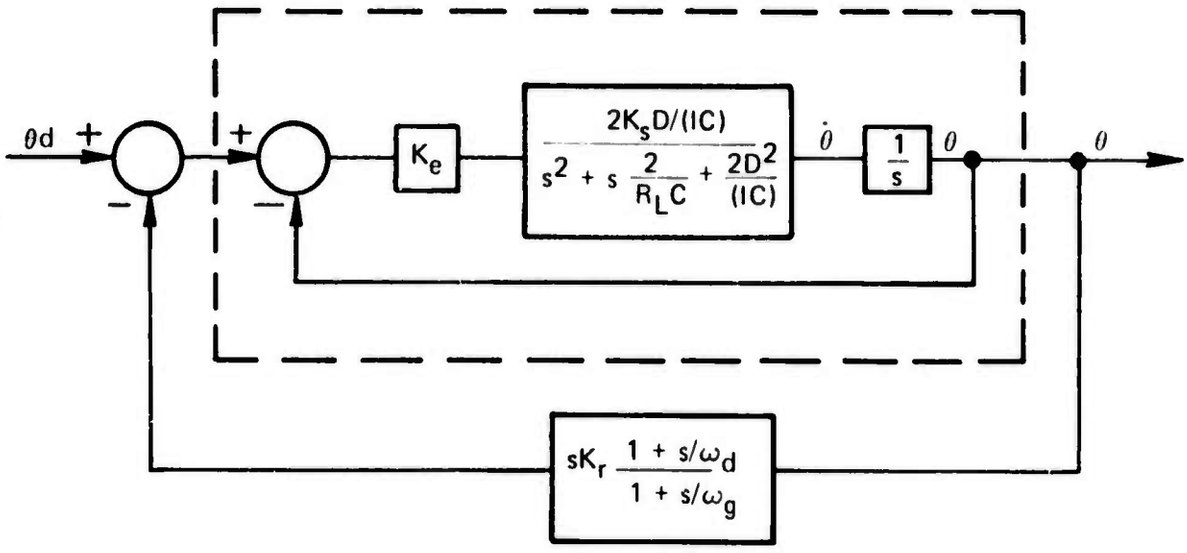

(a) Conventional

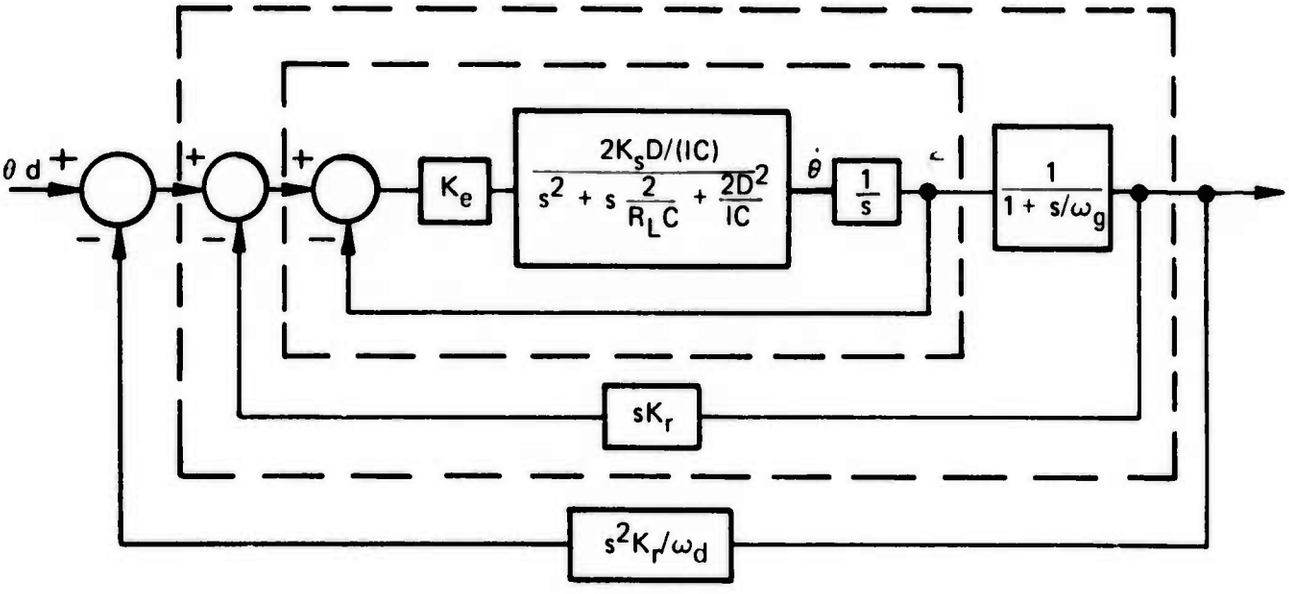

(b) Redrawn for Root Locus Work.

Figure VII-22

Block Diagram

Position Feedback with Lead Filter on Rate Feedback

For frequencies below the lead frequency ω_d the effective compensation appears close to a unity gain with no dynamics. For frequencies above the lead frequency ω_d but still below the lag frequency ω_g the compensation appears like the zero $(1 + s/\omega_d)$, thus achieving differentiation and phase lead. Above the lag frequency the filter looks like pure gain ω_g/ω_d with no phase lead. The lag pole reflects practical constraints on differentiating signals. It also offers a way of limiting the phase lead to where it is needed.

The second block diagram is functionally equivalent to the first but has been redrawn to separate the lead frequency parameter prior to the root locus procedure.

Figure VII-23 shows a two stage root locus process to examine the effects of rate lead compensation. The first root locus begins with the poles of the pure position error system and the pole of the lead compensator. Here a specific value of position error gain K_e and compensator pole frequency ω_g is assumed. The lead frequency loop is assumed to be open, i.e., $1/\omega_d = 0$. The motion of the poles is examined for increasing rate feedback gain K_r. This determines the poles of the subsystem contained in the outer dotted line box of Figure VII-22b. Using this locus a value of K_r is now chosen to fix the poles, and the next stage of the root locus procedure proceeds. The new feedback path is represented by the gain s^2K_r/ω_d in Figure VII-22. Since K_r has just been determined, this locus depends only on $1/\omega_d$ as the varying parameter. The root locus shows that for a range of ω_d the resonant poles have been damped as the poles converge on the real axis. However, increasing $1/\omega_d$ (decreasing ω_d) further will ultimatedly only slow the system down as the poles move closer to the origin. Obviously the exact path of the resonant poles will depend on the values of the open loop poles and zeros. For certain values the resonant poles may move directly toward the origin without damping first. Work is needed in this area to determine how best to design the rate feedback lead compensator.

Figure VII-24 shows a simulation of the same non-linear system using position feedback and lead compensation on rate feedback. The performance has improved considerably.

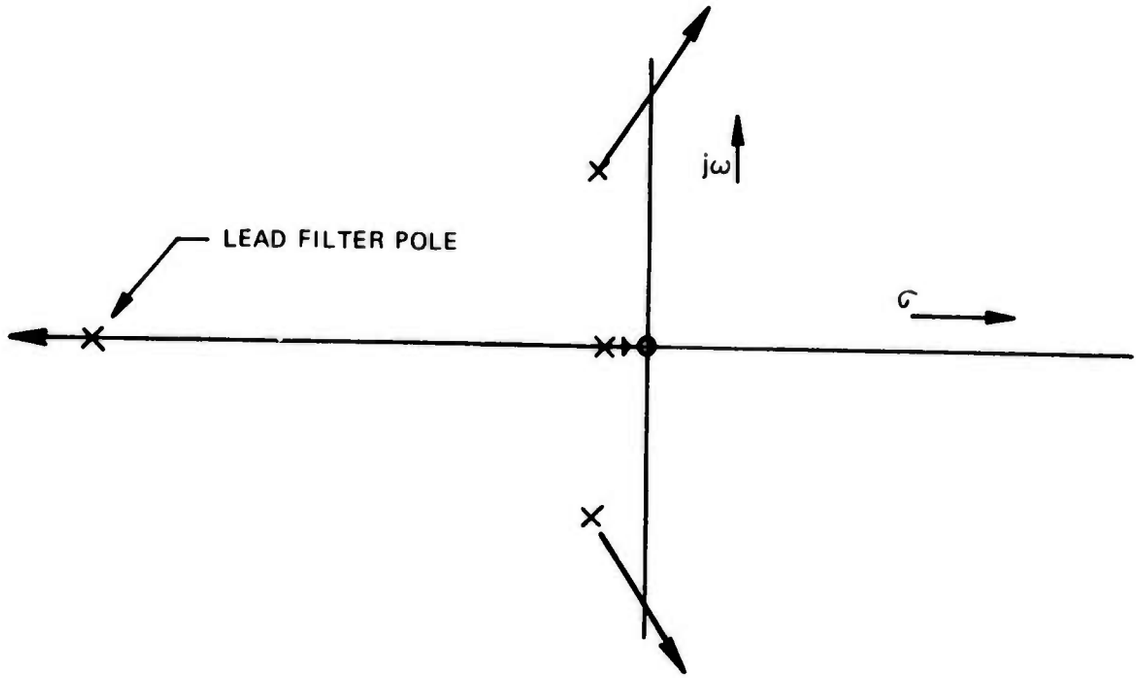

(a) First Stage of Root Locus, $\frac{1}{\omega_d} = 0$. Locus of closed loop poles as rate feedback gain K_r is increased.

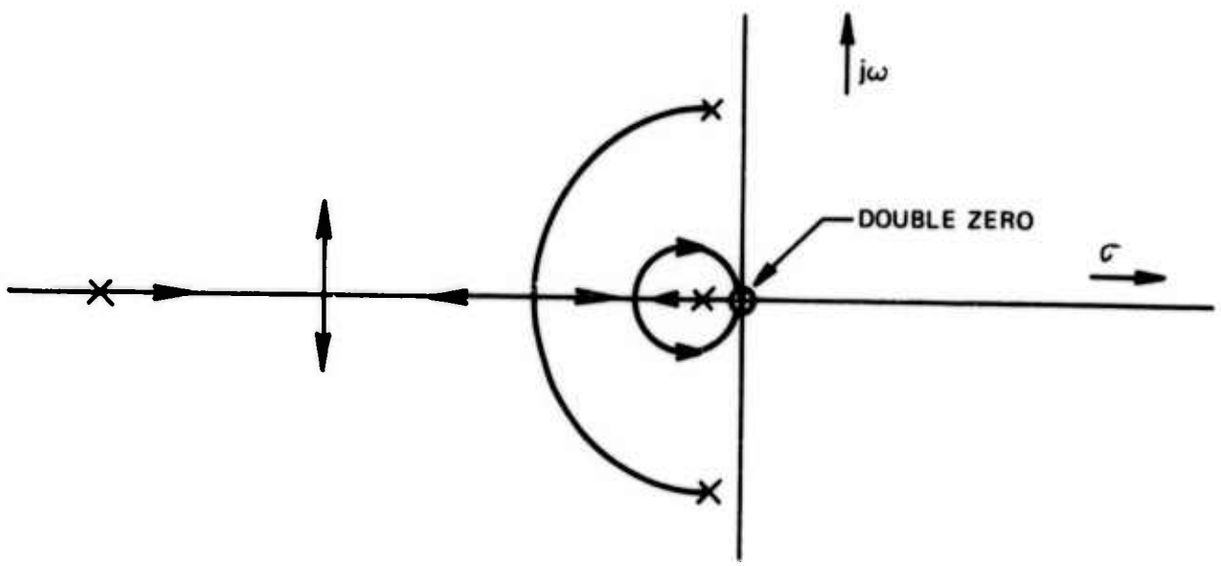

(b) Second Stage of Root Locus, K_r fixed. Locus of closed loop poles as $\frac{1}{\omega_d}$ increases.

Figure VII-23

Root Locus of Position Feedback with Lead Filter on Rate Feedback

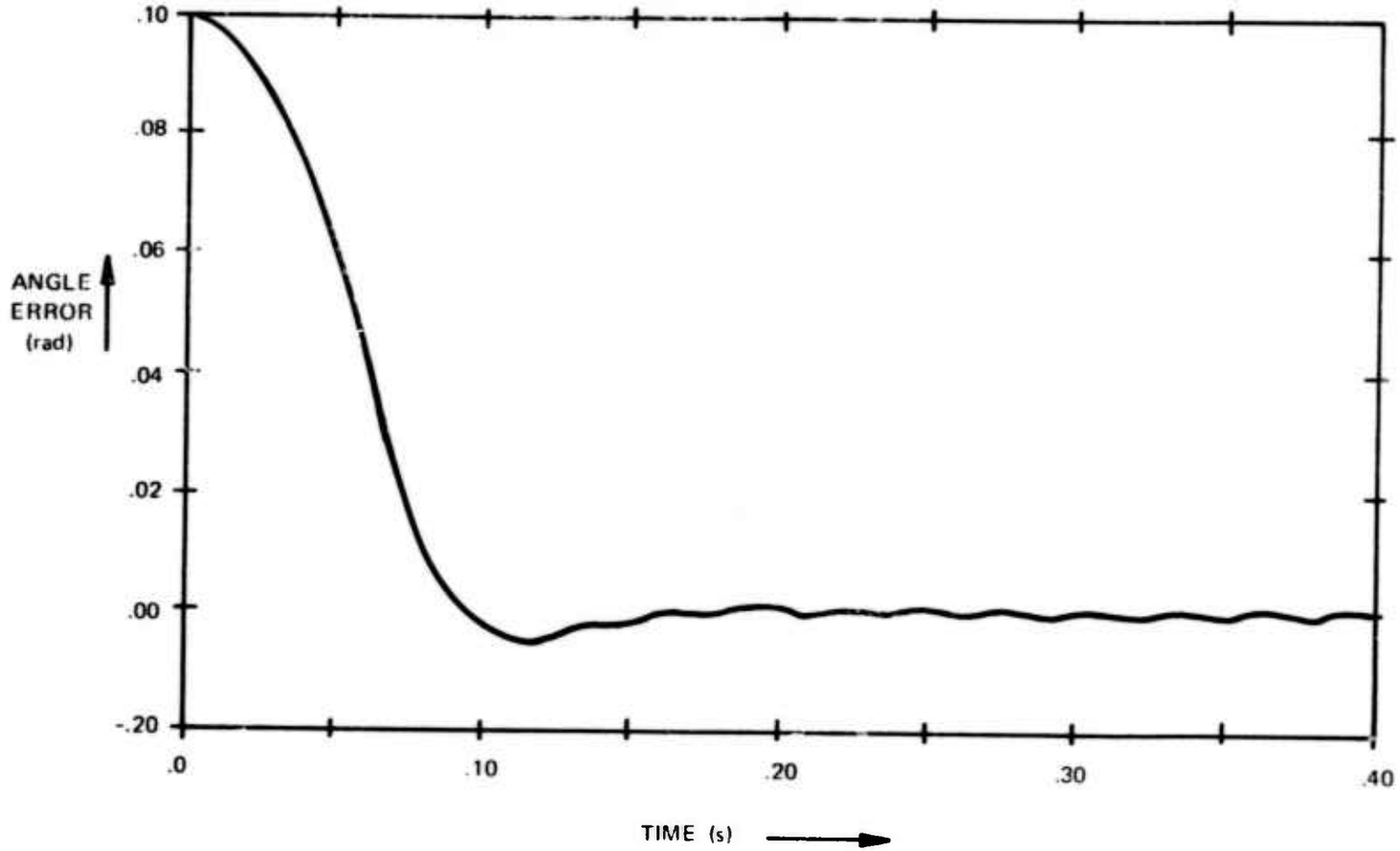

Figure VII-24

Simulated Step Response Using
Position Feedback and Lead
Compensation Rate Feedback

d. Position, rate, and pressure feedback

In the previous section it was explained that acceleration feedback would damp the resonant poles. Besides lead compensation on the rate signal, another way to obtain an acceleration signal is to use pressure feedback. Pressure sensors are placed on both sides of the actuator and used to measure the pressure difference acting on the rotary vane. Because this pressure drop is proportional to the torque of the actuator, and because torque on an inertial load is proportional to acceleration, then this pressure drop can be taken as proportional to the load acceleration.

Figure VII-25 shows a block diagram indicating the use of position, rate, and pressure feedback. Also in the figure is a root locus indicating how the poles move for increasing pressure feedback gain for a given set of position and rate feedback gains. It can be seen that increasing pressure feedback will tend to increase the frequency (speed up) of the dominant real pole—up to a point. Excessive pressure feedback will then bring lightly damped low frequency resonant poles.

An alternative way to conceive of pressure feedback is to think of the pressure loop as creating a pressure or torque servo in the middle of the entire system. Then the position error and rate signal can be thought of as driving a torque source in a stable, conventional position servo.

Finally, Figure VII-26 shows a step response of the simulated system using an appropriate amount of pressure feedback. Notice that the response is smooth, quick, and without oscillation.

4. Discussion

When position, rate, and pressure feedback are all used, then there are three parameters to adjust in the simplified third order system. Theoretically, it should be possible to arbitrarily assign the three pole positions and compute the required position, rate, and pressure gains to achieve them.

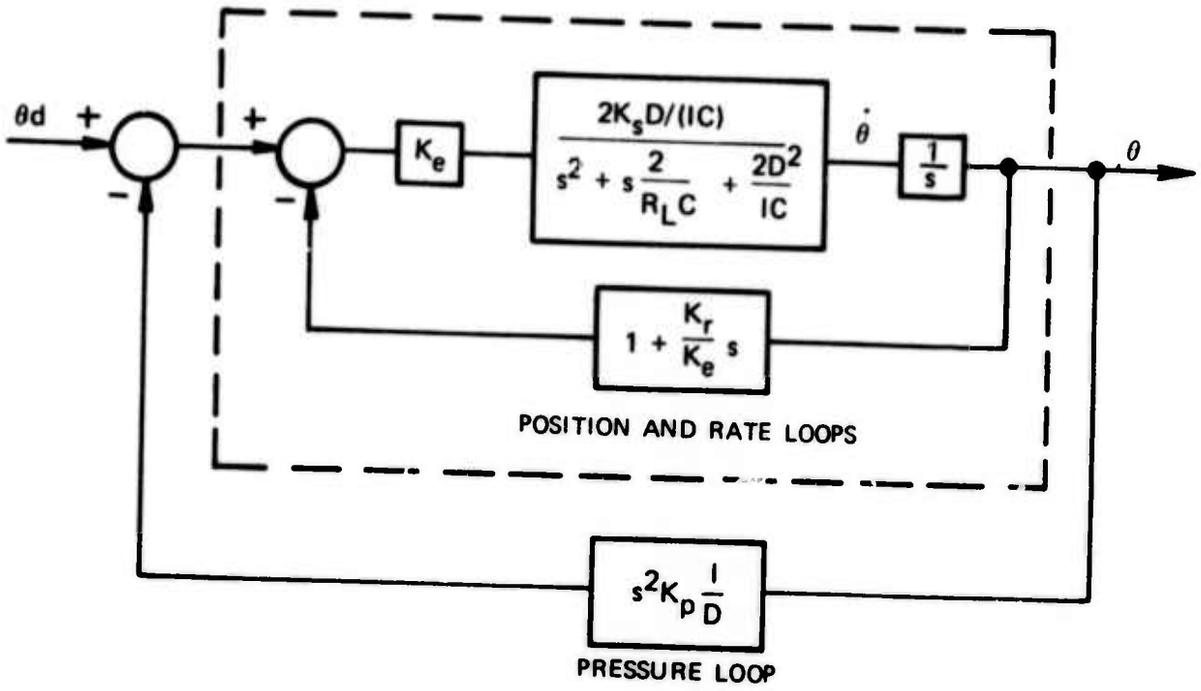

(a) Block Diagram.

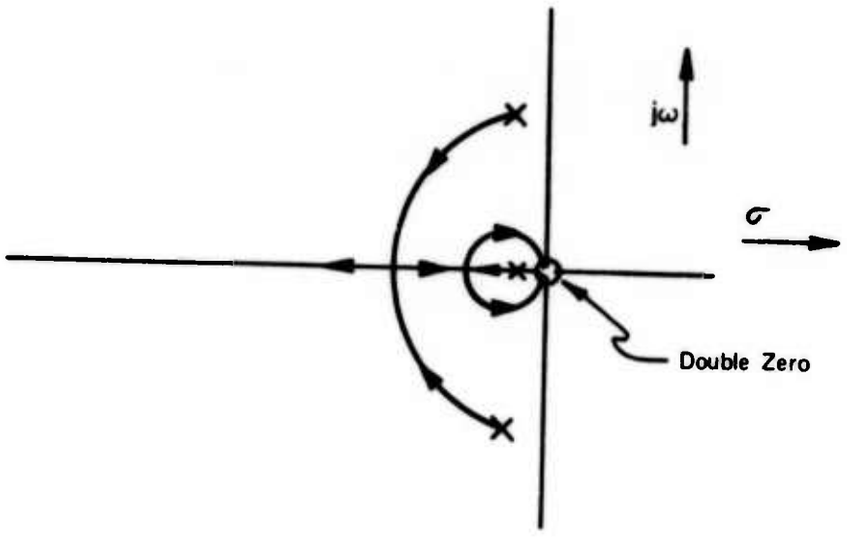

(b) Root Locus of Closed Loop Poles, fixed K_e, K_r. Pressure Feedback Gain K_p increasing.

Figure VII-25
Position, Rate, and Pressure Feedback

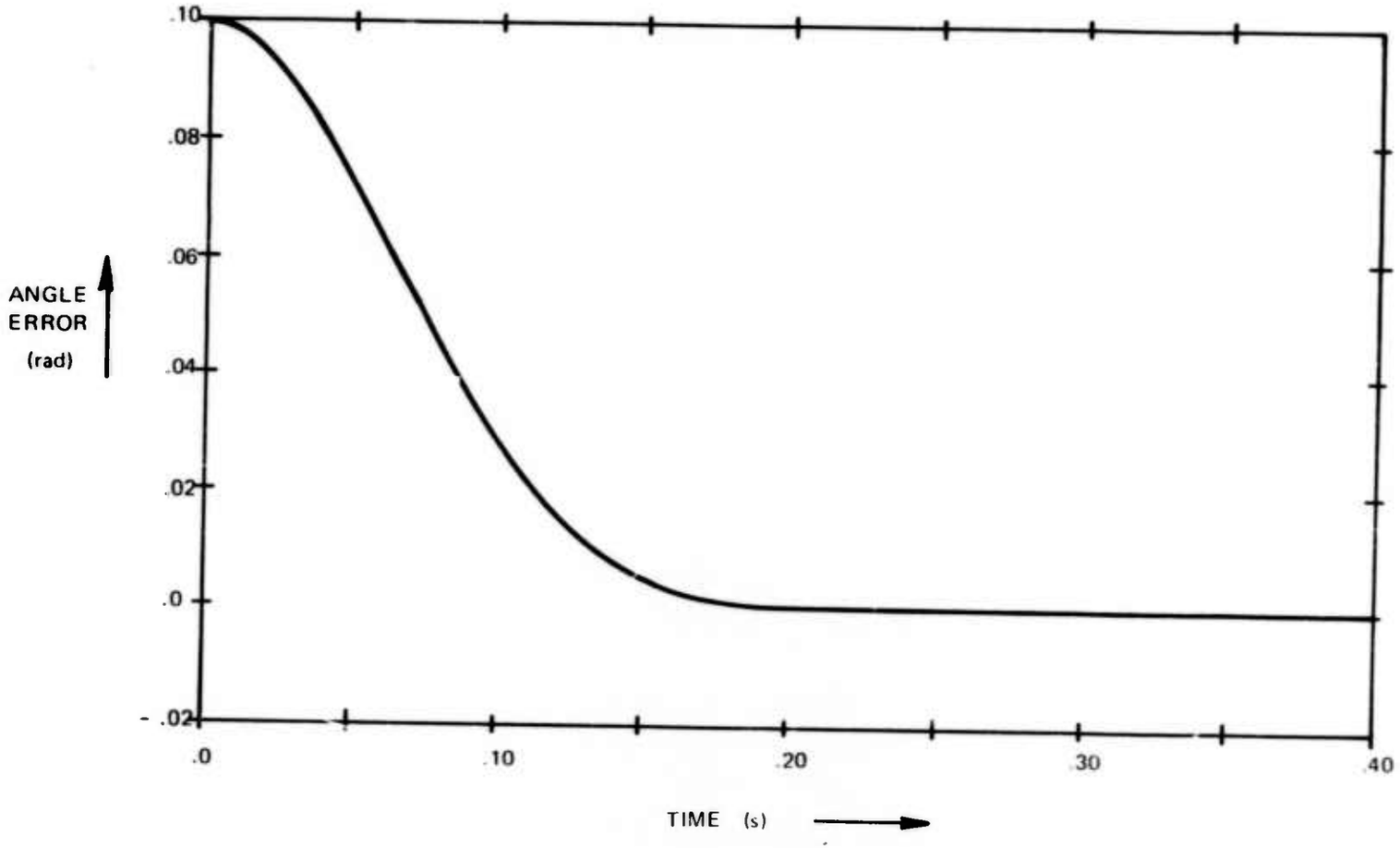

Figure VII-26

Simulated Step Response Using Appropriate Position, Rate, and Pressure Feedback

This technique was tried with the simulation program. Using the simplified model, gains were chosen which were used in the non-linear simulation. The results were inconsistent: while certain values of gains obviously produced reasonable performance (as was shown in the preceding section on pressure feedback), it was not always possible to obtain desired performance. Apparently, the simplified model was too simple to use this way when trying to specify high control frequencies and speed up the response of the control system. Certain higher frequency dynamic components of the control system begin to influence the behavior of the low frequency poles of the simplified model. In particular, the hydraulic valve dynamics and the angle sensing resolver dynamics, both included in the computer simulation, have detrimental effects. Also, the non-linearities included in the simulation may be responsible for some of the problems. Here a more sophisticated pole placement technique including the valve and resolver dynamics is required. The simplified technique does seem to give satisfactory results for control frequency bandwidths less than 10Hz when used in conjunction with the simulation program. Since at this time it is not believed that control frequencies above 10Hz are necessary, or even desirable, then the simplified design technique should prove adequate when used with the simulation program.

It would be desirable to check the simulation program with experimental data. Work in this area is going on now. The experimental equipment includes a commercial rotary vane actuator, hydraulic supply pump and accumulator, inertial load mounted on actuator, a potentiometer for position feedback, a tachometer for rate feedback, pressure sensors in the actuator, and electronics for breadboarding control systems. The qualitative performance of the types of control systems discussed above has been tested and verified. In particular, the addition of pressure feedback was seen to greatly improve performance. Present work is concerned with two areas: First, quantitative comparison of simulation and experiment. Difficulties here include measurement of hard to measure quantities, such as effective fluid modulus and the presence of effects in the experimental equipment not represented in the model of the manipulator actuators. In particular, the commercial rotary actuator used has seals

with rubbing contact leading to significant stiction effects. This type of friction was not included in the simulation. The second primary area of work is the addition of computer control. A PDP9 with A/D and D/A equipment is being used to experiment with the problems of computer control, such as update rates of command and measurement.

Other possibilities for future work in this area include the use of more sophisticated signal filters called observers. Their function is to use the measured signals, such as rate signal or electric current through the valve, to estimate needed signals that are not measured, such as pressure drop in the actuator. This could be very helpful since not only can pressure sensors be expensive, but they also require additional design work on the actuators and instrumentation circuitry to read them. Some preliminary simulation work has shown that a pressure observer designed on the basis of the simplified linearized model can work well for estimating pressure in the non-linear simulation but only when operating in regions where the linear model is most accurate. When the actuator system is operating outside this region the observer performance deteriorates. Consequently, control schemes which would use observers in place of genuine sensors would also deteriorate. Work here has proceeded only in analysis and simulation. Experiments will be done when additional electronic hardware is available.

E. Hydraulic Control Servo Experiments

In support of the theoretical work in the previous part of this section, we have an ongoing program of hydraulic control experiments. The apparatus is illustrated in Figure VII-27. It consists of a hydraulic power supply, a commercial rotary vane actuator, position and rate sensors, and servo electronics. The apparatus can be operated from a signal generator or under computer control. So far the experiments have been utilized to verify our models of rotary vane actuators and to provide values for physical constants for use in computer simulations. Work under way is aimed at testing out the various control configurations outlined above. Work with pressure sensors has been completed and their stabilizing properties, as predicted by the theory, have been amply

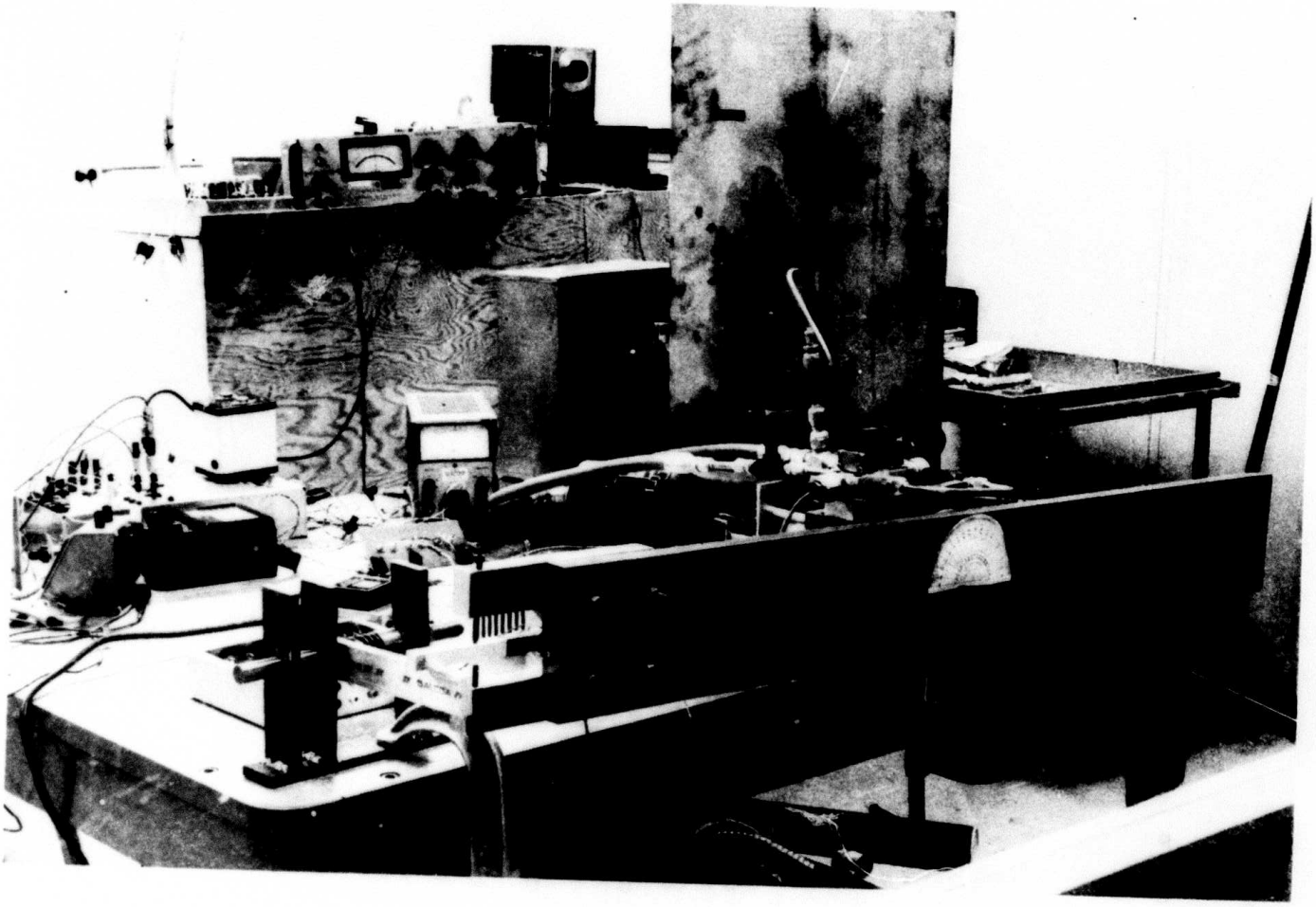

Figure VII-27 Hydraulic Servo Force Feedback Sensor Experimental Hardware

verified. The figure also shows a one degree of freedom force sensor which will be utilized in force feedback servo experiments in connection with the above mentioned companion NSF funded work.

VIII. CONSLUSIONS AND RECOMMENDATIONS FOR FURTHER WORK

A. Conclusions

This report contains three major themes:

- development of a science of manipulator design
- linking that science with the problem of industrial assembly
- study of a particular arm geometry to determine the technological requirements for high performance and operational reliability

The contributions to manipulator design science cover aspects of geometry, kinematics, actuators, servo controls, structure, sensors and task execution strategies. It has been shown that these aspects of arm design and use interact strongly and must be considered together in formulating a design. New design tools have been developed for achieving this. The impetus for any design problem must be a goal for the proposed system. Our efforts were directed at the problem of industrial assembly, where economic and technological success demand high performance arms — arms with strength, high speed, high accuracy and resolution, and rapid, efficient use of sensory information. This set of requirements was combined with a particular choice of scale to produce the geometry which was studied in detail and to focus on problems which arise in other scales, such as mini-robot. Because of this emphasis the design is simple and straightforward. Thus, its potential reliability as a piece of equipment to support laboratory experiments is much higher than commercial or experimental hardware currently in existence. In addition, its capabilities cover a broader spectrum than any currently existing laboratory equipment. Hence, it can support a broader spectrum of experimental activity or tasks.

The requirements of assembly have two aspects: gross motions, which are large, rapid, largely free of sensory feedback and reasonably well understood, and fine motions of two parts interacting as they are assembled. The fine motions are quite small, highly dependent on sensory feedback and thus far not well understood despite some laboratory assembly demonstrations. These demonstrations, both in private industry

and universities, are ad hoc and pragmatic, showing that a particular arm (not specifically designed for assembly) can put some small, well machined smooth parts together. None of these demonstrations has produced any data [except, in one case, the completion time, (an industrial experiment), which was uneconomically slow by a factor of two] shedding light on the class of task attempted in any of the following key areas:

- what design factors in the arm contribute to or detract from success in the demonstrated task, or in other types of tasks
- what control strategies work in this case and which do not — where else will they work
- what sensory information is really necessary to accomplish this or other kinds of tasks
- what forces and torques are being generated during the demonstration tasks
- what is needed to perform these or other tasks more rapidly and reliably

Until a better understanding of the process of assembly is achieved, these demonstrations will be of no value in generating a science of assembly capable of making valid performance predictions with respect to arms and control strategies.

B. Recommendations

Work funded by NSF* is going on at the C. S. Draper Laboratory to study the assembly process, classify and analyze tasks, develop control strategies and use the above to specify hardware and software requirements for industrial assembly systems. In the course of this work, a number of strategies, models, and factors influencing success have emerged. These models need to be tested. The strategies assume employment of novel designs in sensors, servo control organization and actuators. Details of the actuators and sensors have been developed during the current work and are discussed in this report. To carry on this work a high performance computer controlled manipulator arm should be built. Its major contribu-

*NSF-RANN Grant GI-39432X and GI-43787

tions to the research would be as follows:

- a high performance base upon which to test strategy and task models; design and construction of the arm would be sufficiently precise that extraneous and non-reproducible factors influencing the experimental results (structural flexure, sloppiness in transmissions, etc.) could be avoided.
- an accurate, reproducible test instrument capable of executing commanded motions or generating commanded forces and torques quite precisely, so that reliable data on interaction between parts could be obtained; no such data presently exist.
- a device which can be systematically degraded to determine the performance requirements of strategies, the adequacy of error analysis predictions and the usefulness of low cost substitutes for implementing strategies which would be by then well understood.

The questions of size and kinematic arrangement of this arm remain open. None of the design tools developed or used in this research is committed to any particular size or shape of arm. On the contrary, they are applicable to most sizes and all shapes. Two issues need to be resolved before a specific size and shape are selected:

1. if the desired size is quite small, then new technology may be required for actuators and transmissions, and aspects of scaling laws for materials and other items need to be studied in more detail

2. study on this design and on the assembly process revealed the distinction between gross and fine motions. Virtually all existing arms were designed as gross motion devices. We have determined that the requirements for fine motion conflict sufficiently often with requirements for gross motion to make feasible the idea of having two "arms" available for study — one capable of gross motions, accurate positioning and smooth application of force, the other capable of fine motions of high resolution and high speed. A frank assessment of the POPEYE design is that it will be capable of gross motions and some fine motions but for research on fine motion it might be better to ultimately specify a less accurate arm and devote resources to a companion fine motion device. Thus, while POPEYE would make valuable contributions to the science of assembly, we do not claim at this time that it can do assembly by itself or than it even vaguely resembles an industrially satisfactory configuration. Some device designed with foreknowledge of assembly requirements is needed, however, to advance assembly science.

REFERENCES

1. Nevins, J. L., Whitney, D. E. and Simunovic, S. N., "System Architecture for Assembly Machines," C. S. Draper Lab Report No. R-764, November 1973.

2. Nevins, J. L., Whitney, D. E., et. al., "Exploratory Research in Industrial Modular Assembly," C. S. Draper Lab Report No. R-800, March 1974.

3. Nevins, J. L. and Whitney, D. E., "The Force Vector Assembler Concept," C. S. Draper Lab Report No. E-2754, March 1973, presented at First International Symposium on Robot and Manipulator Systems, Udine, Italy, September 1973.

4. Paul, R. P., "Modeling, Trajectory Calculation and Servoing of a Computer Controlled Arm," Stanford University Artificial Intelligence Lab Memo AIM-177, November 1972.

5. Book, W. J., "Modeling, Design and Control of Flexible Manipulator Arms," M. I. T. Mech. Eng. Dept. PhD Thesis. April 1974.

6. Maizza-Neto, O., "Modal Analysis and Control of Flexible Manipulators," M. I. T. Mech. Eng. Dept. PhD Thesis, August 1974.

7. Whitney, D. E., and Scott, P., "The Shaft Windup Problem," C. S. D. L. Internal Memo No. MAT 170, October 1973.

8. Whitney, D. E., "The Mathematics of Coordinated Control of Prosthetic Arms and Manipulators," ASME Journal of Dynamic Systems, Measurement and Control, December 1972, pp 303-309.

9. Doherty, H. J., "Fine Motion Stability of a Manipulator," M. I. T. Mech. Eng. Dept. S. M. Thesis, June 1974.

Survey of Commercial Industrial Robots

	DOF	Accuracy	Control System	Price, $ 1972	Floor Area
Corona	4	± 3mm	D.C. Servo-Mag Tape	15K	800x1000 mm
Fujikoshi	4	± 1mm	Hydr. Cyl. -Mag Tape	-	1530x730 mm
Hawker Siddeley	3	± 3mm	Hydr. -Computer	37.5K	1188x711 mm
Howa	5	± 1.0mm	EL-Hydr.	-	1380x900 mm
Kawauchi Tekko	5	± 1.0mm	Hydr. -Mag Tape	2.8K	1300x750 mm
Kojin	5	± 2.0mm	Hydr. -May Tape	11K	650x1270 mm
Liberator	4	± 0.4mm	Elect-Hydr.	20 to 25K	1320x610 mm
Scheinman	6	± 1.3mm	D.C. Motors	10K	
Sunstrand	5	± .3mm	EL. Motor-Mag Tape	25 to 30K	410x410 mm
Tesa	5	± .1mm	D.C. & Stepper-Mag Tape	-	750x750 mm-control 600x600 mm-Arm
Tokyo Keiki	6	± 1mm	Hydr. (A to D)	12.5K	1900x1300 mm
Tokyo Sokuhan	5	± 1mm	D.C. Motor-POT Input	12.5K	1300x1000 mm
Tralle Fabrikken	4	± 2mm	Hydr. -Mag Tape	20K	1400x750 mm
Versatran	4	0.8mm-1 horz vert	Hydr. -Mag	12 to 25K	
Unimate	6	± 2mm	Hydr. -Mag Tape	37.5K	1500x1500-arm 1200x450-control

Derivation and Simplification of Hydraulic System Equations

We begin the derivation by discussing the nature of the flow through the valve orifices. For any given valve opening, the pressure drop across either orifice is ideally proportional to the square of the flow through the orifice with the sense of the pressure drop in the direction of the flow. The proportional constant varies with the area of the orifice opening so that a flow-pressure relationship is obtained as illustrated in Figure AII-1. Notice that for the largest valve orifice opening, corresponding to valve spoolposition $x_s = 1.0$, the greatest flow is obtained for any given pressure drop. When the valve is closed, $x_s = 0$, there is of course no flow no matter what the pressure drop ΔP. In the following derivation the orifice flow function will be expressed as

$$q = f_q(x_s, \Delta P)$$

where q = flow through orifice

ΔP = pressure drop across orifice

x_s = valve spool position, relative to full travel

When the orifice is ideal the flow function is

$$f_q(x_s, \Delta P) = \begin{cases} K_V \left| x_s \sqrt{|\Delta P|} \right| & \text{for } \Delta P \geq 0 \\ -K_V \left| x_s \sqrt{|\Delta P|} \right| & \text{for } \Delta P < 0 \end{cases} \qquad \text{AII-1}$$

In the non-linear simulation program the ideal flow function is used.

The fluid capacitance, or compliance, in either actuator chamber is proportional to the volume and inversely proportional to the effective fluid modulus

$$C_1(\theta) = \frac{V_1(\theta)}{\beta}$$

$$C_2(\theta) = \frac{V_2(\theta)}{\beta} \qquad \text{AII-2}$$

Figure AII-1

Ideal Valve Orifice Pressure/Flow Relationship

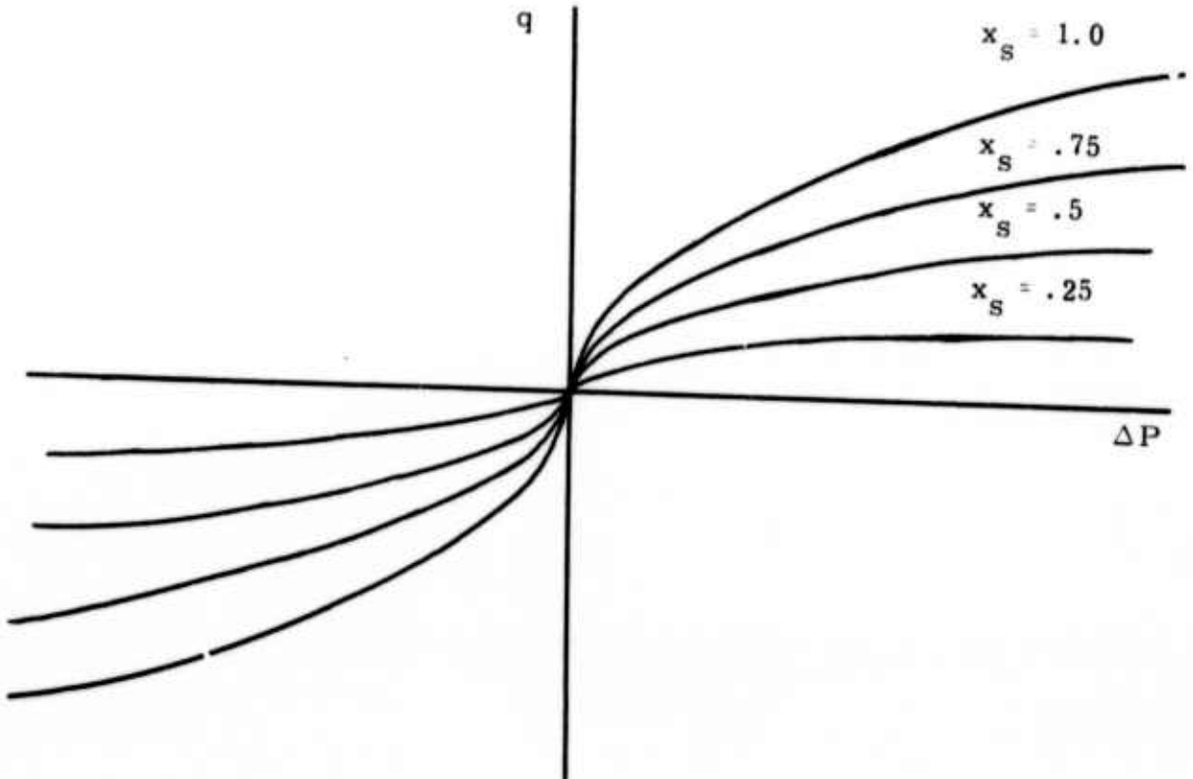

q: flow

ΔP: pressure drop

x_s: valve spool position (size of orifice)

where $C_1(\theta)$ = fluid capacitance in left chamber of Figure VII-16

$C_2(\theta)$ = fluid capacitance in right chamber

$V_1(\theta)$ = actuator fluid volume on left side of actuator vane in Figure VII-16

$V_2(\theta)$ = actuator fluid volume on right side

β = effective fluid modulus

Notice that the volume, and therefore capacitance, of the fluid on one side of the vane is a function of the position of the vane.

The rate of change of pressure in either chamber is equal to the net flow into the chamber divided by the fluid capacitance of the chamber. The net flow into the left hand chamber is

$$-q_L - q_V + q_1$$

where q_L = actuator leakage flow from left chamber to right

q_V = apparent flow due to displacement of the actuator vane

q_1 = flow through the left hand orifice

The net flow into the right chamber is

$$+q_L + q_V - q_2$$

where q_2 = flow through the right hand orifice.

Consequently the equations for pressure rate are

$$\frac{dP_1}{dt} = \frac{1}{C_1(\theta)}[-q_L - q_V + q_1]$$

$$\frac{dP_2}{dt} = \frac{1}{C_2(\theta)}[+q_L + q_V - q_2] \qquad \text{AII-3}$$

We now derive expressions for these flows. The leakage flow q_L past the actuator vane can be expressed as

$$q_L = \frac{P_1 - P_2}{R_L} \qquad \text{AII-4}$$

where R_L is the leakage resistance.

The effective flow due to motion of the actuator vane is the rate at which the vane appears to displace volume.

$$q_V = D\omega \qquad \text{AII-5}$$

where D = displacement of actuator vane

ω = rate of rotation of vane

The flows through the valve orifices can be expressed in terms of the orifice flow function,

$$q_1 = f_q(x_s,\ P_u - P_1) \qquad \text{AII-6}$$

$$q_2 = f_q(x_s,\ P_2 - P_D)$$

$$\text{where } \left.\begin{aligned} P_u &= P_s \\ P_D &= P_E \end{aligned}\right\} \quad \text{for } x_s \geq 0$$

$$\left.\begin{aligned} P_u &= P_E \\ P_D &= P_s \end{aligned}\right\} \quad \text{for } x_s < 0 \qquad \text{AII-7}$$

Equations AII-7 which are discussed in Section VII-D, indicate which orifice is connected to supply pressure and which is connected to exhaust pressure. This depends on the valve spool position x_s. Substituting these expressions for the flows into equations AII-3 we obtain the non-linear chamber equations

$$\frac{dP_1}{dt} = \frac{1}{C_1(\theta)}\left[-\frac{P_1-P_2}{R_L} - D\omega + f_q(x_s,\ P_u - P_1)\right]$$

$$\frac{dP_2}{dt} = \frac{1}{C_2(\theta)}\left[+\frac{P_1-P_2}{R_L} + D\omega - f_q(x_s,\ P_2 - P_D)\right] \qquad \text{AII-8}$$

subject to constraint equations AII-7. Notice that these equations are non-linear not only because of the non-linear flow functions f_q, but also because the capacitances C_1 and C_2 vary with the position of the vane.

We now consider the effect of an inertial load imposed on the actuator. The characteristic equation of the load is

$$I\frac{d\omega}{dt} = \text{torque on load} = D(P_1 - P_2) \qquad \text{AII-9}$$

where I = rotary inertia of load which is equivalently expressed as follows

$$\begin{aligned} \frac{d\omega}{dt} &= \frac{D}{I}(P_1 - P_2) \\ \frac{d\theta}{dt} &= \omega \end{aligned} \qquad \text{AII-10}$$

Now we finally can present the set of non-linear equations for a rotary hydraulic actuator and load:

$$\begin{aligned} \frac{dP_1}{dt} &= \frac{1}{C_1(\theta)}\left[-\frac{P_1 - P_2}{R_L} - D\omega + f_q\,(x_s,\ P_u - P_1)\right] \\ \frac{dP_2}{dt} &= \frac{1}{C_2(\theta)}\left[+\frac{P_1 - P_2}{R_L} + D\omega - f_q\,(x_s,\ P_2 - P_D)\right] \\ \frac{d\omega}{dt} &= \frac{D}{I}(P_1 - P_2) \\ \frac{d\theta}{dt} &= \omega \end{aligned} \qquad \text{AII-11}$$

where $\left.\begin{aligned} P_u &= P_s \\ P_D &= P_E \end{aligned}\right\}$ for $x_s \geq 0$

$\left.\begin{aligned} P_u &= P_E \\ P_D &= P_s \end{aligned}\right\}$ for $x_s < 0$

These equations can be simplified to a linear form by making a series of assumptions as discussed in Section VII-D. They are essentially the following:

1. $C_1(\theta) = C_2(\theta) = C$

2. $q_1 = f_q\,(x_s,\ P_u - P_1) \cong K_s x_s$

   $q_2 = f_q\,(x_s,\ P_2 - P_D) \cong K_s x_s$

3. $\Delta P = P_1 - P_2$

Substitution of these relations in the non-linear equations AII-11 gives:

$$\frac{dP_1}{dt} = \frac{1}{C}\left[-\frac{\Delta P}{R_L} - D\omega + K_s x_s\right] \qquad \text{AII-12}$$

$$\frac{dP_2}{dt} = \frac{1}{C}\left[+\frac{\Delta P}{R_L} + D\omega - K_s x_s\right] \qquad \text{AII-13}$$

$$\frac{d\omega}{dt} = \frac{D}{I}\Delta P \qquad \text{AII-14}$$

Notice that the number of necessary equations has been reduced by one because θ no longer plays a part in the functional relationships. Furthermore, the second equation (AII-13) may be subtracted from the first (AII-12) to yield

$$\frac{d\Delta P}{dt} = \frac{1}{C}\left[-\frac{2\Delta P}{R_L} - 2D\omega + 2K_s x_s\right] \qquad \text{AII-15}$$

$$\frac{d\omega}{dt} = \frac{D}{I}\Delta P$$

or, in matrix form,

$$\begin{bmatrix} \dot{\Delta P} \\ \dot{\omega} \end{bmatrix} = \begin{bmatrix} -\frac{2}{R_L C} & -\frac{2D}{C} \\ \frac{D}{I} & 0 \end{bmatrix} \begin{bmatrix} \Delta P \\ \omega \end{bmatrix} + \begin{bmatrix} \frac{2K_s}{C} \\ 0 \end{bmatrix} x_s \qquad \text{AII-16}$$

Notice that the system order is again reduced by one because the pressure difference ΔP is the important variable, not the values of the pressures themselves.

Appendix III

Abstracts of Theses Performed Under this Contract

a. "A General Planar Positioning Device" by Jonathan David Rock

b. "Design of an Automatic Assembly System Multipurpose End Effector", by Thomas Barry Lyons

A GENERAL, PLANAR

POSITIONING DEVICE

by

JONATHAN DAVID ROCK

Submitted to the Department of Mechanical Engineering

on

June 17, 1974

In partial fulfillment of the requirements for the

degree of Master of Science

A planar positioning device for small motions with the three degrees of freedom x, y, and theta and force feedback is designed. Initially, a model for a six degree of freedom positioning device is discussed and the kinematic equations for motion are derived.

A preliminary analysis of the planar positioning device is made utilizing a computer program to determine how the actuators should be positioned so that maximum forces and torques can be exerted.

Some of the commercial actuators and servo-sensors that are available are looked at and components are chosen. The positioning device is then designed and analyzed, with layout and detailed drawings being included within. An alternate method for obtaining the same three degrees of freedom is considered.

Future research should include control strategies for the positioning device and the design of a six degree of freedom positioning device with force feedback for small motions.

Thesis Supervisor: Daniel E. Whitney

Title: Associate Professor of Mechanical Engineering

DESIGN OF AN AUTOMATIC ASSEMBLY SYSTEM

MULTIPURPOSE END EFFECTOR

by

THOMAS BARRY LYONS

Submitted to the Department of Mechanical Engineering on

May 9, 1974

In partial fulfillment of the requirements for the degree of

Master of Science

A design of an end effector for an experimental automatic assembly system is developed. The operating parameters of the system are explained along with possible uses. The design criteria are payload = 10 Kg. (22 lbs.), maximum jaw opening = 10 cm (4 inches), maximum dynamic load due to normal task operation = 100 Newtons (22 lbf), and actuation is pneumatic using 100 psi shop air. We also try to minimize weight, deflection of the jaws under load, and actuation time, while maximizing strength and jaw spring constant. The final design is approximately 20 cm (8 inches) long, has a mass of just over one kilogram (2.2 lbs.) and has a maximum jaw closing force of over 445 Newtons (100 lbs.).

A kinematic synthesis of a gripper whose jaws remain parallel and whose jaw tips move in a straight line is discussed and laid out graphically. Compliance of the system is analyzed for various loading conditions. This design is compared to a parallelogram gripper and a sliding mechanism gripper, showing the benefits and drawbacks of each. The input stroke of the pneumatic actuator is related to the position of the jaws and overall spring constant of the unit. The actuation system for the end effector is analyzed and various gripping surfaces are discussed. Detailed working drawings are included.

Thesis Supervisor: Daniel E. Whitney
Title: Associate Professor of Mechanical Engineering